A SYNTHETIC, STRUCTURAL AND THEORETICAL INVESTIGATION OF PENTADENTATE SCHIFF BASE LIGANDS

By

SHAUN O. SOMMERER

A DISSERTATION PRESENTED TO THE GRADUATE SCHOOL
OF THE UNIVERSITY OF FLORIDA IN PARTIAL FULFILLMENT
OF THE REQUIREMENTS FOR THE DEGREE OF
DOCTOR OF PHILOSOPHY

UNIVERSITY OF FLORIDA

1991

ACKNOWLEDGMENTS

I wish to thank my research director Gus J. Palenik for his help and guidance during the course of this project, Gaines Martin and Tom Cundari for the helpful discussions concerning the work presented in Chapter 5, and John David Baker for his introduction, help and patients in ZINDO land.

There are a myriad of other people who have helped me in the course of this project and in making my way through graduate school. I thank all of you and leave you with this wish (which I borrowed from B. Dylan)

.... may your heart always be joyful,
may your song always be sung,
and may you stay forever young.

TABLE OF CONTENTS

ACKNOWLEDGMENTS ii

LIST OF TABLES iv

LIST OF FIGURES vi

ABSTRACT vii

CHAPTERS

1 INTRODUCTION 1

2 PENTAGONAL BIPYRAMIDAL COMPLEXES OF Sn(IV), Ti(III), AND Cu(II) 6
Introduction 6
Experimental 7
Results and Discussion 27

3 A NOVEL PENTAGONAL BIPYRAMIDAL IRON COMPOUND: UNCONNECTED Fe(II) AND Fe(III) MOLECULES WITHIN THE SAME ASYMMETRIC UNIT 38
Introduction 38
Experimental 39
Results and Discussion 41

4 PENTAGONAL BIPYRAMIDAL COMPLEXES OF Cr(III) WHICH DISPLAY A STATIC JAHN-TELLER DISTORTION 54
Introduction 54
Experimental 55
Results and Discussion 57

5 SYNTHESIS AND CRYSTAL STRUCTURE OF A WATER SOLUBLE CATIONIC (η^3,η^3-$C_{10}H_{16}$)Ru(IV) COMPLEX: CHLORO[(1-3-η:6-8-η)-2,7-DIMETHYLOCTADIENEDIYL]SEMICARBAZIDE RUTHENIUM(IV) CHLORIDE DIHYDRATE 84
Introduction 84
Experimental 85
Results and Discussion 92
Conclusion 100

6 A THEORETICAL INVESTIGATION OF THE ELECTRONIC AND STRUCTURAL PROPERTIES OF THE LIGAND DAPSC AND THE PENTAGONAL BIPYRAMIDAL COMPLEX DIAQUO-(2,6-DIACETYLPYRIDINEBIS(SEMICARBAZONE)) IRON(II) 101
Introduction 101
Calculations 104
Discussion 115

APPENDIX 127

REFERENCES 140

BIOGRAPHICAL SKETCH 145

LIST OF TABLES

Table 2-1 Crystal Data for $Sn(DAPSC)Cl_2^{2+}$, $Ti(DAPBAH)Cl_2$, and $Cu(DAPAAH)Cl(H_2O)$. 10

Table 2-2 Atomic Parameters for $Sn(DAPSC)Cl_2^{2+}$ 11

Table 2-3 Atomic Parameters for $Ti(DAPBAH)Cl_2$ 12

Table 2-4 Atomic Parameters for $Cu(DAPAAH)Cl(H_2O)$ . . 13

Table 2-5 Bond Distances and Angles for $Sn(DAPSC)Cl_2^{2+}$ 14

Table 2-6 Bond Distances and Angles for $Ti(DAPBAH)Cl_2$ 15

Table 2-7 Bond Distances and Angles for $Cu(DAPAAH)Cl(H_2O)$ 17

Table 2-8 Anisotropic U values for $Sn(DAPSC)Cl_2^{2+}$ . . 18

Table 2-9 Anisotropic U values for $Ti(DAPBAH)Cl_2$ . . 20

Table 2-10 Anisotropic U values for $Cu(DAPAAH)Cl(H_2O)$ 22

Table 2-11 Hydrogen Atomic Parameters for $Sn(DAPSC)Cl_2^{2+}$ 24

Table 2-12 Hydrogen Atomic Parameters for $Ti(DAPBAH)Cl_2$ 25

Table 2-13 Hydrogen Atomic Parameters for $Cu(DAPAAH)Cl(H_2O)$ 26

Table 3-1 Atomic Parameters for Fe(II)/(III) $(DAPSC)Cl(H_2O)$ 44

Table 3-2 Bond Distances and Angles for Fe(II)/(III) $(DAPSC)Cl(H_2O)$ 46

Table 3-3 Anisotropic U values for Fe(II)/(III) $(DAPSC)Cl(H_2O)$ 48

Table 3-4 Hydrogen Atomic Parameters for Fe(II)/(III) $(DAPSC)Cl(H_2O)$ 50

Table 3-5 Bond Lengths Observed Within the Immediate Coordination Sphere for Fe(II)/(III) $(DAPSC)Cl(H_2O)$ and related compounds . 52

Table 4-1 Crystal Data for $Cr(DAPSC)(H_2O)_2$ and $Cr(DAPBAH)(H_2O)_2$ 58

Table 4-2 Atomic Parameters for $Cr(DAPSC)(H_2O)_2$ . . . 59

Table 4-3 Atomic Parameters for $Cr(DAPBAH)(H_2O)_2$ . . 60

Table 4-4 Bond Distances and Angles for $Cr(DAPSC)(H_2O)_2$ 62

Table 4-5 Bond Distances and Angles for $Cr(DAPBAH)(H_2O)_2$ 63

Table 4-6 Anisotropic U values for $Cr(DAPSC)(H_2O)_2$. 66

Table 4-7 Anisotropic U values for $Cr(DAPBAH)(H_2O)_2$. 68

Table 4-8 Hydrogen Atomic Parameters for $Cr(DAPSC)(H_2O)_2$ 71

Table 4-9 Hydrogen Atomic Parameters for $Cr(DAPSC)(H_2O)_2$ 72

Table 4-10 Bond Distances Within the Coordination Sphere for $Cr(DAPSC)(H_2O)_2$ and $Cr(DAPBAH)(H_2O)_2$ 76

Table 5-1 Crystal Data for $(\eta^3,\eta^3\text{-}C_{10}H_{16})$Semicarbazide Ru(IV) Chloride 87

Table 5-2 Atomic Parameters for $(\eta^3,\eta^3\text{-}C_{10}H_{16})$ Semicarbazide Ru(IV) Chloride 88

Table 5-3 Bond Distances and Angles for $(\eta^3,\eta^3\text{-}C_{10}H_{16})$ Semicarbazide Ru(IV) Chloride 89

Table 5-4 Anisotropic U values for $(\eta^3,\eta^3\text{-}C_{10}H_{16})$ Semicarbazide Ru(IV) Chloride 90

Table 5-5 Hydrogen Atomic Parameters for $(\eta^3,\eta^3\text{-}C_{10}H_{16})$ Semicarbazide Ru(IV) Chloride 91

Table 5-6 Summary of the Ru-Cl Bond Distance 99

Table 6-1 Bond Distances and Angles for the Geometrically Optimized DAPSC 107

Table 6-2 Bond Distances and Angles for the Geometrically Optimized $Fe(DAPSC)(H_2O)_2^{2+}$ 120

Table 6-3 A Summary of the Bond Distances Within the Immediate Coordination Sphere for an Fe^{2+} Center in Singlet, Triplet and Quintet Spin States 121

Table 6-4 Relative Total Energies of the Three Optimized Spin States 122

LIST OF FIGURES

Figure 1-1 Graphic Representation of the Ligands DAPSC, DAPBAH and DAPAAH 4

Figure 2-1 An ORTEP Representation of $[Sn(DAPSC)Cl_2]^{2+}$ 28

Figure 2-2 An ORTEP Representation of $Ti(DAPBAH)Cl_2$ 31

Figure 2-3 An ORTEP Representation of $[Cu(DAPAAH)Cl(H_2O)]^+$ 35

Figure 3-1 An ORTEP Representation of an Fe(II/III) DAPSC Complex 43

Figure 4-1 An ORTEP Representation of $[Cr(DAPSC)(H_2O)_2]^{2+}$ 74

Figure 4-2 An ORTEP Representation of $[Cr(DAPBAH)(H_2O)_2]^{2+}$ 75

Figure 4-3 Crystal Field Splitting Diagram for a Pentagonal Bipyramidal Field 78

Figure 4-4 A Representation of the Half-Conjugated Monoanion form of DAPSC 81

Figure 5-1 An ORTEP Representation of $(\eta^3,\eta^3\text{-}C_{10}H_{16})$ Semicarbazide Ru(IV) Chloride 94

Figure 5-2 A Representation of the Bonding, Non-bonding and Anti-bonding Molecular Orbitals for a 3-electron η^3-allyl function 96

Figure 6-1 Representations of the DAPSC Ligand in Low Energy Conformations 105

Figure 6-2 A Representation of DAPSC in the Optimum Geometry as Determined by ZINDO . . . 108

Figure 6-3 An Illustration of the Relative Total Energy vs. the Angle of Rotation for DAPSC with One Semicarbazone "arm" Locked Forward 111

Figure 6-4 An Illustration of the Relative Total Energy vs. the Angle of Rotation for DAPSC with One Semicarbazone "arm" Locked Backward 113

Figure 6-5 An Illustration of the Possible Spin States for an Fe^{2+} (d^6) Ion 114

Figure 6-6 Coordinate System and Atom Numbering Scheme 118

Figure 6-7 A Representation of $[Fe(DAPSC)(H_2O)_2]^{2+}$ in the Optimum Geometry as Determined by ZINDO 119

Abstract of Dissertation Presented to the Graduate School of the University of Florida in Partial Fulfillment of the Requirements for the degree of Doctor of Philosophy

A SYNTHETIC, STRUCTURAL AND THEORETICAL INVESTIGATION OF PENTADENTATE SCHIFF BASE LIGANDS

By

SHAUN O. SOMMERER

May 1991

Chairman: Dr. Gus J. Palenik
Major Department: Chemistry

The pentadentate Schiff base ligands 2,6-diacetylpyridinebis(semicarbazone), DAPSC, 2,6-diacetylpyridinebis(benzoic acid hydrazone), DAPBAH, and 2,6-diacetylpyridinebis-(acethydrazone), DAPATD, were used to isolate Sn^{4+}, Ti^{3+}, and Cu^{2+}, respectively, in pentagonal bipyramidal, PBP, geometry. The complexes were characterized by X-ray diffraction studies, and the structural details of each complex are reported and discussed. A unique Fe-DAPSC PBP species is also reported which has been characterized by an X-ray diffraction study, and evidence is put forth to show that in one of the molecules, the Fe atom is formally 2+ where in the other molecule the Fe atom is formally 3+.

Two PBP Cr^{3+} complexes are reported which are markedly distorted in the equatorial plane. Both structures have been characterized by X-ray diffraction techniques and solution

magnetic moments show both species to be high spin d^3 complexes. A group theoretical treatment of the possible spin states resulting from the d^3 configuration shows that a Jahn-Teller distortion is possible in a D_{5h} ligand field. The equatorial distortion observed in both complexes is finally shown to actually be a combination of effects, namely the deprotonation of the ligand combined with a Jahn-Teller distortion.

A theoretical study of the ligand DAPSC is presented which employed several techniques. Molecular mechanics calculations (MM2 type) (corroborated by MOPAC calculations) showed that there were three configurations of the ligand which corresponded to energy minima. Using the program ZINDO, a complete geometry optimization of DAPSC was preformed, the rotation barriers of the semicarbazone "arms" of DAPSC were determined, and several geometry optimizations on a DAPSC molecule perturbed by an Fe^{2+} ion were preformed. The purpose of these calculations was to determine the low energy conformation of DAPSC as well as the effects of spin state multiplicity on the geometry of both the ligand and the Fe-DAPSC complex. The geometry and bond distances observed in the optimized Fe-complex are in excellent agreement with what has been observed in the solid state for a similar $[Fe(DAPSC)Cl_2]$ complex as determined by X-ray diffraction studies.

CHAPTER 1

INTRODUCTION

Seven-coordinate transition metal complexes are less common since they cannot achieve as efficient a structural form as the nearest coordination neighbors six and eight. Moreover, in progressing from six to seven coordination, a much less effective packing arrangement is achieved. Since seven-coordination has, in the general case, a potential surface that is not distinguished by a deep minimum corresponding to one polytopal[1] form, the number of monoisomorphic polyhedra with seven vertices is large (34)[2]. The pentagonal bipyramid (PBP), capped octahedron, and capped trigonal prism are considered to be the three ideal polyhedra for CN = 7 with PBP geometry, being the most common arrangement found in monomers and dimers throughout the periodic table[3]. The role of seven-coordination is significant when viewed in the light of reaction intermediates or transition states in associative reactions of 6-coordinate complexes, oxidative addition reactions of 5-coordinate complexes, and dissociative reactions of 8-coordinate complexes[4]. Therefore, systematic investigations of 7-

coordinate complexes can provide added insight to these important areas of chemistry.

A very efficient way of forming pentagonal bipyramidal (PBP) complexes (C.N. = 7) is with pentadentate ligands that can occupy the pentagonal plane, particularly if the ligand is at least partly conjugated[5]. The two types of pentadentate ligands that have been used successfully in this fashion to achieve PBP geometry are either macrocyclic in nature or noncyclic. A disadvantage of the macrocyclic type ligands is that the size of the ligands central "hole" is of critical importance in determining which metal-cations the ligand will hold effectively. If the match between the metal-cation and the "hole" size is incorrect, puckering of the pentagonal girdle results causing distortion and possible instability. Noncyclic pentadentate ligands on the other hand are not hindered to the same extent by the metal-cation size constraint since the "hole" is not bound on all sides; consequently, this type of ligand is more versatile in achieving PBP geometry as it can accommodate metal atoms of different sizes by increasing the L-M-L angle not spanned by a chelate ring. Accordingly, noncyclic pentadentate ligands offer the potential for the development of a wide based coordination chemistry due to the inherent flexibility of these ligands.

In order to study seven-coordinate chemistry of the transition metals a series of noncyclic pentadentate ligands

was designed which would consistently produce PBP geometry[6]. Three of these ligands are depicted in Figure 1.

DAPSC, DAPBAH, and DAPAAH have been used successfully to produce several complexes which exhibit PBP geometry. DAPSC especially has been found to react with virtually all +2 and +3 ions of groups 3, 12, and 13 as well as the elements Ti to Cu[6-16]. Although the usual result is PBP geometry, higher coordination numbers are found with the larger +3 ions[13,14].

DAPBAH and DAPAAH mimic the coordination sites of DAPSC but vary in the functional groups directed away from the coordinated metal. With the replacement of the $-NH_2$ function of the acid hydrazide with either a $-C_6H_5$ function to give DAPBAH, or a $-CH_3$ function giving DAPATD, the solution chemistry of the complex would be expected to change, especially in terms of the solubility for a particular complex in aqueous verses an organic media. Although DAPBAH and DAPAAH have been used less extensively, previous results[15] have demonstrated that these ligands are quite reactive with many of the transition metals.

Several intriguing aspects concerning the chemistry and structure of these pentadentate ligands emerged during the initial investigation[6] which merited further examination. As a consequence, a research project was designed to analyze the coordination chemistry and structure of these ligands with the following goals in mind: first, to advance the on going study of seven-coordinate chemistry by preparing new seven-

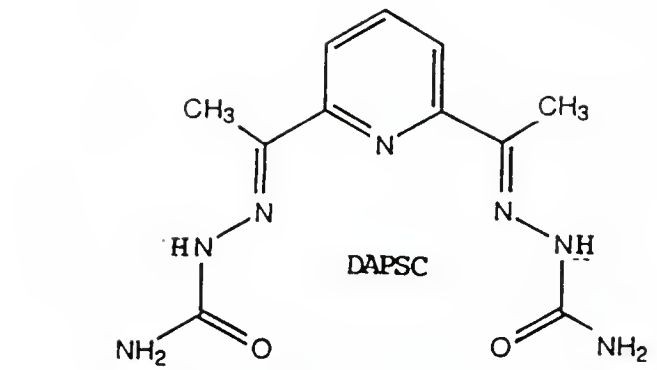

DAPSC

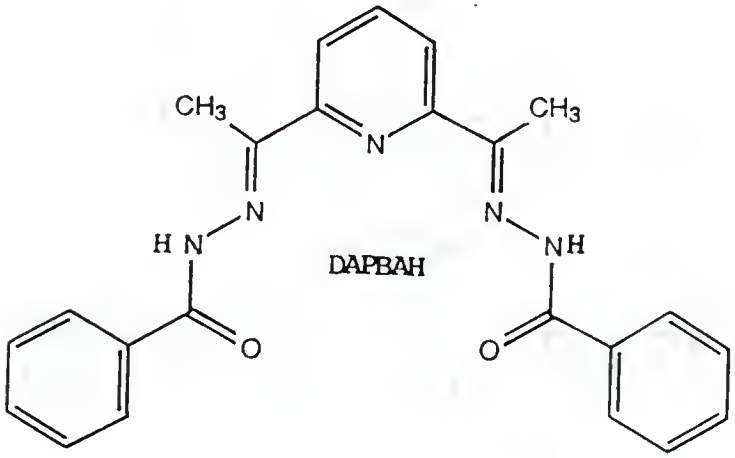

DAPBAH

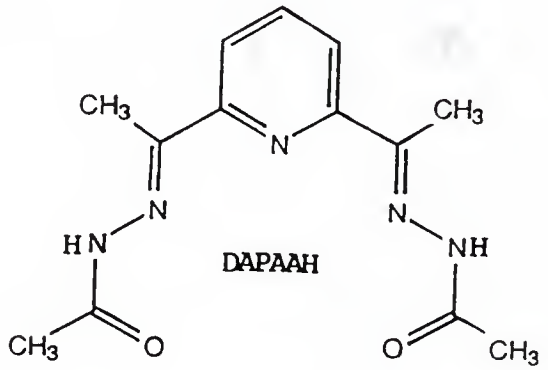

DAPAAH

Figure 1-1. 2.6-diacetylpyridinebis(semicarbazone, (DAPSC), 2,6-diacetylpyridinebis(benzoic acid hydrazone), (DAPBAH), and 2,6-diacetylpyridinebis(acethydrazone), (DAPAAH).

coordinate complexes of metals not yet isolated with the three pentadentate ligands; second, to investigate further the structural aspects of PBP complexes exhibiting unusual distortions within the coordination sphere; third, to study the structural characteristics of these pentadentate ligands; and, finally, to explore the reaction chemistry observed with these ligands. To accomplish this work, general laboratory procedures were used for the synthesis with an emphasis on obtaining single crystals for X-ray diffraction studies and structural determination.

The following chapters report the experimental work which was preformed and discuss what was learned regarding the chemistry and structure of DAPSC, DAPBAH, and DAPAAH.

CHAPTER 2

PENTAGONAL BIPYRAMIDYL COMPLEXES OF Sn(IV), Ti(III), AND Cu(II).

Introduction

The synthesis and structural characterization by X-ray diffraction techniques of $Sn(DAPSC)Cl_2^{2+}$, $Ti(DAPBAH)Cl_2^{+}$ and $Cu(DAPAAH)(H_2O)Cl^{+}$ is addressed in this chapter. This set of complexes demonstrates the versatility of the respective ligands in the study of 7-coordinate chemistry since each of these complexes was found to exhibit PBP geometry.

The PBP Sn(IV) complex was unexpectedly isolated from aqueous solution during investigations involving $(CH_4N)_3[Pt(SnCl_3)_5]$. This is a unique complex in that it is the first example of a water soluble seven-coordinate Sn(IV) complex in which a pentadentate ligand was used. With the isolation of the $Ti(DAPBAH)Cl_2^{+}$ complex, there is now an example of each of the first transition series (i. e. Sc - Zn) in a PBP field coordinated by a pentadentate ligand. Finally, this report of the $Cu(DAPAAH)(H_2O)Cl^{+}$ complex marks the first account of DAPAAH being used to isolate a Cu(II) ion in PBP geometry.

Experimental

Materials. All materials and solvents were reagent grade and used as supplied from the manufacturer except where noted.

Preparation of $[Sn(DAPSC)Cl_2]Cl_2 \cdot 2H_2O$ (I). Both $(CH_3NH)_3[Pt(SnCl_3)_5]$ (0.632g, 0.4 mmole) and DAPSC (0.113g, 0.4 mmole), prepared by methods previously described[9,17], were slurried together in 40 mL of H_2O. HCl was added drop-wise until the pH = 1.00. As the solution cleared to a yellow/brown color, a fine black precipitate was evident in the solution. A dark yellow/brown solution void of black precipitate was obtained after filtering through a fine glass frit. Slow evaporation of the filtrate gave yellow crystals within four days.

Preparation of $Ti(DAPBAH)Cl_2^+$, (II). In a dry box with an Argon atmosphere, $TiCl_3$ (0.151g, 1.0 mmole) was weighed out and placed into a dry Schlenk flask containing a magnetic stirring bar. The flask was sealed with a rubber septum and removed from the dry box. By means of a needle and syringe, 2,6-diacetylpyridine (0.168g, 1.0 mmole) dissolved in 20 mL absolute ethanol was added to the flask. Next, benzoic acid hydrazide (0.272g, 2.0 mmole) dissolved in 20 mL of absolute ethanol was added by needle and syringe. The closed mixture was stirred for three hours after which the solvent was removed by vacuum. The Schlenk flask containing the dry crude solid was placed back into the dry box and the rubber septum was removed. Acetonitrile (30 mL), previously dried over

P_2O_{10}, was added and the mixture was stirred for two hours. The mixture was then filtered through a fine glass frit and a clear dark red solution was obtained. The volume of this solution was reduced to 13 mL and then placed into an Erlenmyer flask, sealed, removed from the dry box, and placed in a freezer (-10 °C). Air stable red single crystals were obtained after three weeks.

Preparation of $Cu(DAPAAH)Cl_2$, (III). Acethydrazide (0.156g, 2.0 mmole), $CuCl_2 \cdot 2H_2O$ (0.170g, 1 mmole), and 2,6-diacetylpyridine (0.168g, 1.0 mmole), were combined in 30 mL of a 50/50 mixture of ethanol/water solution. This solution was then heated to 58°C and stirred for one-half hour. A dark green solution was the result of this reaction which was then filtered through a fine glass frit while warm. A crop of dark green crystals were removed after eight days. The density of these crystals was measured at 1.57 g/cm^3 by floatation techniques.

X-ray Crystallography. Crystals having the dimensions 0.15 x 0.17 x 0.23 mm, 0.18 x 0.20 x 0.25 mm, and 0.10 x 0.14 x 0.15 mm for I, II, and III, respectively, and suitable for diffraction studies, were mounted on the end of a glass fibers. All subsequent measurements for I and II were made using a Nicolet R3m diffractometer with graphite-monochromated Mo-Kα radiation (λ = 0.71069Å). For compound III, the subsequent measurements were made using a Nicolet P1 diffractometer, up graded to R3m specifications, with

monochromated Cu-Kα radiation (λ = 1.54056Å) with a nickel filter in place.

The cell dimensions for each of the three compounds were determined by a least squares refinement of 25 automatically centered reflections. A variable-speed (1° - 29.3°) 2θ scan technique was used to measure the intensity data from 0° to 50°, 0° to 45°, and 0° to 110° in 2θ for I, II, and III respectively. Two standard reflections were measured every 98 reflections to monitor for any decomposition during the X-ray analysis. No absorption corrections were made. The pertinent crystal data is given in Table 2-1.

Structure Refinement. The data reduction, structure solution and final refinement were performed using the NRCVAX (PC-Version)[18] package of programs. The Sn, Ti and Cu atoms and all non-hydrogen atoms were located by the heavy-atom method (Patterson and Fourier syntheses) and refined anisotropically by full-matrix least squares. The hydrogen atoms were located using a difference Fourier map and refined isotropically. The models converged to an R of 0.047, 0.061, and 0.061 with Rw values of 0.061, 0.086, and 0.068 for I, II, and III respectively. The final positional parameters for non-hydrogen atoms are given in Tables 2-2 to 2-4. The final bond distances involving the non-hydrogen atoms and bond angles are listed in Tables 2-5 to 2-7 with the anisotropic thermal parameters given in Tables 2-8 to 2-10. Tables 2-11 to 2-13 list the final positional parameters for the hydrogen atoms.

Table 2-1. Crystal Data

	I	II	III
formula	$Sn(DAPSC)Cl_2^{+}2Cl^{-}\cdot 2H_2O$	$Ti(DAPBAH\text{-}H)Cl_2$	$Cu(DAPAAH)\cdot 3H_2O$
MW	$SnC_{11}N_7O_4H_{19}Cl_4$	$TiC_{23}N_5O_2H_{20}Cl_2$	$CuC_{13}N_5O_5H_{21}Cl_2$
a, Å	573.81	497.09	360.33
b, Å	9.213(2)	8.611(5)	7.977(1)
c, Å	13.391(4)	13.986(5)	13.265(2)
β, deg	16.856(7)	20.228(8)	18.810(2)
Vol., $Å^3$	95.60(3)	100.40(4)	99.26(1)
Z	2069.6	2396.1	1964.6
ϱ_{calc}, g/cm^3	4	4	4
space group	1.83	1.39	1.22
μ, cm^{-1}	P $2_1/n$	P $2_1/c$	P $2_1/c$
Data used with (Inet>2.5σInet)	87.2	6.1	43.0
R^a	2832	1955	2056
$R_w{}^b$	4.7	6.1	6.1
	6.1	8.6	6.8

$$R^{a}=\sum \frac{|F_o|-|F_c|}{|F_c|}$$

$$R_w^{b}=\left[\frac{\sum w(|F_o|-|F_c|)^2}{\sum w|F_o|^2}\right]^{1/2}$$

Table 2-2. Atomic Parameters for I, x,y,z and Biso. E.S.Ds. refer to the last digit printed.

	x/a	y/b	z/c	Biso
Sn	.7209 (1)	.8794 (1)	.1567 (1)	2.01 (2)
Cl1	.7977 (3)	.7284 (2)	.2187 (1)	3.3 (1)
Cl2	.6410 (3)	1.0346 (2)	.1010 (1)	3.14 (9)
O1	.5462 (6)	.8820 (5)	.2303 (3)	2.7 (2)
O2	.5548 (7)	.8033 (5)	.0844 (3)	2.9 (3)
N3	.8018 (7)	.9612 (5)	.2706 (4)	2.1 (3)
N4	.9554 (7)	.9285 (5)	.1551 (4)	2.1 (3)
N5	.8062 (8)	.8419 (5)	.0391 (4)	2.2 (3)
N1	.4690 (10)	.9221 (7)	.3494 (5)	3.5 (4)
N2	.6985 (7)	.9660 (6)	.3238 (4)	2.6 (3)
N6	.7071 (9)	.8016 (6)	-.0146 (4)	2.8 (3)
N7	.4779 (10)	.7322 (7)	-.0344 (5)	3.3 (4)
C1	.5683 (10)	.9225 (7)	.2994 (5)	2.5 (3)
C2	.9313 (10)	.9952 (7)	.2845 (5)	2.6 (3)
C3	.9911 (13)	1.0438 (10)	.3594 (6)	3.8 (5)
C4	1.0211 (9)	.9794 (6)	.2176 (5)	2.3 (3)
C5	1.1647 (10)	1.0122 (7)	.2174 (6)	3.0 (4)
C6	1.2383 (10)	.9893 (8)	.1532 (6)	3.4 (4)
C7	1.1722 (10)	.9348 (8)	.0897 (6)	3.0 (4)
C8	1.0287 (10)	.9064 (6)	.0920 (5)	2.5 (3)
C9	.9410 (10)	.8556 (6)	.0256 (5)	2.3 (3)
C10	1.0033 (12)	.8258 (8)	-.0488 (6)	3.0 (4)
C11	.5773 (10)	.7790 (6)	.0140 (5)	2.5 (3)
W1	.7343 (10)	.8522 (7)	.5155 (5)	4.6 (4)
W2	.8857 (11)	.3283 (8)	.8452 (6)	6.4 (5)
C13	.6830 (3)	.7146 (2)	.8170 (1)	4.1 (1)
C14	.6672 (3)	1.0786 (2)	.4759 (1)	3.9 (1)

Biso is the Mean of the Principal Axes of the Thermal Ellipsoid

Table 2-3. Atomic Parameters for II, x,y,z and Biso. E.S.Ds. refer to the last digit printed.

	x/a	y/b	z/c	Biso
Ti	.1286 (2)	.5235 (2)	.2035 (1)	3.83(9)
C11	.1899 (4)	.3800 (2)	.1565 (2)	5.5 (2)
C12	.0230 (4)	.6553 (2)	.2488 (2)	5.1 (2)
O1	.3430 (8)	.5435 (5)	.2567 (3)	4.1 (3)
O2	.2329 (8)	.6027 (5)	.1430 (3)	4.0 (3)
N1	.2837 (11)	.4531 (8)	.3435 (5)	4.6 (5)
N2	.1449 (11)	.4488 (7)	.2991 (4)	4.2 (4)
N3	-.0988 (10)	.4548 (6)	.2098 (5)	4.0 (4)
N4	-.0443 (12)	.5505 (7)	.1121 (5)	4.6 (5)
N5	.0077 (13)	.6035 (7)	.0630 (5)	5.0 (5)
C1	.3824 (12)	.5089 (8)	.3170 (5)	3.6 (5)
C2	.0297 (13)	.4009 (8)	.3162 (6)	3.9 (5)
C3	.0332 (17)	.3486 (12)	.3788 (8)	5.8 (7)
C4	-.1156 (13)	.4032 (8)	.2659 (7)	4.3 (6)
C5	-.2559 (16)	.3599 (9)	.2719 (8)	5.8 (7)
C6	-.3795 (15)	.3724 (12)	.2197 (10)	7.6 (9)
C7	-.3661 (15)	.4267 (11)	.1627 (9)	6.4 (8)
C8	-.2236 (15)	.4637 (9)	.1591 (7)	5.0 (6)
C9	-.1859 (14)	.5169 (10)	.1030 (7)	5.5 (7)
C10	-.3003 (22)	.5329 (14)	.0397 (12)	7.2 (9)
C11	.1534 (15)	.6284 (9)	.0836 (6)	4.4 (6)
CA1	.5386 (12)	.5293 (7)	.3565 (5)	3.3 (5)
CA2	.6388 (12)	.5910 (9)	.3321 (5)	4.3 (6)
CA3	.7859 (14)	.6167 (10)	.3711 (6)	5.4 (7)
CA4	.8275 (14)	.5770 (11)	.4327 (6)	5.6 (7)
CA5	.7313 (16)	.5127 (10)	.4574 (6)	6.0 (7)
CA6	.5869 (12)	.4898 (9)	.4193 (6)	4.7 (6)
CB1	.2364 (16)	.6874 (8)	.0389 (6)	4.4 (6)
CB2	.1549 (17)	.7096 (10)	-.0248 (7)	6.1 (7)
CB3	.236 (3)	.7605 (13)	-.0664 (8)	8.3 (9)
CB4	.394 (3)	.7862 (11)	-.0466 (9)	8.4 (9)
CB5	.4721 (19)	.7591 (10)	.0186 (8)	6.7 (8)
CB6	.3915 (17)	.7135 (9)	.0605 (6)	5.1 (7)

Biso is the Mean of the Principal Axes of the Thermal Ellipsoid

Table 2-4. Atomic Parameters for III, x,y,z and Biso. E.S.Ds. refer to the last digit printed.

	x/a	y/b	z/c	Biso
Cu	.2545 (1)	.2823 (1)	.0028 (1)	2.75(5)
Cl1	.5138 (3)	.2839 (2)	.0733 (1)	4.21(9)
Cl2	-.0564 (3)	.2043 (2)	-.2091 (1)	5.8 (1)
W1	.0241 (9)	.2864 (5)	-.0570 (4)	4.1 (3)
W2	.5683 (20)	.2810 (10)	.7348 (7)	8.1 (7)
W3	.7701 (9)	.3874 (5)	-.0181 (5)	6.0 (4)
O1	.1665 (7)	.4146 (4)	.0634 (3)	3.5 (3)
O2	.3326 (7)	.4122 (4)	-.0641 (3)	3.9 (3)
N1	.4056 (8)	.2911 (5)	-.1383 (3)	3.5 (3)
N2	.3539 (8)	.2213 (5)	-.0918 (3)	3.1 (3)
N3	.2438 (8)	.1128 (4)	.0035 (4)	3.2 (3)
N4	.1379 (8)	.2276 (4)	.0964 (3)	3.0 (3)
N5	.0872 (8)	.3007 (5)	.1405 (3)	3.3 (3)
C1	.3925 (10)	.3899 (6)	-.1174 (4)	3.4 (4)
C2	.4543 (13)	.4662 (10)	-.1661 (6)	5.0 (5)
C3	.3546 (10)	.1255 (6)	-.1060 (4)	3.5 (4)
C4	.4052 (16)	.0797 (10)	-.1718 (6)	5.4 (6)
C5	.2987 (10)	.0628 (6)	-.0501 (4)	3.2 (4)
C6	.3011 (12)	-.0427 (7)	-.0488 (6)	4.2 (4)
C7	.2461 (13)	-.0911 (6)	.0069 (6)	4.5 (4)
C8	.1891 (12)	-.0389 (6)	.0612 (5)	4.1 (5)
C9	.1900 (10)	.0662 (6)	.0584 (4)	3.1 (3)
C10	.1312 (10)	.1328 (6)	.1132 (4)	3.3 (3)
C11	.0735 (16)	.0917 (8)	.1781 (5)	5.0 (5)
C12	.1030 (10)	.3971 (6)	.1167 (4)	3.1 (4)
C13	.0396 (14)	.4767 (8)	.1616 (5)	4.3 (4)

Biso is the Mean of the Principal Axes of the Thermal Ellipsoid

Table 2-5. Bond Distances(Å) and Angles(°) for I

Sn - Cl1	2.354(2)	N5 - C9	1.297(11)
Sn - Cl2	2.368(2)	N1 - C1	1.304(11)
Sn - O1	2.127(5)	N2 - C1	1.360(12)
Sn - O2	2.123(6)	N6 - C11	1.367(12)
Sn - N3	2.272(7)	N7 - C11	1.322(12)
Sn - N4	2.260(7)	C2 - C3	1.479(13)
Sn - N5	2.259(6)	C2 - C4	1.477(12)
O1 - C1	1.282(10)	C4 - C5	1.395(12)
O2 - C11	1.267(10)	C5 - C6	1.368(14)
N3 - N2	1.371(9)	C6 - C7	1.386(14)
N3 - C2	1.277(12)	C7 - C8	1.381(13)
N4 - C4	1.348(10)	C8 - C9	1.481(13)
N4 - C8	1.347(10)	C9 - C10	1.484(12)
N5 - N6	1.336(10)		

Cl1-Sn-Cl2	176.94(8)	C4-N4-C8	120.4(7)
Cl1-Sn-O1	88.1(2)	Sn-N5-N6	114.3(5)
Cl1-Sn-O2	90.6(2)	Sn-N5-C9	123.0(6)
Cl1-Sn-N3	88.8(2)	N6-N5-C9	122.7(7)
Cl1-Sn-N4	90.5(2)	N3-N2-C1	115.5(7)
Cl1-Sn-N5	94.8(2)	N5-N6-C11	114.4(7)
Cl2-Sn-O1	89.6(2)	O1-C1-N1	121.8(8)
Cl2-Sn-O2	90.9(2)	O1-C1-N2	120.9(7)
Cl2-Sn-N3	88.6(2)	N1-C1-N2	117.4(8)
Cl2-Sn-N4	90.0(2)	N3-C2-C3	125.2(8)
Cl2-Sn-N5	88.2(2)	N3-C2-C4	113.1(7)
O1-Sn-O2	78.4(2)	C3-C2-C4	121.7(8)
O1-Sn-N3	72.8(2)	N4-C4-C2	115.2(7)
O1-Sn-N4	141.4(2)	N4-C4-C5	120.8(8)
O1-Sn-N5	149.7(2)	C2-C4-C5	124.0(8)
O2-Sn-N3	151.1(2)	C4-C5-C6	118.4(9)
O2-Sn-N4	140.3(2)	C5-C6-C7	121.0(9)
O2-Sn-N5	71.5(2)	C6-C7-C8	118.3(8)
N3-Sn-N4	68.6(2)	N4-C8-C7	121.1(8)
N3-Sn-N5	137.3(2)	N4-C8-C9	114.8(8)
N4-Sn-N5	68.9(2)	C7-C8-C9	124.0(8)
Sn-O1-C1	118.3(5)	N5-C9-C8	113.1(7)
Sn-O2-C11	119.1(6)	N5-C9-C10	124.5(8)
Sn-N3-N2	112.5(5)	C8-C9-C10	122.4(8)
Sn-N3-C2	123.3(5)	O2-C11-N6	120.2(8)
N2-N3-C2	124.1(7)	O2-C11-N7	122.1(9)
Sn-N4-C4	119.6(5)	N6-C11-N7	117.7(8)
Sn-N4-C8	119.9(6)		

Table 2-6. Bond Distances(Å) and Angles(°) for II

Ti - Cl1	2.322(4)	C4 - C5	1.377(16)
Ti - Cl2	2.316(4)	C5 - C6	1.368(24)
Ti - O1	1.982(7)	C6 - C7	1.40(3)
Ti - O2	1.983(7)	C7 - C8	1.346(20)
Ti - N2	2.179(9)	C8 - C9	1.442(22)
Ti - N3	2.205(9)	C9 - C10	1.486(22)
Ti - N4	2.188(9)	C11 -CB1	1.498(18)
O1 - C1	1.298(12)	CA1 - CA2	1.374(15)
O2 - C11	1.320(14)	CA1 - CA6	1.378(15)
N1 - N2	1.361(13)	CA2 - CA3	1.413(15)
N1 - C1	1.336(14)	CA3 - CA4	1.354(18)
N2 - C2	1.295(14)	CA4 - CA5	1.376(19)
N3 - C4	1.373(17)	CA5 - CA6	1.377(16)
N3 - C8	1.351(16)	CB1 - CB2	1.386(17)
N4 - N5	1.377(16)	CB1 - CB6	1.378(20)
N4 - C9	1.289(17)	CB2 - CB3	1.38(3)
N5 - C11	1.296(17)	CB3 - CB4	1.39(3)
C1 - CA1	1.464(14)	CB4 - CB5	1.42(3)
C2 - C3	1.459(19)	CB5 - CB6	1.349(20)
C2 - C4	1.463(16)		

Cl1-Ti-Cl2	169.9(2)	N1-C1-CA1	118.8(9)
Cl1-Ti-O1	95.0(2)	N2-C2-C3	126.5(11)
Cl1-Ti-O2	93.9(2)	N2-C2-C4	113.8(10)
Cl1-Ti-N2	88.1(3)	C3-C2-C4	119.8(10)
Cl1-Ti-N3	85.2(2)	N3-C4-C2	112.4(9)
Cl1-Ti-N4	88.4(3)	N3-C4-C5	121.9(12)
Cl2-Ti-O1	93.8(2)	C2-C4-C5	125.7(12)
Cl2-Ti-O2	93.0(2)	C4-C5-C6	116.7(14)
Cl2-Ti-N2	89.9(3)	C5-C6-C7	122.4(12)
Cl2-Ti-N3	84.7(2)	C6-C7-C8	117.6(13)
Cl2-Ti-N4	86.6(3)	N3-C8-C7	122.1(14)
O1-Ti-O2	77.0(3)	N3-C8-C9	112.6(11)
O1-Ti-N2	71.4(3)	C7-C8-C9	125.3(13)
O1-Ti-N3	141.2(3)	N4-C9-C8	114.7(11)
O1-Ti-N4	149.3(4)	N4-C9-C10	122.1(17)
O2-Ti-N2	148.4(3)	C8-C9-C10	123.3(15)
O2-Ti-N3	141.7(3)	O2-C11-N5	122.2(11)
O2-Ti-N4	72.3(4)	O2-C11-CB1	118.3(11)
N2-Ti-N3	69.8(4)	N5-C11-CB1	119.5(11)
N2-Ti-N4	139.3(4)	C1-CA1-CA2	120.0(9)
N3-Ti-N4	69.4(4)	C1-CA1-CA6	121.4(9)
Ti-O1-C1	121.1(6)	CA2-CA1-CA6	118.6(9)
Ti-O2-C11	119.7(7)	CA1-CA2-CA3	121.2(10)
N2-N1-C1	107.9(8)	CA2-CA3-CA4	118.1(11)
Ti-N2-N1	118.2(7)	CA3-CA4-CA5	121.7(10)

Table 2-6 (cont.)

Ti-N2-C2	123.7(8)	CA4-CA5-CA6	119.4(11)
N1-N2-C2	118.1(9)	CA1-CA6-CA5	121.0(11)
Ti-N3-C4	120.2(7)	C11-CB1-CB2	117.9(12)
Ti-N3-C8	120.6(9)	C11-CB1-CB6	119.7(10)
C4-N3-C8	119.2(10)	CB2-CB1-CB6	122.3(12)
Ti-N4-N5	116.3(7)	CB1-CB2-CB3	117.0(14)
Ti-N4-C9	122.6(10)	CB2-CB3-CB4	122.1(14)
N5-N4-C9	121.1(11)	CB3-CB4-CB5	118.4(14)
N4-N5-C11	109.5(10)	CB4-CB5-CB6	119.8(15)
O1-C1-N1	121.2(9)	CB1-CB6-CB5	120.3(12)
O1-C1-CA1	120.0(9)		

Table 2-7. Bond Distances(Å) and Angles(°) for III

Cu - Cl1	2.270(2)	N4 - N5	1.378(9)
Cu - W1	1.996(7)	N4 - C10	1.300(10)
Cu - O1	2.264(5)	N5 - C12	1.367(10)
Cu - O2	2.280(5)	C1 - C2	1.501(14)
Cu - N2	2.216(6)	C3 - C4	1.491(13)
Cu - N3	2.250(6)	C3 - C5	1.466(12)
Cu - N4	2.239(6)	C5 - C6	1.400(12)
O1 - C12	1.217(9)	C6 - C7	1.360(16)
O2 - C1	1.213(10)	C7 - C8	1.371(15)
N1 - N2	1.381(9)	C8 - C9	1.395(11)
N1 - C1	1.377(11)	C9 - C10	1.490(11)
N2 - C3	1.299(10)	C10 - C11	1.476(12)
N3 - C5	1.337(10)	C12 - C13	1.491(12)
N3 - C9	1.332(10)		

Cl1-Cu-W1	177.5(2)	C3-C5-C6	125.1(8)
N2-N1-C1	114.4(6)	C5-C6-C7	118.7(8)
N1-N2-C3	121.0(6)	C6-C7-C8	121.5(8)
C5-N3-C9	122.6(6)	C7-C8-C9	118.2(9)
N5-N4-C10	120.4(6)	N3-C9-C8	119.8(7)
N4-N5-C12	114.2(6)	N3-C9-C10	116.0(6)
O2-C1-N1	121.7(7)	C8-C9-C10	124.2(8)
O2-C1-C2	123.5(9)	N4-C10-C9	112.0(7)
N1-C1-C2	114.8(8)	N4-C10-C11	126.1(8)
N2-C3-C4	125.4(9)	C9-C10-C11	121.9(8)
N2-C3-C5	113.3(7)	O1-C12-N5	121.4(7)
C4-C3-C5	121.3(8)	O1-C12-C13	123.8(7)
N3-C5-C3	115.7(7)	N5-C12-C13	114.8(7)
N3-C5-C6	119.2(8)		

Table 2-8. U values *100 for I.
E.S.Ds. refer to the last digit printed

	U11(σ)	U22	U33	U12	U13	U23
Sn	2.81(3)	2.78(3)	2.09(3)	-.21(3)	.41 (2)	-.09 (2)
Cl1	4.89(14)	3.33(12)	4.31(13)	.23(10)	.30 (10)	.72 (10)
Cl2	4.13(13)	3.71(12)	4.15(12)	.78(10)	.74 (10)	.81 (10)
O1	2.6 (3)	5.0 (4)	2.6 (3)	-.8 (3)	.75 (23)	-.6 (3)
O2	4.0 (4)	4.5 (4)	2.6 (3)	-1.0 (3)	.5 (3)	-.6 (3)
N1	4.5 (5)	5.6 (5)	3.3 (4)	-.4 (4)	1.3 (4)	-.3 (4)
N2	2.1 (4)	4.4 (4)	3.3 (4)	-.0 (3)	.6 (3)	-.9 (3)
N3	1.8 (3)	3.5 (4)	2.9 (3)	.3 (3)	.2 (3)	-.1 (3)
N4	2.0 (3)	3.3 (4)	2.6 (3)	.3 (3)	.3 (3)	.5 (3)
N5	3.2 (4)	2.8 (4)	2.4 (3)	-.1 (3)	.5 (3)	.0 (3)
N6	4.9 (5)	3.6 (4)	2.2 (4)	-.4 (4)	.8 (3)	-.9 (3)
N7	4.5 (5)	5.1 (5)	3.0 (4)	-1.0 (4)	.3 (4)	1.0 (4)
C1	3.3 (5)	3.5 (5)	3.0 (4)	.0 (4)	.9 (4)	1.0 (4)
C2	3.8 (5)	3.2 (5)	2.8 (4)	.7 (4)	-.1 (4)	-.2 (4)
C3	4.2 (6)	6.4 (8)	3.8 (6)	-.7 (6)	-.0 (5)	-1.4 (5)
C4	2.4 (4)	2.8 (4)	3.3 (4)	-.4 (4)	-.7 (3)	.2 (4)
C5	2.9 (5)	4.3 (5)	3.9 (5)	-.8 (4)	-.5 (4)	.5 (4)
C6	2.9 (5)	5.0 (6)	4.8 (5)	-.5 (4)	.1 (4)	1.3 (5)
C7	3.0 (5)	4.6 (6)	3.8 (5)	.5 (4)	1.0 (4)	.8 (4)
C8	3.8 (5)	3.1 (5)	2.7 (4)	.5 (4)	.7 (4)	.6 (3)

Table 2-8. (cont.).

	U11(σ)	U22	U33	U12	U13	U23
C9	3.5 (5)	2.6 (4)	2.8 (4)	.6 (4)	.7 (3)	.7 (3)
C10	4.5 (6)	3.9 (6)	3.3 (5)	.2 (5)	1.8 (4)	-.2 (4)
C11	4.2 (5)	2.5 (4)	2.7 (4)	.0 (4)	-.3 (4)	-.1 (3)
W1	5.5 (5)	6.1 (5)	5.8 (5)	-.7 (4)	1.0 (4)	.4 (4)
W2	7.2 (6)	9.2 (7)	8.2 (6)	.8 (6)	1.5 (5)	-2.5 (5)
C13	5.85(16)	6.62(17)	3.07(12)	1.05(14)	-.25 (11)	-1.46 (11)
C14	6.85(17)	4.51(13)	3.68(12)	1.18(13)	1.83 (11)	1.32 (11)

Anisotropic Temperature Factors are of the form --
Temp=-2*Pi*Pi*(h*h*u11*astar*astar+---+2*h*k*u12*astar*bstar+---)

Table 2-9. U values *100 for II.
E.S.Ds. refer to the last digit printed

	U11(σ)	U22	U33	U12	U13	U23
Ti	4.4 (1)	5.3 (1)	4.6 (1)	-.3 (1)	.17(9)	-.5 (1)
Cl1	5.4 (2)	7.1 (2)	8.0 (2)	1.1 (2)	-.01(16)	-2.1 (2)
Cl2	8.2 (2)	5.1 (2)	6.4 (2)	-.4 (2)	2.4 (2)	-.5 (2)
O1	5.6 (5)	5.8 (5)	4.0 (4)	-1.3 (4)	.2 (4)	.3 (4)
O2	4.9 (5)	5.9 (5)	3.9 (4)	-.1 (4)	-.3 (4)	.2 (4)
N1	5.5 (6)	6.9 (7)	4.5 (6)	-1.3 (6)	-.2 (5)	.1 (5)
N2	5.7 (6)	5.5 (6)	4.7 (6)	-.9 (5)	1.0 (5)	.0 (5)
N3	3.2 (5)	4.5 (6)	7.3 (7)	-.6 (4)	.2 (5)	-2.1 (5)
N4	5.6 (7)	6.4 (7)	5.3 (6)	1.4 (6)	.3 (5)	-.7 (5)
N5	6.9 (7)	6.5 (7)	5.4 (6)	1.6 (6)	.3 (6)	-.9 (6)
C1	5.0 (7)	4.3 (7)	4.2 (7)	-1.0 (6)	1.0 (6)	-.3 (5)
C2	4.4 (7)	4.0 (6)	6.6 (8)	-.8 (6)	1.6 (6)	-.2 (6)
C3	7.3 (9)	7.3 (10)	7.7 (11)	-3.6 (8)	2.2 (8)	-2.6 (9)
C4	4.5 (7)	3.7 (6)	8.4 (9)	-.8 (6)	1.6 (6)	-1.6 (6)
C5	5.4 (8)	5.2 (8)	12.0 (12)	-1.6 (7)	3.2 (8)	-.4 (8)
C6	2.9 (8)	9.9 (13)	16.4 (17)	-.7 (8)	2.6 (10)	-2.4 (12)
C7	3.1 (8)	7.6 (10)	13.1 (14)	.9 (7)	-.2 (8)	-2.6 (10)
C8	6.2 (9)	4.5 (7)	8.0 (9)	.9 (7)	.8 (7)	-1.8 (7)
C9	4.3 (8)	7.9 (10)	7.9 (10)	1.7 (7)	-1.1 (7)	-3.2 (8)
C10	5.4 (11)	9.8 (15)	10.2 (13)	2.7 (9)	-3.4 (9)	-2.0 (11)

Table 2-9 (cont.).

	U11(σ)	U22	U33	U12	U13	U23
C11	6.0 (8)	5.7 (8)	5.0 (7)	1.7 (7)	.7 (6)	-1.3 (6)
CA1	4.7 (6)	3.5 (6)	4.1 (6)	-.6 (5)	.5 (5)	.2 (5)
CA2	4.1 (7)	8.2 (9)	4.3 (7)	-.1 (6)	.9 (5)	.5 (6)
CA3	4.6 (7)	10.1 (11)	5.8 (8)	-2.9 (7)	1.0 (6)	-.7 (8)
CA4	4.4 (7)	9.9 (11)	6.1 (9)	-1.7 (7)	-1.2 (6)	.3 (8)
CA5	7.8 (10)	8.3 (10)	5.8 (8)	-1.7 (8)	-1.2 (7)	2.0 (7)
CA6	3.9 (7)	7.2 (9)	6.2 (8)	-1.1 (6)	-.2 (6)	2.0 (7)
CB1	7.6 (9)	4.9 (7)	4.3 (7)	.7 (7)	1.1 (6)	.3 (6)
CB2	10.3 (11)	7.5 (9)	5.3 (8)	3.1 (9)	.9 (8)	1.9 (7)
CB3	15.9 (18)	10.0 (13)	5.9 (10)	2.6 (13)	2.2 (12)	1.7 (9)
CB4	18.5 (19)	6.2 (10)	9.4 (14)	1.7 (13)	8.3 (14)	1.8 (10)
CB5	11.3 (12)	5.6 (9)	9.4 (12)	-.2 (9)	4.0 (10)	.5 (8)
CB6	10.1 (11)	5.0 (8)	4.8 (8)	-.2 (8)	2.6 (8)	.2 (6)

Anisotropic Temperature Factors are of the form --

Temp=-2*Pi*Pi*(h*h*u11*astar*astar+---+2*h*k*u12*astar*bstar+---)

Table 2-10. U values *100 for III.
E.S.Ds. refer to the last digit printed

	U11(σ)	U22	U33	U12	U13	U23
Cu	4.36(7)	2.95(6)	3.20(6)	.26(6)	.85(5)	-.10(5)
C11	5.7 (1)	5.2 (1)	5.1 (1)	-.1 (1)	.7 (1)	-.4 (1)
C12	9.3 (2)	8.2 (2)	4.5 (1)	.1 (2)	1.6 (1)	-.7 (1)
W1	5.8 (4)	5.0 (4)	4.9 (4)	1.6 (3)	1.7 (3)	-.8 (3)
W2	10.2 (6)	12.3 (11)	8.9 (9)	.7 (10)	3.5 (7)	-3.0 (11)
W3	7.2 (5)	4.8 (4)	11.8 (7)	.5 (4)	4.6 (5)	.4 (4)
O1	6.8 (4)	3.5 (3)	3.6 (3)	.2 (3)	2.2 (3)	.28(25)
O2	7.0 (4)	4.2 (3)	4.1 (3)	.3 (3)	2.5 (3)	-.1 (3)
N1	5.1 (4)	5.1 (4)	3.4 (4)	-.4 (4)	1.1 (3)	-.4 (3)
N2	4.4 (4)	4.1 (4)	3.4 (3)	-.1 (3)	.4 (3)	-.5 (3)
N3	4.8 (4)	2.5 (3)	4.5 (4)	.2 (3)	.1 (3)	-.3 (3)
N4	4.8 (4)	3.2 (4)	3.5 (3)	.1 (3)	.6 (3)	.2 (3)
N5	5.7 (4)	4.1 (4)	3.1 (4)	.6 (3)	1.7 (3)	.1 (3)
C1	4.5 (5)	4.7 (5)	3.7 (5)	-.2 (4)	.5 (4)	.3 (4)
C2	5.8 (7)	7.4 (7)	6.1 (7)	-.9 (7)	1.4 (7)	1.5 (5)
C3	3.6 (5)	4.8 (6)	4.7 (5)	.8 (4)	.1 (4)	-1.2 (4)
C4	8.0 (9)	7.1 (8)	5.2 (6)	1.6 (7)	.8 (6)	-2.4 (6)
C5	4.2 (5)	3.1 (5)	4.8 (5)	.5 (4)	.2 (4)	-.9 (4)
C6	5.1 (6)	3.8 (6)	6.8 (7)	.8 (4)	.5 (5)	-1.9 (5)
C7	6.4 (6)	2.0 (4)	8.5 (7)	.2 (5)	.0 (5)	-.5 (5)

Table 2-10 (cont.).

	U11(σ)	U22	U33	U12	U13	U23
C8	5.3 (6)	3.4 (5)	6.8 (7)	-.2 (4)	.5 (5)	1.2 (5)
C9	4.2 (5)	3.1 (5)	4.2 (5)	-.3 (4)	-.2 (4)	.1 (4)
C10	4.4 (5)	4.0 (5)	3.9 (5)	-.4 (4)	.2 (4)	.4 (4)
C11	9.4 (9)	4.7 (6)	5.0 (6)	-1.1 (6)	1.8 (6)	1.1 (5)
C12	4.6 (5)	3.5 (5)	3.6 (5)	.4 (4)	.7 (4)	.2 (4)
C13	6.8 (7)	5.2 (6)	4.6 (6)	1.6 (5)	2.1 (5)	.4 (5)

Anisotropic Temperature Factors are of the form --

Temp=-2*Pi*Pi*(h*h*u11*astar*astar+---+2*h*k*u12*astar*bstar+---)

Table 2-11. Hydrogen Atomic Parameters x,y,z and Biso for I. E.S.Ds. refer to the last digit printed.

	x/a		y/b		z/c		Biso
H1(N1)	.397	(12)	.910	(8)	.339	(6)	3.2
H2(N1)	.489	(11)	.955	(7)	.385	(5)	3.2
H3(N2)	.711	(11)	1.017	(7)	.368	(5)	3.2
H4(C3)	.956	(11)	1.026	(8)	.405	(6)	3.2
H5(C3)	1.092	(12)	1.014	(7)	.373	(5)	3.2
H6(C3)	1.013	(11)	1.110	(8)	.349	(5)	3.2
H7(C5)	1.209	(11)	1.047	(7)	.261	(6)	3.2
H8(C6)	1.355	(11)	1.007	(7)	.154	(5)	3.2
H9(C7)	1.238	(11)	.914	(7)	.051	(5)	3.2
H10(C10)	1.072	(12)	.865	(8)	-.063	(6)	3.2
H11(C10)	.931	(11)	.811	(7)	-.096	(6)	3.2
H12(C10)	1.030	(11)	.756	(8)	-.046	(5)	3.2
H13(N6)	.742	(11)	.774	(8)	-.055	(6)	3.2
H14(N7)	.483	(12)	.728	(8)	-.073	(6)	3.2
H15(N7)	.395	(12)	.720	(8)	-.009	(6)	3.2
H16(W1)	.694	(12)	.847	(8)	.556	(6)	3.2
H17(W1)	.741	(11)	.921	(8)	.512	(6)	3.2

Biso is the Mean of the Principal Axes of the Thermal Ellipsoid

Table 2-12. Hydrogen Atomic Parameters x,y,z and Biso for II. E.S.Ds. refer to the last digit printed.

	x/a		y/b		z/c		Biso
H1(C3)	.144	(13)	.357	(8)	.401	(5)	4.7
H2(C3)	.011	(12)	.374	(8)	.402	(5)	4.7
H3(C3)	.017	(12)	.262	(8)	.382	(5)	4.7
H4(N1)	.265	(12)	.510	(8)	.370	(5)	4.7
H5(C6)	-.264		.314		.314		4.7
H6(C6)	-.491		.336		.220		4.7
H7(C7)	-.470		.438		.127		4.7
H8(C10)	-.361	(17)	.564	(10)	.041	(8)	4.7
H9(C10)	-.349	(12)	.471	(8)	.022	(5)	4.7
H10(C10)	-.288	(13)	.570	(8)	-.002	(5)	4.7
H11(CA2)	.607		.618		.281		4.7
H12(CA3)	.868		.662		.352		4.7
H13(CA4)	.936		.600		.465		4.7
H14(CA5)	.767		.482		.507		4.7
H15(CA6)	.509		.442		.439		4.7
H16(CB2)	.033		.690		-.039		4.7
H17(CB3)	.177		.785		-.115		4.7
H18(CB4)	.453		.829		-.079		4.7
H19(CB5)	.597		.774		.036		4.7
H20(CB6)	.446		.693		.111		4.7

Biso is the Mean of the Principal
Axes of the Thermal Ellipsoid

Table 2-13. Hydrogen Atomic Parameters x,y,z and Biso for III. E.S.Ds. refer to the last digit printed.

	x/a	y/b	z/c	Biso
H1(C2)	.362	.493	-.179	4.7
H2(C2)	.531	.465	-.161	4.7
H3(N1)	.461	.275	-.188	4.7
H4(C4)	.347	.096	-.204	4.7
H5(C4)	.517	.088	-.184	4.7
H6(C4)	.381	.001	-.174	4.7
H7(C6)	.340	-.064	-.083	4.7
H8(C7)	.247	-.150	.005	4.7
H9(C8)	.141	-.061	.092	4.7
H10(C11)	-.054	.097	.185	4.7
H12(C11)	.113	.031	.182	4.7
H13(C11)	.120	.127	.220	4.7
H14(N5)	.022	.215	-.317	4.7
H15(C13)	.138	.509	.170	4.7
H16(C13)	-.028	.454	.195	4.7
H17(C13)	-.041	.503	.134	4.7
H18(W1)	-.041	.297	-.045	4.7
H19(W1)	.005	.275	-.096	4.7
H20(W2)	.568	.293	.700	4.7
H21(W2)	.569	.235	.745	4.7
H22(W3)	.664	.370	.005	4.7
H23(W3)	.750	.384	.034	4.7

Biso is the Mean of the Principal
Axes of the Thermal Ellipsoid

Results and Discussion

Sn(DAPSC)Cl_2^{2+} The crystals were found to contain monomeric Sn(DAPSC)Cl_2^{2+} cations and display PBP geometry which is easily seen in Figure 2-1. Surprisingly, the complex was obtained from aqueous solution and is very water soluble since all related compounds[19-21] were isolated from organic media. Oxidation of Sn^{2+} to Sn^{4+} is known[21] to occur in aqueous solutions exposed to the air and has been observed to occur in a structurally similar complex[19]. Indeed, a similar oxidation has occurred in this instance. As noted above, a fine black precipitate fell out as the solution cleared, which suggests that a reduction of the Pt^{2+} starting material to Pt^0 occurred. Whether or not this was a direct result of the Sn oxidation is not clear. This is the first example of a metal oxidation taking place in the presence of DAPSC and being stabilized by the ligand. DAPSC tends to have a more reducing nature as is observed in the Fe^{2+} and Co^{2+} systems[6].

Compounds such as $(CH_3NH)_3[Pt(SnCl_3)_5]$ and Pt(II)/Sn(II) mixtures have been of interest for some time due to the observed capability of these species to homogeneously catalyze the hydroformylation, carbonylation, and hydrogenation reactions[22]. Common to most of the discussion regarding possible mechanisms for these reactions is the postulated presence of free $SnCl_3^-$ ions in solution liberated by ligand dissociation. The $[Pt(SnCl_3)_5]^{3-}$ species has long-term

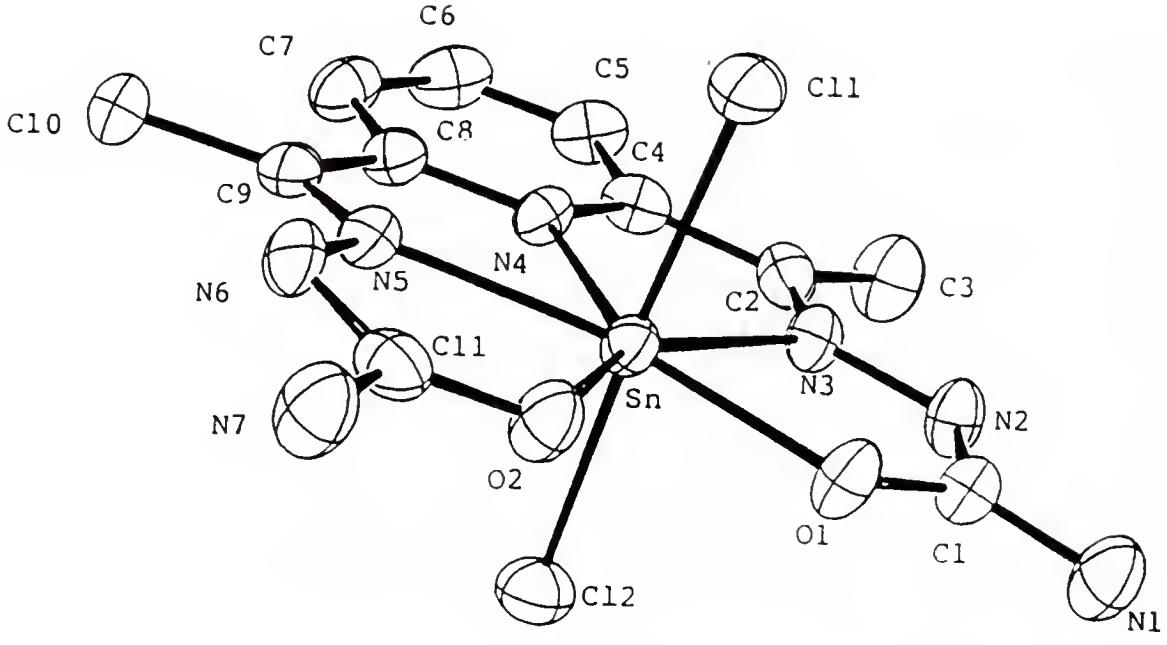

Figure 2-1. An ORTEP representation of $Sn(DAPSC)Cl_2^{2+}$

stability in the presence of protic solvents, although in HCl solutions metallic Pt is slowly precipitated[23] as we also observed. Hence, in a HCl solution of $(CH_3NH)_3[Pt(SnCl_3)_5]$ with pH = 1.00 the concentration of free $SnCl_3^-$ is probably quite high and the likely source of the Sn atom for coordination by DAPSC. Attempts to prepare the title complex in good yield directly from $SnCl_2 \cdot 2H_2O$ and DAPSC in HCl and methanol/H_2O solutions failed even when excess halide was added in the form of KCl which promotes[24] the formation of $SnCl_3^-$.

The geometry about the Sn-cation can be described as a slightly distorted pentagonal bipyramid. A slight distortion is apparent in the pentagonal equatorial plane as evidenced by the lengths of the respective sides O1-O2 2.685(7), O1-N3 2.611(8), N3-N4 2.553(9), N4-N5 2.555(9), and N5-O2 2.560(9)Å. The axial chlorides also contribute to the observed distortion since they are not exactly linear and make an angle of 176.94(8)°. A least-squares plane drawn through the five coordinating atoms in the equatorial girdle shows little deviation from planarity with the average of the deviations being 0.034(7)Å. The Sn ion can be considered to lie in the equatorial plane since it deviates only 0.019(3)Å out of the plane made by the five equatorial donors. Dimensions within the neutral ligand are similar to those observed in related structures with no irregularities. There is evidence of

several hydrogen-bonds with in the asymmetric unit. Most notable are the interactions between N2 - Cl4, N6 - Cl3, and N7 - W1 with distances (H ••• Cl) of 2.053(10), 2.289(10), and 1.863(10)Å with bond angles of 152(1), 143(1), and 156(1)° respectively.

The two Sn - Cl distances appear to be significantly different, t_o = 4.09[25], although they appear to be chemically equivalent. However an analysis of the various intermolecular contacts involving Cl1 and Cl2 indicates that the two Cl atoms have slightly different environments which could account for the small but significant difference. The Sn - Cl distances are slightly shorter than that of 2.395(7) and 2.387(7)Å found in $[Sn(dappc)Cl_2]^{2+}$ [20]. However the Sn - O and Sn -N distances are slightly longer than in the $[Sn(dappc)Cl_2]^{2+}$ complex which suggests that the Sn - Cl distance may be influenced by non bonded interactions. The much longer Sn - Cl bond distance of 2.446(3)Å when the trans atom is carbon suggests a trans influence may be operative in Sn compounds. The Sn - Cl distance of 2.362(4)Å in tris(tropolonato)monochlorotin(IV) chloroform solvate[26] would support this view. Unfortunately, there are not a sufficient number of seven-coordinate Sn(IV) complexes for a detailed comparison.

It has been suggested[27] that tin in a seven-coordinate environment prefers pentagonal bipyramidal geometry; however,

our result may be attributed to the planar pentadentate nature of the ligand rather than any stereochemical preference by the metal[3].

Ti(DAPBAH)Cl_2 The pentagonal bipyramidyl nature of this complex is easily seen in Figure 2-2. With the isolation of this complex, there are now examples of each of the first row transition metals (Sc - Zn) in PBP geometry coordinated in part by planar pentadentate ligands. Seven coordinate Ti complexes are known though most involve combinations of mono- and bidentate ligands to arrive at a coordination number of seven. This complex is unique in that a pentadentate ligand has been used.

Preliminary experiments demonstrated that DAPSC does indeed react with $TiCl_3$, however crystalline products were never evident in any of the reaction mixtures. Combining our experience from previous experiments which have shown that DAPSC works best in aqueous or semiaqueous solution together with the fact that $TiCl_3$ is extremely sensitive to water suggested that neither this ligand or this solvent system would be favorable for an attempt to obtain a PBP complex of Ti^{3+}. However, due to the high solubility of benzoic acid hydrazide in organic media, the ligand DAPBAH emerged as a better choice and the best of the three pentadentate ligands to use for a reaction with Ti^{3+}.

The ligand DAPBAH is not as soluble in pure ethanol as

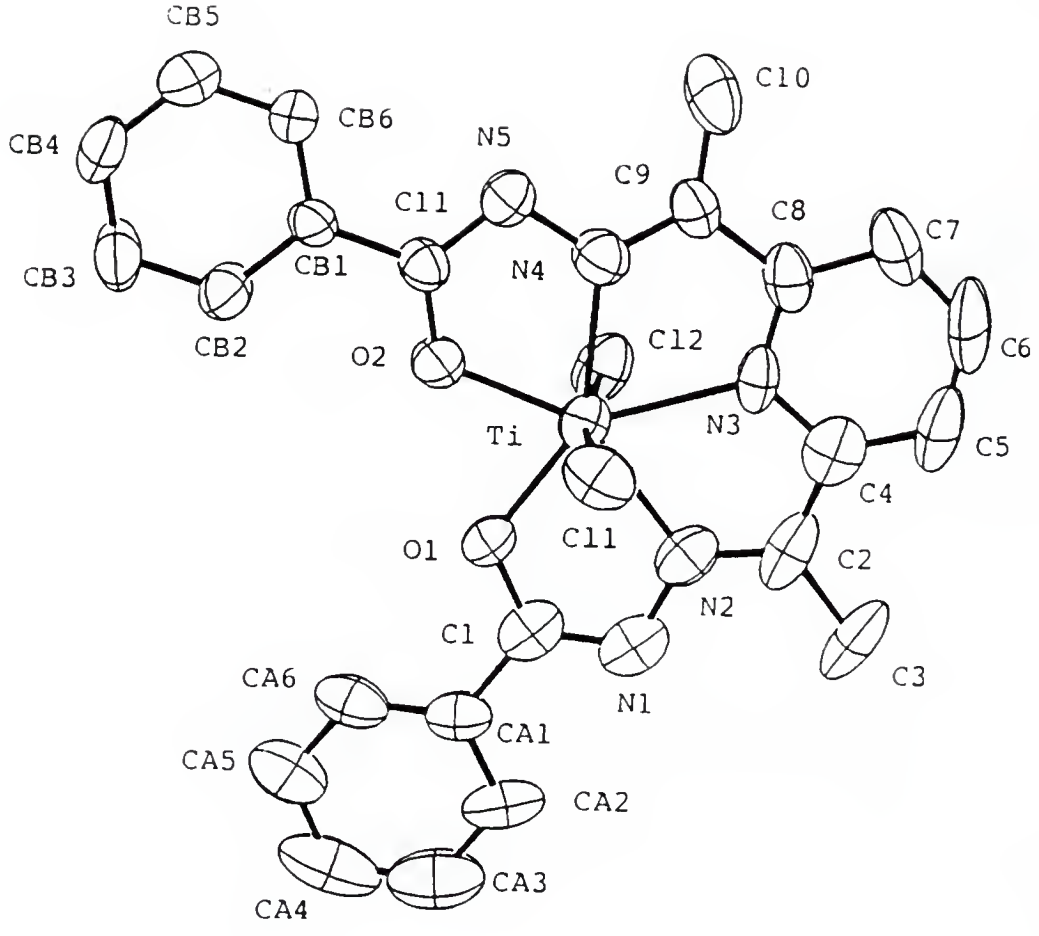

Figure 2-2. An ORTEP representation of $Ti(DAPBAH)Cl_2$

are 2,6-diacetylpyridine and benzoic acid hydrazide separately. Consequently, the complex had to be prepared by a template type reaction rather than by combining the ligand directly with Ti^{3+}. Although two equivalents of water were produced in the reaction forming the Schiff base ligand, no deleterious results were detected in the course of the reaction.

The Ti-cation can be described as being at the center of a distorted pentagonal bipyramid with distortions occurring in both the equatorial plane and axial positions. The distortion observed in the equatorial plane has two contributions: first and foremost is the formation of a monoanion resulting from the deprotonation of the ligand at N1. Upon deprotonation, the entire side of the ligand becomes conjugated as well as negatively charged. The 3^+ center now has a stronger attraction to this side of the ligand as is evidenced in the shorter Ti-N2 bond of 2.179(9)Å verses the Ti-N4 bond of 2.188(9)Å. Similarly, the distance between O1 and N2 in the pentagonal plane is 2.434(9)Å verses a distance of 2.188(9)Å from O2 to N4. The shorter side reflects a contraction in that "arm" of the ligand due to the conjugation and increased attraction towards the cationic center. The second contribution to the distortion is a minor Jahn-Teller effect due to the degeneracy of the possible electron configurations for a d^1 species in a PBP field. Since the orbitals

potentially occupied by the single d-electron are not strongly bonding, the distortion resultant from this effect is small. Distortions due to the Jahn-Teller effect and the formation of monoanions in these types of complexes will be examined at length and in greater detail in chapter four.

An angle of 169.86(15)°, significantly less than the expected 180°, is made by the atoms Cl1 - Ti - Cl2. Since there appears to be no other intermolecular contacts between the axial Cl^-s and other molecules in the asymmetric unit, the distortion must be the result of an intermolecular electronic effect. Pentadentate ligands of this type are known to have some inherent flexibility especially between the "arms". This complex provides an excellent example of this as illustrated by the deviations of O1 and O2 from the least squares plane calculated for Ti, N2, N3, and N4. All four of these atoms show deviations of less than 0.002(9)Å but O1 deviates +0.051(8)Å and O2 deviates -0.010(8)Å. In essence, DAPBAH has twisted slightly with one oxygen moving up and the other down perpendicular to the equatorial plane. The electronic effects from the two oxygens is the most likely contributor to the axial distortion since the associated electron density would repel the axial chloride ions to some degree.

<u>Cu(DAPAAH)(H_2O)Cl</u>$^+$ The crystals were found to contain monomeric Cu(DAPAAH)(H_2O)Cl^+ cations which display PBP geometry as can be seen in Figure 2-3. Although the axial ligands

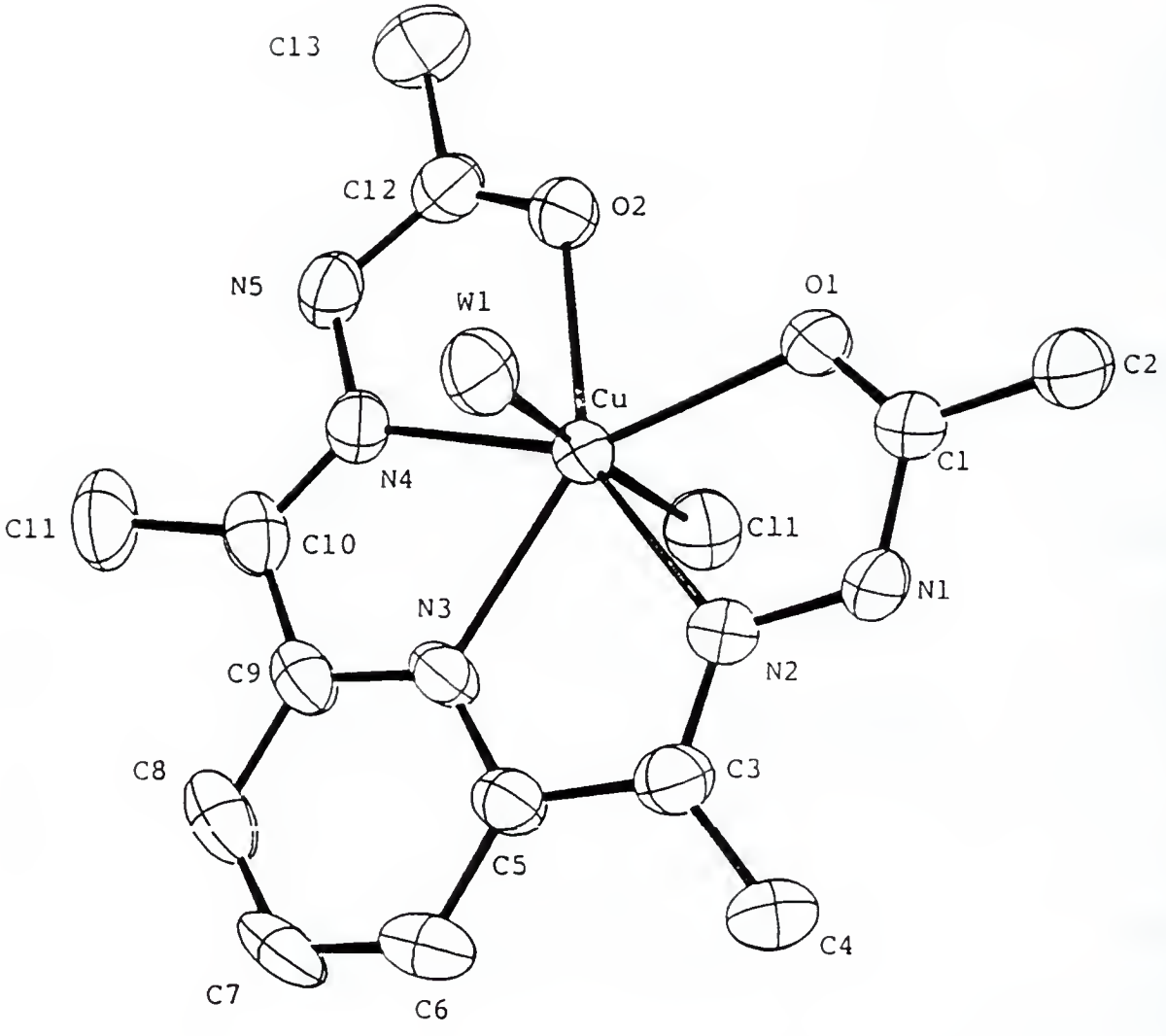

Figure 2-3. An ORTEP representation of Cu(DAPAAH)Cl(H_2O)$^+$

differ (i.e. one Cl^- and one H_2O) there appears to be no disorder occurring. The geometry about the Cu-cation can be described as being a somewhat disordered pentagonal bipyramid. The distortion is apparent in the pentagonal equatorial plane as evidenced by the length of the O1-O2 side being 2.921(7)Å while the other four sides average length is 2.574(8)Å ± 0.022(8). This distortion apparently does not affect the planarity of the equatorial plane since a least-squares plane drawn through the five coordinating atoms comprising the equatorial plane shows that there is little deviation from planarity with average deviations of 0.031(8)Å out of the plane for the five equatorial atoms. The Cu ion can be considered to lie in the equatorial plane since it deviates only 0.061(3)Å out of the plane.

The bond lengths exhibited both within the coordination sphere and throughout the ligand are very nearly the same as those found in the previously reported $[Cu(DAPSC)Cl(H_2O)]^+$ complex[16]. The major difference is found in the replacement of an axial Cl^- with a H_2O molecule. An uncoordinated Cl^- is closely associated with the cation through a hydrogen bond to the axial H_2O with a O-H $\cdots$ Cl distance of 2.30(3)Å. There also appears to be some interaction between the two uncoordinated H_2O molecules found in the asymmetric unit and the axial Cl^- with the closest contact being a hydrogen bond between W3 and Cl1 with a O-H $\cdots$ Cl distance of 2.20(3)Å.

Attempts to isolate IV by a similar method to the aforementioned complex ($[Cu(DAPSC)Cl(H_2O)]^+$) from a pure aqueous solution failed due to the insolubility of the 2,6-diacetylpyridine. In other experiments where the DAPAAH ligand was prepared separately and then reacted with the Cu ion, solubility problems were again encountered in pure aqueous media though upon the addition of either ethanol or methanol to the aqueous solution, the reaction appeared to progress rapidly and clear dark green solutions were obtained. The $Cu(DAPAAH)ClH_2O^+$ crystals were found to be much more soluble in ethanol, methanol and ethanol/water solutions than in pure H_2O. This observations suggest that the methyl groups directed outward from the complex have an effect to some extent on the solubility of this complex.

CHAPTER 3

A NOVEL PENTAGONAL BIPYRAMIDAL IRON COMPOUND: UNCONNECTED Fe(II) AND Fe(III) MOLECULES WITHIN THE SAME ASYMMETRIC UNIT.

Introduction

In the preceding chapter it was noted that the ligand DAPSC reacts with all the metals of the first transition series and that in each case the result has usually been the formation of seven-coordinate complexes displaying PBP geometry. A particularly interesting system which we have come upon in this series is that of the iron-DAPSC complexes.

Fe(II)[7] and Fe(III)[9] cations coordinated by DAPSC have been isolated and structurally characterized by means of X-ray structure studies. Both compounds were obtained from the same reaction mixture. However, in addition to these two compounds, a third product was isolated from the same reaction mixture which appeared to have a different crystal habit than the two compounds previously characterized. In order to determine the composition of the third product, an investigation of the crystal structure by means of an X-ray analysis was undertaken.

Previous attempts at determining the structure of this product were unsuccessful. Thus, a more detailed experimental

section outlining the crystallographic work is presented in addition to the normal experimental details.

Experimental

Materials. All chemicals were reagent grade and used as supplied.

Preparation of $[Fe(DAPSC)Cl\ H_2O]^{2+/3+}$. DAPSC (0.5546g, 2 mmole) prepared by the method previously described[9] was combined with $FeCl_3 \cdot H_2O$ (0.5406g, 2 mmole) in 50 mL deionized H_2O. The pH was lowered to 1.00 with HCl and stirred for 1.5 hours. A deep red solution resulted which was filtered and allowed to slowly evaporate. After 16 days the product was obtained, the second of two red products. The first red product, the Fe(III)-DAPSC, formed red needles some of which were quite long. The second product was dark red "chunks" which are easily distinguishable from the first red product. No green product (Fe(II)) was visible at this point.

Crystallography. A dark red crystal suitable for an X-ray study having the dimensions 0.18 x 0.21 x 0.25 mm was mounted on the end of a glass fiber. All subsequent measurements were made using a Nicolet R3m diffractometer with graphite-monochromated Mo-Kα radiation (λ = 0.71069Å). The cell dimensions were determined by a least squares refinement of 25 automatically centered reflections in the 2θ range 3.63° - 24.56°. A variable-speed (1° - 29.3°) 2θ scan technique

was used to measure the intensity data from 2.0° to 46.0° degrees in 2θ corresponding to hkl values of 0 to 10, 0 to 18, and -22 to 22 respectively. Two standard reflections were measured every 98 reflections to monitor for any decomposition during the X-ray analysis. No absorption correction was made. There were 2543 unique reflections measured of which 2473 with an Inet > 2.5σ(Inet) were used in the analysis. The density of the compound was found to be 1.68 g/cm^3 by flotation which when taken together with the unit cell volume of 1808.4 Å^3 suggested that there were four molecules per unit cell assuming a molecular weight of ~450 g/mole. From an analysis of the systematic absences, either of the space groups $P2_1$ or $P2_1/m$ were possible though from an evaluation of the intensity statistics P 2_1 appeared to be the best choice. The data reduction, structure solution and final refinement were performed using the NRCVAX (PC-Version)[18] package of programs. The Fe atoms and all non-hydrogen atoms were located by the heavy-atom method (Patterson and Fourier syntheses) and refined anisotropically by full-matrix least squares. The hydrogen atoms were located using a difference Fourier map and refined isotropically. The model converged to an R of 0.036 and a Rw of 0.039. The largest shift/e.s.d. in the last cycle was 0.213. A final difference fourier synthesis had a maximum peak of 0.530 and a minimum peak of -0.560 e Å^{-3} and was featureless.

Results and Discussion

As noted previously, the structural solution for this compound was somewhat involved. The direct method routines of both the SHELXTL[28] and NRCVAX (PC-version)[18] software packages failed to arrive at a reasonable initial solution for this compound. This is often the case when noncentrosymmetric crystals are encountered and caution must be exercised when using "black-box" solving routines in these situations. We were eventually able to arrive at an initial solution for the structure by locating the Fe atoms from a Patterson map though with two heavy atoms in the asymmetric unit, four Fe vectors resulted which had to be properly sorted out. Upon the correct phasing of the Fe atoms, the positions of the remaining non-hydrogen atoms were easily determined from subsequent Fourier syntheses.

The refinement of this model proceeded smoothly and the resulting structural parameters contained nothing irregular or abnormal. To check if any symmetry elements had been overlooked, the program MISSYM which is part of the NRCVAX (PC-version)[18] software package was run using the atomic parameters from the final model. MISSYM checks the structural data and can detect possible missing symmetry which may have been described in the wrong space group. Upon running the program no additional symmetry was detected. This result together with the smooth refinement and intensity statistics

which indicated a noncentrosymmetric structure confirms that $P2_1$ was indeed the correct space group for this structure.

The PBP nature of the two cations is easily seen in Figure 3-1. The final atom coordinates are given in Table 3-1 and bond distances and angles are given in Table 3-2. The final anisotropic thermal parameters are given in Table 3-3 and the final coordinates for the hydrogen atoms are provided in Table 3-4.

The presence of only five anions in the asymmetric unit implies that one Fe-cation is formally 2+ and the other 3+ which is highly unusual indeed. The possibility does exist that an additional anion is present in the form of a deprotonated ligand or water molecule though this is doubtful for several reasons. First the hydrogen atoms bonded to N2, N6, N9, and N13 are known to be acidic and it has been pointed out previously that DAPSC can in fact undergo deprotonation at one of these sites with the semicarbazone arm then acting as monoanion and carrying an overall negative charge[29]. However, all hydrogen atoms associated with the ligand were clearly found in a Fourier difference map, so both ligands are fully protonated and neither has undergone deprotonation. Second, the two coordinated and two uncoordinated H_2O molecules in the asymmetric unit could have undergone deprotonation leaving a OH^- anion, but this is highly unlikely since the compound was isolated from a highly acidic solution.

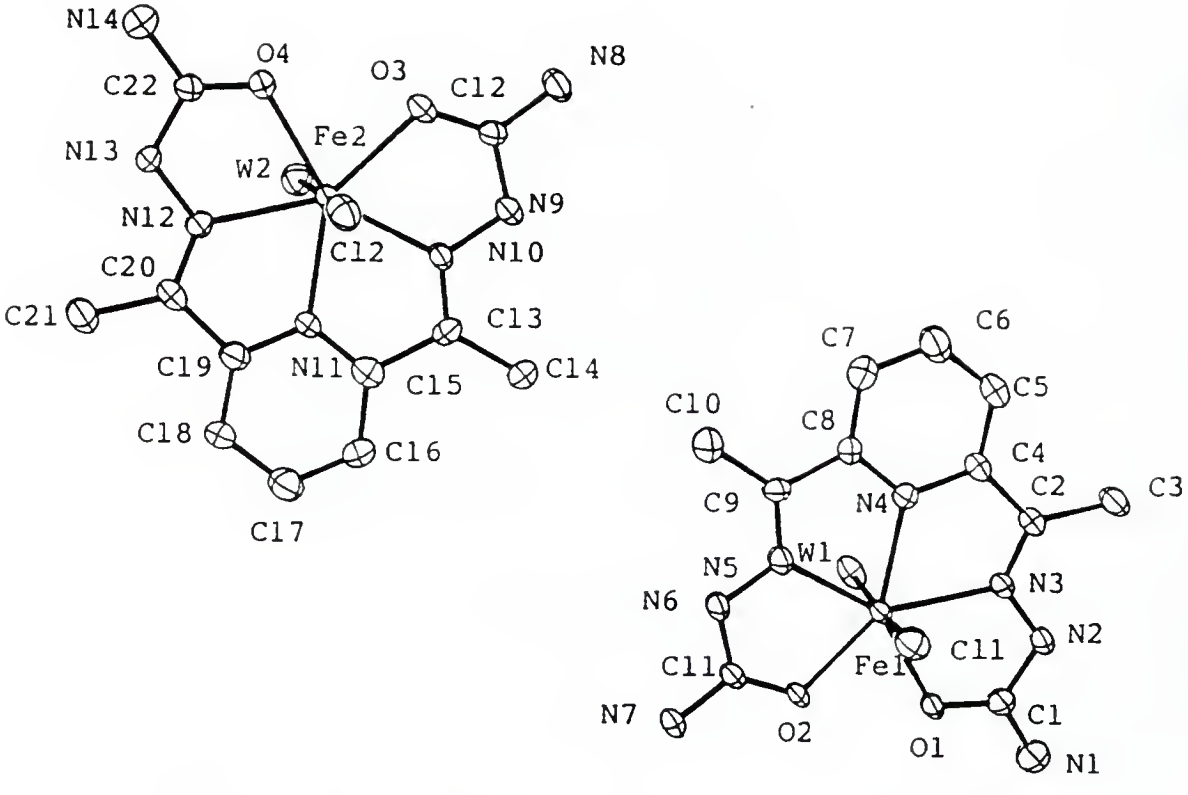

Figure 3-1. An ORTEP representation of the Fe(II/III)-DAPSC complex.

Table 3-1. Atomic Parameters x,y,z and Biso.
E.S.Ds. refer to the last digit printed.

	x	y	z	Biso
Fe1	.1524 (2)	.5000	.4175 (1)	1.8 (4)
Fe2	.7548 (2)	.3115 (1)	1.0514 (1)	1.8 (4)
C11	-.1406 (3)	.5035 (2)	.4685 (1)	2.8 (8)
C12	.4228 (3)	.2893 (1)	1.1062 (1)	2.6 (8)
W1	.4227 (7)	.5049 (4)	.3735 (3)	2.9 (2)
W2	1.0449 (7)	.3208 (4)	1.0112 (3)	2.8 (2)
O1	.0447 (8)	.4731 (3)	.3098 (3)	2.4 (2)
O2	.1719 (8)	.3534 (3)	.4064 (3)	2.2 (2)
O3	.7544 (8)	.4630 (4)	1.0598 (3)	2.6 (2)
O4	.8690 (8)	.3369 (4)	1.1652 (3)	2.8 (2)
N1	-.0908 (11)	.5284 (5)	.2036 (4)	3.3 (3)
N2	.0321 (10)	.6291 (4)	.2918 (4)	2.3 (3)
N3	.1013 (9)	.6352 (4)	.3612 (3)	1.9 (3)
N4	.2433 (9)	.6140 (4)	.4912 (3)	2.1 (3)
N5	.2733 (9)	.4439 (4)	.5226 (3)	2.2 (3)
N6	.2788 (10)	.3485 (5)	.5263 (4)	2.3 (3)
N7	.2180 (9)	.2136 (4)	.4631 (4)	2.3 (3)
N8	.7272 (10)	.6005 (5)	.9984 (4)	2.7 (3)
N9	.6466 (9)	.4637 (4)	.9388 (4)	2.3 (3)
N10	.6521 (9)	.3683 (4)	.9450 (3)	1.9 (2)
N11	.7067 (9)	.1979 (4)	.9716 (3)	1.8 (3)
N12	.8358 (9)	.1770 (4)	1.1038 (3)	2.0 (3)
N13	.9052 (10)	.1815 (4)	1.1759 (3)	2.4 (3)
N14	1.0061 (11)	.2766 (5)	1.2710 (4)	3.4 (3)
C1	-.0050 (12)	.5408 (6)	.2689 (4)	2.4 (3)
C2	.1388 (11)	.7130 (5)	.3923 (4)	2.0 (3)
C3	.1115 (12)	.8065 (6)	.3571 (5)	2.8 (3)
C4	.2181 (10)	.7030 (5)	.4682 (4)	1.9 (3)
C5	.2617 (11)	.7761 (6)	.5166 (5)	2.6 (4)
C6	.3267 (13)	.7563 (6)	.5884 (5)	3.2 (4)
C7	.3479 (13)	.6663 (6)	.6113 (5)	3.0 (4)
C8	.3061 (11)	.5953 (5)	.5608 (4)	2.1 (3)
C9	.3239 (10)	.4943 (6)	.5780 (4)	2.1 (3)

Table 3-1 (cont.).

	x	y	z	Biso
C10	.3915 (15)	.4647 (7)	.6536 (5)	3.7 (4)
C11	.2199 (10)	.3069 (5)	.4633 (4)	2.0 (3)
C12	.7111 (10)	.5070 (6)	1.0026 (4)	2.0 (3)
C13	.6159 (10)	.3172 (6)	.8871 (4)	2.1 (3)
C14	.5639 (13)	.3516 (6)	.8119 (4)	2.9 (4)
C15	.6431 (11)	.2165 (6)	.9036 (4)	2.3 (3)
C16	.6081 (12)	.1462 (6)	.8501 (4)	2.7 (4)
C17	.6489 (13)	.0562 (6)	.8700 (5)	3.1 (4)
C18	.7241 (11)	.0355 (6)	.9432 (4)	2.3 (3)
C19	.7470 (11)	.1084 (6)	.9917 (4)	2.2 (3)
C20	.8199 (11)	.0990 (5)	1.0688 (4)	2.2 (3)
C21	.8619 (12)	.0053 (6)	1.1040 (5)	2.9 (3)
C22	.9261 (12)	.2701 (5)	1.2025 (4)	2.4 (3)
C13	.8797 (3)	.7394 (2)	.1446 (1)	3.3 (2)
C14	.3949 (3)	.2004 (1)	.6431 (1)	2.5 (2)
C15	.1171 (4)	.0688 (2)	.3107 (1)	3.7 (2)
W3	.4179 (10)	.0893 (5)	.1835 (4)	4.4 (3)
W4	.5128 (12)	.3840 (6)	.2638 (4)	5.5 (4)

Biso is the Mean of the Principal
Axes of the Thermal Ellipsoid

Table 3-2. Bond Distances(Å) and Angles(°)

Fe1 - Cl1	2.2644(22)	Fe2 - C12	2.5631(23)
Fe1 - W1	2.067(5)	Fe2 - W2	2.174(5)
Fe1 - O1	2.095(5)	Fe2 - O3	2.184(5)
Fe1 - O2	2.124(5)	Fe2 - O4	2.207(5)
Fe1 - N3	2.218(6)	Fe2 - N10	2.183(6)
Fe1 - N4	2.193(6)	Fe2 - N11	2.195(6)
Fe1 - N5	2.203(6)	Fe2 - N12	2.223(6)
O1 - C1	1.265(9)	O3 - C12	1.237(9)
O2 - C11	1.260(9)	O4 - C22	1.233(9)
N3 - N2	1.331(9)	N10 - N9	1.378(9)
N3 - C2	1.275(10)	N10 - C13	1.293(9)
N4 - C4	1.357(10)	N11 - C15	1.316(10)
N4 - C8	1.342(10)	N11 - C19	1.367(10)
N5 - N6	1.376(9)	N12 - N13	1.374(8)
N5 - C9	1.275(10)	N12 - C20	1.290(10)
N1 - C1	1.318(10)	N8 - C12	1.353(10)
N2 - C1	1.359(10)	N9 - C12	1.372(9)
N6 - C11	1.338(10)	N13 - C22	1.368(10)
N7 - C11	1.342(10)	N14 - C22	1.343(10)
C2 - C3	1.497(11)	C13 - C14	1.474(11)
C2 - C4	1.467(10)	C13 - C15	1.492(12)
C4 - C5	1.394(11)	C15 - C16	1.411(12)
C5 - C6	1.387(13)	C16 - C17	1.374(13)
C6 - C7	1.366(13)	C17 - C18	1.436(12)
C7 - C8	1.392(12)	C18 - C19	1.370(11)
C8 - C9	1.491(12)	C19 - C20	1.470(11)
C9 - C10	1.488(11)	C20 - C21	1.515(12)

Cl1-Fe1-W1	176.5(2)	C8-C9-C10	119.4(7)
Cl1-Fe1-O1	93.2(2)	O2-C11-N6	121.2(7)
Cl1-Fe1-O2	96.9(1)	O2-C11-N7	121.8(7)
W1-Fe1-O1	88.7(2)	N6-C11-N7	117.0(7)
W1-Fe1-O2	86.4(2)	N9-N10-C13	119.8(6)
O1-Fe1-O2	75.7(2)	C15-N11-C19	120.0(6)
Fe1-O1-C1	118.9(5)	N13-N12-C20	121.7(6)
Fe1-O2-C11	118.0(5)	N10-N9-C12	112.2(6)
N2-N3-C2	122.3(6)	N12-N13-C22	113.9(6)

Table 3-2 (cont.)

C4-N4-C8	120.7(6)	O3-C12-N8	122.4(7)
N6-N5-C9	121.5(6)	O3-C12-N9	121.9(7)
N3-N2-C1	114.1(6)	N8-C12-N9	115.7(6)
N5-N6-C11	113.5(6)	N10-C13-C14	125.8(8)
O1-C1-N1	121.8(7)	N10-C13-C15	111.7(6)
O1-C1-N2	119.7(7)	C14-C13-C15	122.4(7)
N1-C1-N2	118.5(7)	N11-C15-C13	114.9(7)
N3-C2-C3	125.6(7)	N11-C15-C16	122.3(7)
N3-C2-C4	113.0(7)	C13-C15-C16	122.8(7)
C3-C2-C4	121.4(7)	C15-C16-C17	117.8(8)
N4-C4-C2	114.7(6)	C16-C17-C18	120.3(8)
N4-C4-C5	119.9(7)	C17-C18-C19	117.2(7)
C2-C4-C5	125.3(7)	N11-C19-C18	122.3(7)
C4-C5-C6	119.1(8)	N11-C19-C20	113.7(7)
C5-C6-C7	120.3(8)	C18-C19-C20	124.0(7)
C6-C7-C8	118.8(8)	N12-C20-C19	113.7(7)
N4-C8-C7	121.2(7)	N12-C20-C21	123.9(7)
N4-C8-C9	114.4(6)	C19-C20-C21	122.4(7)
C7-C8-C9	124.5(7)	O4-C22-N13	120.4(7)
N5-C9-C8	111.8(6)	O4-C22-N14	124.6(7)
N5-C9-C10	128.7(8)	N13-C22-N14	115.0(7)

Table 3-3. U values *100.
E.S.Ds. refer to the last digit printed

	U11(σ)	U22	U33	U12	U13	U23
FE1	2.94(5)	1.32(5)	2.35(5)	-.05(5)	-.49(4)	-.08(5)
FE2	2.95(5)	1.51(5)	2.28(5)	-.10(5)	-.55(4)	.17(5)
CL1	3.4 (1)	2.09(9)	5.0 (1)	-.31(9)	.18(9)	.2 (1)
CL2	3.3 (1)	3.1 (1)	3.4 (1)	-.17(9)	-.09(8)	.15(9)
W1	3.8 (3)	3.1 (3)	4.2 (3)	-.4 (3)	.3 (3)	-.3 (3)
W2	3.2 (3)	2.9 (3)	4.4 (3)	.2 (3)	-.4 (2)	.1 (3)
O1	5.2 (4)	1.4 (3)	2.7 (3)	.1 (2)	-1.4 (3)	.2 (2)
O2	4.6 (3)	1.1 (3)	2.7 (3)	.0 (2)	-.7 (2)	-.1 (2)
O3	4.9 (4)	1.5 (3)	3.5 (3)	.0 (3)	-.9 (3)	-.1 (2)
O4	5.8 (4)	2.0 (3)	2.8 (3)	.1 (3)	-1.6 (3)	.0 (2)
N1	5.3 (5)	3.8 (5)	3.4 (4)	.1 (4)	-1.1 (3)	.0 (3)
N2	4.2 (4)	1.6 (3)	2.8 (4)	.2 (3)	-.6 (3)	.3 (3)
N3	3.1 (4)	1.6 (3)	2.6 (3)	.4 (3)	-.2 (3)	.0 (3)
N4	3.4 (4)	2.1 (3)	2.4 (3)	-.1 (3)	-.5 (3)	.0 (3)
N5	3.4 (4)	2.0 (4)	2.8 (3)	.4 (3)	-.8 (3)	.1 (3)
N6	4.2 (4)	1.7 (3)	2.9 (4)	.3 (3)	-1.1 (3)	.3 (3)
N7	3.9 (4)	1.6 (3)	3.2 (4)	.6 (3)	-.3 (3)	.2 (3)
N8	3.9 (4)	1.8 (4)	4.3 (4)	.1 (3)	-1.0 (3)	.2 (3)
N9	3.8 (4)	1.7 (3)	3.1 (4)	-.1 (3)	-.5 (3)	.0 (3)
N10	3.0 (3)	1.5 (3)	2.7 (3)	.0 (3)	-.7 (3)	.2 (3)
N11	3.0 (3)	1.5 (3)	2.4 (3)	-.1 (3)	-.2 (3)	-.2 (3)
N12	2.8 (3)	2.3 (4)	2.5 (3)	.0 (3)	-1.0 (3)	.0 (3)
N13	4.8 (4)	2.1 (4)	2.1 (3)	.0 (3)	-1.4 (3)	.1 (3)
N14	6.2 (5)	3.7 (4)	3.1 (4)	.0 (4)	-1.2 (4)	-.1 (3)
C1	4.0 (5)	2.7 (4)	2.6 (4)	.2 (4)	-.8 (4)	-.2 (4)
C2	2.8 (4)	1.7 (4)	3.1 (4)	.0 (3)	.0 (3)	.0 (3)

Table 3-3 (cont.).

	U11(σ)	U22	U33	U12	U13	U23
C3	4.5 (5)	1.9 (4)	4.1 (5)	.1 (4)	-.6 (4)	-.1 (4)
C4	2.1 (4)	1.7 (4)	3.3 (4)	.1 (3)	-.1 (3)	.1 (3)
C5	3.5 (5)	2.1 (4)	4.4 (5)	.0 (4)	.1 (4)	.3 (4)
C6	4.7 (5)	2.7 (5)	4.7 (5)	.2 (4)	.5 (4)	.5 (4)
C7	4.4 (5)	3.6 (5)	3.2 (5)	.3 (4)	-.2 (4)	.3 (4)
C8	3.4 (5)	2.2 (4)	2.5 (4)	.1 (4)	-.3 (3)	.2 (3)
C9	3.3 (4)	2.4 (4)	2.4 (4)	.0 (4)	-.7 (3)	-.6 (4)
C10	6.6 (6)	3.2 (5)	4.0 (5)	.3 (5)	-1.2 (5)	.4 (4)
C11	3.1 (4)	1.4 (4)	2.9 (4)	.2 (3)	-.1 (3)	-.1 (3)
C12	2.9 (4)	2.0 (4)	2.5 (4)	-.1 (4)	-.6 (3)	-.3 (4)
C13	3.1 (4)	2.9 (4)	1.9 (4)	-.1 (4)	-.3 (3)	.0 (4)
C14	5.5 (6)	2.9 (5)	2.4 (4)	.1 (4)	-.9 (4)	-.1 (4)
C15	2.8 (4)	2.5 (5)	3.4 (4)	-.1 (4)	.3 (3)	-.2 (4)
C16	4.2 (5)	3.4 (5)	2.5 (4)	-.2 (4)	-.6 (4)	-.3 (4)
C17	4.4 (5)	3.1 (5)	4.2 (5)	-.3 (4)	.1 (4)	-.4 (4)
C18	3.8 (5)	2.2 (4)	2.9 (4)	-.1 (4)	.0 (4)	-.4 (4)
C19	3.1 (4)	2.3 (4)	3.0 (4)	.0 (4)	-.2 (3)	-.3 (4)
C20	3.0 (4)	1.7 (4)	3.5 (5)	-.1 (3)	.2 (3)	-.1 (4)
C21	4.4 (5)	2.4 (4)	4.3 (5)	.3 (4)	-.4 (4)	.1 (4)
C22	4.1 (5)	2.1 (4)	2.9 (4)	-.1 (4)	-1.4 (4)	-.3 (4)
CL3	4.9 (1)	3.5 (1)	4.1 (1)	.7 (1)	.0 (1)	1.1 (1)
CL4	3.7 (1)	2.6 (1)	3.4 (1)	-.40(9)	-.31(8)	-.30(9)
CL5	5.9 (1)	3.5 (1)	4.6 (1)	.4 (1)	-.3 (1)	.4 (1)
W3	7.0 (5)	4.1 (4)	5.5 (4)	.0 (4)	.0 (4)	-.1 (3)
W4	9.9 (6)	6.0 (5)	5.0 (4)	1.3 (5)	-.4 (4)	-.8 (4)

Anisotropic Temperature Factors are of the form

Temp=-2*Pi*Pi*(h*h*u11*astar*astar+---+2*h*k*u12*astar*bstar+---)

Table 3-4. Ligand Hydrogen Atomic Parameters x,y,z and Biso.

	x	y	z	Biso
H1(N1)	-.0083	.4996	.1851	3.2
H2(N1)	-.1751	.5412	.2113	3.2
H3(N2)	.0110	.6694	.2611	3.2
H4(C3)	-.2010	.3353	.6303	3.2
H5(C3)	.0088	.8044	.3246	3.2
H6(C3)	-.0264	.3303	.5968	3.2
H7C5)	-.2386	.3430	.5094	3.2
H8(C6)	.3402	.8195	.6205	3.2
H9(C7)	.3718	.6529	.6609	3.2
H10(C10)	.4297	.4216	.6529	3.2
H11(C10)	-.4994	.4879	.6650	3.2
H12(C10)	.3151	.4682	.6813	3.2
H13(N6)	.3193	.3126	.5743	3.2
H14(N7)	-.2609	.6866	.4966	3.2
H15(N7)	.1658	.1744	.4155	3.2
H16(N8)	.3187	.1321	.0417	3.2
H17(N8)	-.2080	.6298	.0443	3.2
H18(N9)	-.3888	.4878	.8936	3.2
H19(C14)	-.5506	.8003	.2380	3.2
H20(C14)	-.4743	.8987	.1867	3.2
H21(C14)	-.6696	.8921	.2106	3.2
H22(C16)	-.5474	.6594	.2028	3.2
H23(C17)	.3863	.5015	.1719	3.2
H24(C18)	.2388	.4654	.0406	3.2
H25(C21)	.0196	.4956	.8776	3.2
H26(C21)	.0854	.4712	.9317	3.2
H27(C21)	.1906	.4981	.8433	3.2
H28(N13)	.0572	.6371	.7953	3.2
H29(N14)	-.0879	.7769	.7410	3.2
H30(N14)	.0807	.7722	.7251	3.2

Biso is the Mean of the Principal
Axes of the Thermal Ellipsoid

Third, the existence of an OH^- ion in this water soluble compound would imply that it should act as a strong base in aqueous solution. Aqueous solutions of this compound were found to be acidic and not at all basic. Finally, though there is evidence of hydrogen bonding, most notably between N6-H(N6)···Cl4, N2-H(N2)···Cl3, N13-H(N13)···Cl5 with distances between the hydrogen and chloride of 2.10(4), 2.48(4) and 2.45(4)Å respectively, there is no evidence of strong hydrogen bonding involving either of the uncoordinated water molecules as might be expected if one were in fact a OH^- ion.

Additional evidence for an Fe(II)/Fe(III) assignment comes from a comparison of bond lengths within the immediate coordination sphere of each Fe-cation. Table 3-5 shows that Fe1 has much shorter bond lengths within the coordination sphere than does Fe2. Since first row transition metals tend generally to be ionic in nature, it is reasonable to expect that shorter bond lengths would be observed for a 3+ cation as opposed to a cation carrying a 2+ charge. Thus our observations suggest that the Fe1-cation is 3+ and the Fe2-cation is 2+. Furthermore, comparing the coordination sphere bond lengths of the two complexes in this compound with the previously reported Fe(II) and Fe(III) complexes as is shown in Table 2-5, reveals that the bond lengths of Fe2 parallel

Table 3-5. Bond Lengths Observed Within the Immediate Coordination Sphere in Å.

	I	II	III	IV
Fe - Cl	2.506	2.563	2.362	2.261
Fe - O	2.153	2.174	2.325(Cl)	2.067
Fe - O1	2.192	2.207	2.074	2.095
Fe - O2	2.175	2.184	2.131	2.124
Fe - N3	2.195	2.183	2.200	2.218
Fe - N4	2.229	2.195	2.196	2.183
Fe - N5	2.229	2.223	2.203	2.203

Where I = Fe(DAPSC)II, J. Am. Chem. Soc., (1975),16,6505.

II = Fe2 complex discussed in this chapter.

III = Fe(DAPSC)III, Inorg. Chem., (1976), 15, 1814.

IV = Fe1 complex discussed in this chapter.

those observed for the Fe(II) complex and a similar situation exists between Fe1 and the Fe(III) complex.

Due to the unique nature of this compound, we have now begun a theoretical investigation exploring the electronic and conformational characteristics of the associated molecules by preforming semi-empirical geometry optimization calculations. The details of this work will be presented in chapter 6.

CHAPTER 4

PENTAGONAL BIPYRAMIDAL COMPLEXES OF Cr(III) WHICH DISPLAY A STATIC JAHN-TELLER DISTORTION

Introduction

Pentagonal-bipyramidal complexes of Cr(III) are extremely rare and to date only four reports[9,29,30] of such compounds have appeared in the literature. In each instance a planar pentadentate ligand was employed to obtain this unique geometry around the chromium-cation. An intriguing aspect of these complexes is the pronounced asymmetry observed in the equatorial plane of the pentagonal bipyramid. In two of the reports[9,29] this dramatic asymmetry has been attributed to two effects: a static Jahn-Teller[31] distortion arising from orbital degeneracy and the stronger attraction of a negatively charged section of the ligand to the metal cation.

Utilizing both DAPSC and DAPBAH, two new complexes of Cr(III) displaying PBP geometry have been prepared. The reaction of DAPSC with $Cr_2O_7^{2-}$ in a reducing medium produced a Cr(III) cation $[Cr(DAPSC)(H_2O)_2]^{2+}$, a product previously isolated[9] but not structurally characterized. Combining DAPBAH with a solution of Cr^{2+} in 0.6M HCl produced the cation $[Cr(DAPBAH)(H_2O)_2]^{2+}$.

The synthesis and characterization of both PBP-Cr(III) complexes by X-ray diffraction techniques is presented in this chapter. In addition, it is shown by means of a group theoretical treatment that a static Jahn-Teller[31] distortion is indeed possible for a Cr(III) cation in a PBP-field.

Experimental

Materials. The 2,6-Diacetylpyridine purchased from Aldrich, semicarbazide hydrochloride purchased from Eastman Chemicals, and the benzoic acid hydrazide purchased from Pfaltz and Bauer were used as supplied. All other solvents and chemicals were reagent grade.

Preparation of $[Cr(DAPSC)(H_2O)_2]^{2+}(NO_3)_2 \cdot H_2O$, (I). $K_2Cr_2O_7$ (0.0735g, 0.2 mmole) was added to 45 mL H_2O having a pH = 1.00 (conc. HNO_3). DAPSC (0.390g, 1.4 mmole), prepared by the method previously described[9], was then added to this solution. The resulting slurry was stirred and heated to 57° C for 1 hr. The green solution was then filtered through a fine glass frit and cooled to room temp (23° C). At this point pH = 3.30. Slow evaporation of the filtrate gave a crop of brown plates after 23 days.

Preparation of $[Cr(DAPBAH)(H_2O)_2]^{2+}Cl_2 \cdot 4H_2O$, (II). Chromium metal (0.0265g, 0.5 mmole) was placed into 30 mL of a 0.06 M HCl solution (under N_2) to produce a 0.017 M Cr^{2+} solution. DAPBAH (0.2003g, 0.5 mmole), prepared by the method

previously described[15], was then added to this solution. Upon the addition of DAPBAH, the blue Cr^{2+} solution rapidly turned to a yellow/green color. Stirring was continued for 1 hr. after which the N_2 atmosphere was removed and the solution filtered. The filtrate had a pH = 0.90 and no further color changes were observed. Green cubic shaped crystals were obtained in good yield within 24 hrs..

Magnetic Measurements. The magnetic moments of both compounds were determined in a 2% tert-butyl alcohol-water solution by NMR techniques[32]. The average of three measurements for I and II was 4.03 ± 0.04 and 4.07 ± 0.04 respectively.

Data Collection and Structure Refinement. Crystals suitable for diffraction studies were mounted on the end of a glass fiber and all subsequent measurements were made using a Nicolet R3m diffractometer with graphite-monochromated Mo-Kα radiation (λ = 0.71069Å). The unit cell dimensions were determined by a least squares refinement of 25 automatically centered reflections. A variable-speed (1° - 29.3°) 2θ scan technique was used to measure the intensity data from 0° to 50° and 40° in 2θ for the complexes I, and II respectively. Two standard reflections were measured every 98 reflections to monitor for any decomposition during the X-ray analysis. No absorption corrections were made. The pertinent crystal data is given in Table 4-1.

The data reduction, structure solution and final refinement were performed using the NRCVAX (PC-Version)[18] package of programs. All non-hydrogen atoms were located by the heavy-atom method (Patterson and Fourier syntheses) and refined anisotropically by full-matrix least squares. The hydrogen atoms were located by the calculation of a difference Fourier map and refined isotropically for complex I. For complex II, H-atoms were placed at calculated positions and not refined. The final positional parameters are given in Tables 4-2 and 4-3 with the final bond distances involving the non-hydrogen atoms and bond angles listed in Tables 4-4 and 4-5 respectively. The anisotropic thermal parameters are listed in Tables 4-6 and 4-7 and the hydrogen positional parameters are given in Tables 4-8 and 4-9.

Results and Discussion

The crystals of I and II consist of $[Cr(DAPSC)(H_2O)_2]^{2+}$ and $[Cr(DAPBAH)(H_2O)_2]^{2+}$ cations respectively and display PBP geometry which is easily seen in Figures 4-1 and 4-2. The bond lengths observed within each of the coordination spheres are presented in Table 4-10. It is clear from the bond lengths in Table 4-10 that the five bonds in each of the equatorial planes differ significantly from each other. Consequently there is notable distortion of the respective pentagonal bipyramid in each case.

Table 4-1. Crystal Data for I and II

	I	II
Crystal System	Monoclinic	Triclinic
Space Group	$P2_1/n$	$P\bar{1}$
a, Å	11.726	14.404
b, Å	14.730	14.689
c, Å	11.856	15.102
α, °	90	62.56
β, °	105.52	75.17
γ, °	90	74.90
Vol., Å^3	1973	2703
mol. wt.	508.34	601.90
Z	4	4
d(calcd), g/cm^3	1.71	1.48
Crystal Size, mm^3	0.10 x 0.12 x 0.18	0.09 x 0.11 x 0.17
μ, cm^{-1}	11.4	6.4
Data with I > 2.5 σI	2580	2509
R[a], %	4.4	7.0
Rw[b], %	4.6	8.3

$$R^{a}=\sum \frac{|F_o|-|F_c|}{|F_c|}$$

$$R_w^{b}=\left[\frac{\sum w(|F_o|-|F_c|)^2}{\sum w|F_o|^2}\right]^{1/2}$$

Table 4-2. Atomic Parameters x,y,z and Biso for Compound I. E.S.Ds. refer to the last digit printed.

	x	y	z	Biso
Cr	.08266(6)	.60588(4)	.23319(5)	2.04 (2)
W1	-.0838 (3)	.6001 (3)	.1449 (3)	2.7 (1)
W2	.2469 (3)	.6178 (2)	.3282 (3)	3.1 (1)
O1	.0307 (2)	.5761 (2)	.3865 (2)	2.4 (1)
O2	.0959 (3)	.4725 (1)	.2355 (2)	2.5 (1)
N1	.1028 (3)	.7389 (2)	.1458 (3)	2.3 (1)
N2	.0390 (3)	.7390 (2)	.3300 (3)	2.5 (1)
N3	.0057 (3)	.7227 (2)	.4287 (3)	2.8 (2)
N4	-.0251 (4)	.6107 (3)	.5502 (3)	3.4 (2)
N5	.1342 (3)	.5777 (3)	.0854 (3)	2.2 (2)
N6	.1477 (3)	.4875 (2)	.0616 (3)	2.4 (1)
N7	.1329 (4)	.3485 (2)	.1398 (4)	3.1 (2)
C1	.1373 (4)	.7326 (3)	.0469 (3)	2.5 (2)
C2	.1552 (4)	.8078 (3)	-.0160 (4)	3.3 (2)
C3	.1370 (5)	.8927 (3)	.0261 (4)	3.8 (2)
C4	.1028 (4)	.8997 (3)	.1287 (4)	3.4 (2)
C5	.0860 (4)	.8213 (3)	.1866 (4)	2.5 (2)
C6	.0523 (4)	.8201 (3)	.2978 (4)	2.5 (2)
C7	.0373 (7)	.9035 (4)	.3615 (6)	4.1 (3)
C8	.0045 (4)	.6331 (3)	.4550 (3)	2.4 (2)
C9	.1564 (4)	.6392 (4)	.0136 (4)	2.5 (2)
C10	.1984 (6)	.6167 (4)	-.0897 (5)	4.0 (3)
C11	.1254 (3)	.4385 (3)	.1478 (3)	2.3 (2)
N8	.2823 (4)	.6743 (4)	.6070 (4)	4.5 (2)
N9	.4585 (3)	.6637 (2)	.1838 (3)	2.6 (2)
O3	.2832 (4)	.7165 (3)	.5198 (3)	6.7 (2)
O4	.2722 (5)	.7120 (4)	.6935 (4)	8.9 (3)
O5	.2924 (5)	.5918 (4)	.6065 (6)	9.7 (4)
O6	.3972 (3)	.7332 (2)	.1647 (3)	4.2 (2)
O7	.5285 (4)	.6468 (3)	.1239 (4)	5.6 (2)
O8	.4487 (3)	.6095 (2)	.2596 (3)	4.0 (2)
W3	.2524 (4)	.9328 (3)	.7621 (4)	5.8 (2)

Biso is the Mean of the Principal Axes of the Thermal Ellipsoid

Table 4-3. Atomic Parameters x,y,z and Biso for Compound II. E.S.Ds. refer to the last digit printed.

	x	y	z	Biso
Cr1	.6354 (2)	.8579 (2)	.0952 (2)	2.3 (2)
Cr2	.8675 (2)	.40859(2)	.6351 (2)	2.2 (2)
Cl1	.1162 (4)	.1741 (4)	.7679 (4)	4.6 (3)
Cl2	.6169 (4)	.2706 (4)	.6967 (4)	4.7 (3)
Cl3	.9184 (4)	.8115 (4)	.9019 (4)	4.7 (3)
Cl4	.5941 (5)	.6068 (4)	.6941 (4)	5.7 (4)
O1	.6134 (9)	1.0274 (8)	.0454 (8)	3.0 (7)
O2	.6350 (8)	.9153 (7)	-.0514 (7)	2.3 (6)
O3	.8825 (8)	.4664 (7)	.4862 (7)	2.0 (6)
O4	.8711 (9)	.5648 (7)	.5940 (7)	2.7 (6)
W1	.4912 (10)	.8735 (8)	.1230 (8)	3.9 (8)
W2	.7796 (8)	.8456 (8)	.0737 (8)	3.1 (6)
W3	.7203 (9)	.4415 (8)	.6485 (8)	3.0 (7)
W4	1.0119 (9)	.3733 (7)	.6264 (8)	3.3 (7)
N1	.6340 (10)	.7264 (8)	.2435 (8)	1.9 (7)
N2	.6292 (11)	.9058 (9)	.2241 (9)	2.7 (8)
N3	.6312 (10)	1.0109 (9)	.1988 (8)	2.3 (8)
N4	.6435 (11)	.7297 (9)	.0724 (9)	2.6 (9)
N5	.6433 (11)	.7472 (9)	-.0273 (9)	2.6 (8)
N6	.8629 (9)	.2720 (9)	.7853 (9)	1.8 (7)
N7	.8652 (10)	.2848 (10)	.6139 (8)	2.5 (8)
N8	.8632 (11)	.3040 (9)	.5153 (9)	2.8 (8)
N9	.8599 (11)	.4476 (9)	.7776 (9)	2.8 (9)
N10	.8654 (11)	.5488 (9)	.7531 (9)	2.9 (9)
C1	.6303 (13)	.7348 (11)	.3296 (11)	2.3 (9)
C2	.6229 (14)	.6470 (13)	.4216 (11)	3.0 (11)
C3	.6216 (15)	.5539 (12)	.4244 (12)	3.3 (11)
C4	.6247 (15)	.5470 (12)	.3363 (12)	3.3 (12)
C5	.6311 (14)	.6358 (11)	.2452 (13)	3.4 (10)
C6	.6299 (12)	.8388 (11)	.3204 (10)	1.8 (9)
C7	.6231 (15)	.8644 (15)	.4059 (12)	4.0 (12)
C8	.6203 (12)	1.0673 (12)	.1024 (11)	2.2 (9)
C9	.6361 (14)	.6364 (11)	.1468 (12)	3.1 (10)
C10	.6302 (15)	.5453 (13)	.1304 (13)	3.7 (12)
C11	.6391 (14)	.8479 (13)	-.0851 (12)	3.1 (11)
C12	.8624 (11)	.1812 (11)	.7821 (10)	1.5 (8)
C13	.8640 (14)	.0851 (12)	.8725 (12)	3.1 (10)
C14	.8717 (14)	.0865 (12)	.9604 (11)	3.1 (10)
C15	.8755 (15)	.1805 (12)	.9643 (12)	3.3 (11)
C16	.8703 (13)	.2735 (12)	.8719 (11)	2.6 (9)
C17	.8654 (13)	.1881 (11)	.6832 (11)	2.7 (10)
C18	.8680 (17)	.0982 (13)	.6622 (14)	4.6 (13)
C19	.8783 (13)	.4002 (12)	.4537 (11)	2.6 (10)

Table 4-3 (cont).

	x	y	z	Biso
C20	.8665 (15)	.3758 (12)	.8682 (12)	3.5 (11)
C21	.8692 (15)	.3870 (13)	.9612 (13)	3.7 (12)
C22	.8659 (13)	.6071 (12)	.6497 (11)	2.4 (10)
C81	.6147 (14)	1.1835 (11)	.0572 (12)	2.9 (11)
C82	.6275 (16)	1.2414 (12)	-.0454 (12)	3.8 (12)
C83	.6220 (16)	1.3472 (13)	-.0854 (12)	4.1 (12)
C84	.5971 (15)	1.3977 (13)	-.0214 (14)	4.0 (12)
C85	.5821 (17)	1.3399 (14)	.0846 (13)	4.5 (13)
C86	.5924 (14)	1.2321 (12)	.1233 (12)	3.0 (10)
C111	.6360 (13)	.8831 (11)	-.1924 (11)	2.2 (10)
C112	.6325 (13)	.8182 (13)	-.2337 (12)	2.7 (10)
C113	.6276 (15)	.8546 (13)	-.3339 (13)	3.9 (13)
C114	.6258 (16)	.9603 (14)	-.3950 (13)	4.3 (13)
C115	.6308 (16)	1.0250 (14)	-.3577 (13)	4.3 (13)
C116	.6419 (16)	.9872 (12)	-.2565 (11)	3.8 (12)
C191	.8835 (16)	.4349 (12)	.3427 (12)	3.8 (12)
C192	.8739 (16)	.5408 (13)	.2745 (12)	4.0 (12)
C193	.8822 (13)	.5687 (13)	.1718 (12)	3.2 (10)
C194	.9034 (14)	.4942 (12)	.1359 (12)	3.3 (11)
C195	.9045 (18)	.3925 (15)	.2028 (16)	5.5 (15)
C196	.8945 (16)	.3589 (14)	.3076 (13)	4.6 (13)
C221	.8737 (14)	.7203 (12)	.6099 (12)	3.1 (11)
C222	.8844 (15)	.7674 (12)	.6638 (13)	3.7 (12)
C223	.8936 (16)	.8725 (14)	.6167 (14)	4.5 (13)
C224	.8858 (16)	.9291 (12)	.5149 (14)	4.5 (12)
C225	.8714 (16)	.8829 (13)	.4629 (14)	4.0 (12)
C226	.8621 (15)	.7789 (13)	.5056 (12)	3.6 (12)
W5	.8245 (10)	.6335 (8)	.9051 (8)	4.1 (8)
W6	.7073 (13)	1.0800 (10)	.3062 (10)	6.7 (11)
W7	.3229 (15)	.7132 (11)	.5256 (10)	7.7 (12)
W8	.6014 (19)	.2406 (16)	.3560 (17)	12.4 (19)
W9	.9021 (13)	.0596 (11)	.2059 (11)	7.3 (11)

Biso is the Mean of the Principal Axes of the Thermal Ellipsoid

Table 4-4. Bond Lengths (Å) and Bond Angles (°) for I.

Cr - W1	1.955(4)	N7 - C11	1.333(5)
Cr - W2	1.962(3)	C1 - C2	1.382(6)
Cr - O1	2.112(2)	C1 - C9	1.465(6)
Cr - O2	1.970(3)	C2 - C3	1.385(7)
Cr - N1	2.258(3)	C3 - C4	1.383(6)
Cr - N2	2.396(3)	C4 - C5	1.385(6)
Cr - N5	2.043(4)	C5 - C6	1.474(6)
O1 - C8	1.261(5)	C6 - C7	1.478(7)
O2 - C11	1.282(4)	C9 - C10	1.475(7)
N1 - C1	1.342(5)	N8 - O3	1.209(6)
N1 - C5	1.340(5)	N8 - O4	1.199(6)
N2 - N3	1.350(5)	N8 - O5	1.221(8)
N2 - C6	1.276(5)	N9 - O6	1.237(5)
N3 - C8	1.357(5)	N9 - O7	1.246(5)
N4 - C8	1.309(5)	N9 - O8	1.229(4)
N5 - N6	1.376(5)	N5 - C9	1.316(7)
N6 - C11	1.333(5)		

W1-Cr-W2	176.3(2)	C2-C3-C4	119.5(4)
W1-Cr-O1	88.6(1)	C3-C4-C5	119.1(4)
W1-Cr-O2	91.6(1)	N1-C5-C4	121.5(4)
W1-Cr-N5	90.8(2)	N1-C5-C6	114.4(3)
W2-Cr-O1	89.4(1)	C4-C5-C6	124.1(4)
W2-Cr-O2	91.1(1)	N2-C6-C5	111.2(3)
W2-Cr-N5	92.3(2)	N2-C6-C7	125.8(4)
O1-Cr-O2	79.7(1)	C5-C6-C7	122.9(4)
O1-Cr-N5	156.3(1)	O1-C8-N3	118.7(3)
O2-Cr-N5	76.6(1)	O1-C8-N4	123.6(4)
Cr-O1-C8	126.3(2)	N3-C8-N4	117.7(4)
Cr-O2-C11	114.6(2)	N5-C9-C1	113.6(4)
C1-N1-C5	119.1(3)	N5-C9-C10	123.4(5)
N3-N2-C6	120.8(3)	C1-C9-C10	122.9(5)
N2-N3-C8	113.3(3)	O2-C11-N6	124.1(3)
Cr-N5-N6	116.7(3)	O2-C11-N7	119.0(4)
Cr-N5-C9	124.8(3)	N6-C11-N7	117.0(3)
N6-N5-C9	118.6(4)	O3-N8-O4	121.2(6)
N5-N6-C11	108.0(3)	O3-N8-O5	119.0(5)
N1-C1-C2	122.7(4)	O4-N8-O5	119.8(6)
N1-C1-C9	113.8(3)	O6-N9-O7	120.0(4)
C2-C1-C9	123.4(4)	O6-N9-O8	120.5(3)
C1-C2-C3	118.0(4)	O7-N9-O8	119.5(4)

Table 4-5. Bond Lengths (Å) and Angles (°) for II.

Cr1 - O1	2.203(10)	C5 - C9	1.465(24)
Cr1 - O2	1.974(9)	C6 - C7	1.477(22)
Cr1 - W1	1.984(14)	C8 - C81	1.505(21)
Cr1 - W2	1.992(12)	C9 - C10	1.495(23)
Cr1 - N1	2.181(11)	C11 - C111	1.466(22)
Cr1 - N2	2.330(13)	C12 - C13	1.442(20)
Cr1 - N4	2.034(11)	C12 - C17	1.439(21)
Cr2 - O3	1.978(9)	C13 - C14	1.370(24)
Cr2 - O4	2.094(10)	C14 - C15	1.424(23)
Cr2 - W3	2.027(12)	C15 - C16	1.436(21)
Cr2 - W4	1.993(13)	C16 - C20	1.465(22)
Cr2 - N6	2.231(12)	C17 - C18	1.484(23)
Cr2 - N7	1.996(13)	C19 - C191	1.498(21)
Cr2 - N9	2.440(13)	C20 - C21	1.498(24)
O1 - C8	1.278(18)	C22 - C221	1.509(21)
O2 - C11	1.290(18)	C81 - C82	1.371(22)
O3 - C19	1.294(18)	C81 - C86	1.408(22)
O4 - C22	1.236(17)	C82 - C83	1.371(23)
N1 - C1	1.349(19)	C83 - C84	1.40(3)
N1 - C5	1.331(20)	C84 - C85	1.41(3)
N2 - N3	1.415(16)	C85 - C86	1.392(23)
N2 - C6	1.330(18)	C111 - C112	1.375(21)
N3 - C8	1.330(19)	C111 - C116	1.394(21)
N4 - N5	1.408(17)	C112 - C113	1.369(23)
N4 - C9	1.322(19)	C113 - C114	1.390(25)
N5 - C11	1.320(20)	C114 - C115	1.33(3)
N6 - C12	1.359(18)	C115 - C116	1.403(24)
N6 - C16	1.350(20)	C191 - C192	1.409(23)
N7 - N8	1.389(17)	C191 - C196	1.399(25)
N7 - C17	1.320(19)	C192 - C193	1.391(23)
N8 - C19	1.325(20)	C193 - C194	1.368(24)
N9 - N10	1.376(16)	C194 - C195	1.36(3)
N9 - C20	1.296(20)	C195 - C196	1.40(3)
N10 - C22	1.392(19)	C221 - C222	1.342(24)
C1 - C2	1.396(21)	C221 - C226	1.435(23)
C1 - C6	1.468(21)	C222 - C223	1.398(23)
C2 - C3	1.354(23)	C223 - C224	1.39(3)
C3 - C4	1.369(23)	C224 - C225	1.33(3)
C4 - C5	1.395(22)	C225 - C226	1.387(23)

O1-Cr1-O2	76.1(4)	C1-C6-C7	125.0(13)
O1-Cr1-W1	85.9(4)	O1-C8-N3	122.8(14)
O1-Cr1-W2	92.4(4)	O1-C8-C81	117.7(13)
O1-Cr1-N1	133.1(4)	N3-C8-C81	119.5(13)
O1-Cr1-N4	152.5(5)	N4-C9-C5	111.5(13)

Table 4-5 (cont.).

O2-Cr1-W1	91.1(5)	N4-C9-C10	123.1(15)
O2-Cr1-W2	91.5(5)	C5-C9-C10	125.4(13)
O2-Cr1-N1	150.3(4)	O2-C11-N5	123.5(14)
O2-Cr1-N4	76.7(5)	O2-C11-C111	119.4(14)
W1-Cr1-W2	176.4(5)	N5-C11-C111	117.0(13)
W1-Cr1-N1	86.7(5)	N6-C12-C13	120.7(13)
W1-Cr1-N4	90.0(5)	N6-C12-C17	115.4(12)
W2-Cr1-N1	92.2(5)	C13-C12-C17	123.8(14)
W2-Cr1-N4	93.0(5)	C12-C13-C14	118.5(14)
N1-Cr1-N4	73.7(5)	C13-C14-C15	121.4(14)
O3-Cr2-O4	78.7(4)	C14-C15-C16	116.8(14)
O3-Cr2-W3	91.9(4)	N6-C16-C15	121.7(13)
O3-Cr2-W4	89.8(4)	N6-C16-C20	116.5(13)
O3-Cr2-N6	149.9(4)	C15-C16-C20	121.7(14)
O3-Cr2-N7	78.0(4)	N7-C17-C12	111.2(13)
O4-Cr2-W3	89.6(4)	N7-C17-C18	124.4(14)
O4-Cr2-W4	91.2(4)	C12-C17-C18	124.3(13)
O4-Cr2-N6	131.1(4)	O3-C19-N8	122.6(13)
O4-Cr2-N7	156.6(4)	O3-C19-C191	119.3(14)
W3-Cr2-W4	178.2(4)	N8-C19-C191	117.9(14)
W3-Cr2-N6	92.4(4)	N9-C20-C16	110.3(14)
W3-Cr2-N7	89.2(5)	N9-C20-C21	128.8(14)
W4-Cr2-N6	85.9(4)	C16-C20-C21	120.9(14)
W4-Cr2-N7	90.7(5)	O4-C22-N10	120.8(13)
N6-Cr2-N7	72.3(4)	O4-C22-C221	122.9(13)
Cr1-O1-C8	122.0(10)	N10-C22-C221	115.8(12)
Cr1-O2-C11	115.2(9)	C8-C81-C82	121.3(14)
Cr2-O3-C19	113.5(9)	C8-C81-C86	118.2(13)
Cr2-O4-C22	128.2(9)	C82-C81-C86	120.4(14)
Cr1-N1-C1	123.7(9)	C81-C82-C83	120.7(15)
Cr1-N1-C5	115.2(10)	C82-C83-C84	119.9(15)
C1-N1-C5	120.9(12)	C83-C84-C85	120.4(15)
N3-N2-C6	117.2(12)	C84-C85-C86	118.5(15)
N2-N3-C8	108.5(12)	C81-C86-C85	120.0(14)
Cr1-N4-N5	116.3(8)	C11-C111-C112	123.6(14)
Cr1-N4-C9	123.4(10)	C11-C111-C116	117.8(13)
N5-N4-C9	119.8(12)	C112-C111-C116	118.5(14)
N4-N5-C11	108.2(11)	C111-C112-C113	121.8(15)
Cr2-N6-C12	114.2(9)	C112-C113-C114	118.6(15)
Cr2-N6-C16	124.7(9)	C113-C114-C115	121.1(16)
C12-N6-C16	120.8(12)	C114-C115-C116	120.6(16)
Cr2-N7-N8	115.6(9)	C111-C116-C115	118.9(15)
Cr2-N7-C17	126.9(10)	C19-C191-C192	121.9(14)
N8-N7-C17	117.6(12)	C19-C191-C196	118.2(14)
N7-N8-C19	109.6(12)	C192-C191-C196	119.9(15)
N10-N9-C20	120.8(12)	C191-C192-C193	119.6(15)

Table 4-5 (cont.).

N9-N10-C22	109.0(11)	C192-C193-C194	120.6(15)
N1-C1-C2	119.3(14)	C193-C194-C195	119.2(16)
N1-C1-C6	116.9(12	C194-C195-C196	122.8(17)
C2-C1-C6	123.8(14)	C191-C196-C195	117.2(16)
C1-C2-C3	120.5(15)	C22-C221-C222	126.2(14)
C2-C3-C4	119.4(14)	C22-C221-C226	113.0(14)
C3-C4-C5	119.2(14)	C222-C221-C226	120.7(15)
N1-C5-C4	120.7(15)	C221-C222-C223	120.3(16)
N1-C5-C9	115.8(13)	C222-C223-C224	119.2(17)
C4-C5-C9	123.5(14)	C223-C224-C225	120.1(15)
N2-C6-C1	108.3(12)	C224-C225-C226	123.1(17)
N2-C6-C7	126.5(13)	C221-C226-C225	116.3(16)

Table 4-6. U values *100 for I.
E.S.Ds. refer to the last digit printed

	U11(σ)	U22	U33	U12	U13	U23
Cr	3.30(3)	2.29(3)	2.4(3)	-.1(3)	1.2(2)	-.2(3)
W1	3.6(2)	4.0(2)	3.0(2)	-.4(2)	1.3(2)	-.7(2)
W2	3.7(2)	4.8(2)	3.2(2)	-.6(2)	1.2(2)	-.6(2)
O1	4.9(2)	2.1(1)	2.8(1)	.0(1)	2.1(1)	-.0(1)
O2	4.9(2)	2.1(1)	3.0(1)	.1(1)	2.0(1)	-.0(1)
N1	3.6(2)	2.6(2)	2.7(2)	-.3(2)	1.1(1)	.4(1)
N2	4.3(2)	2.2(2)	3.3(2)	-.2(2)	1.8(2)	-.0(1)
N3	6.0(2)	2.0(2)	3.4(2)	-.4(2)	2.8(2)	-.4(2)
N4	8.2(3)	2.2(2)	4.0(2)	.4(2)	4.0(2)	.0(2)
N5	3.4(2)	2.8(2)	2.5(2)	-.2(2)	1.2(2)	-.1(2)
N6	4.0(2)	2.6(2)	2.8(2)	-.0(2)	1.5(2)	-.5(1)
N7	6.5(3)	2.4(2)	3.6(2)	.4(2)	2.4(2)	-.3(2)
C1	3.5(2)	3.2(2)	2.7(2)	-.3(2)	.9(2)	.4(2)
C2	5.4(3)	4.3(3)	3.4(2)	-.5(2)	1.8(2)	1.0(2)
C3	7.0(3)	3.6(2)	4.3(3)	-.4(2)	2.4(2)	1.5(2)
C4	6.0(3)	2.5(2)	4.8(3)	-.6(2)	1.9(2)	.6(2)
C5	3.7(2)	2.4(2)	3.4(2)	-.3(2)	1.0(2)	.3(2)
C6	4.1(2)	2.2(2)	3.5(2)	-.2(2)	1.3(2)	.1(2)
C7	8.8(5)	2.5(3)	5.7(3)	-.2(3)	4.1(4)	-.1(3)
C8	3.9(2)	2.5(2)	3.0(2)	.0(2)	1.4(2)	.0(2)
C9	3.7(2)	3.5(2)	2.6(2)	-.5(2)	1.3(2)	.4(2)
C10	6.8(4)	5.3(4)	4.3(3)	-.8(3)	3.6(3)	-.3(3)
C11	3.2(2)	2.9(2)	2.6(2)	.0(2)	.9(2)	-.6(2)
N8	4.8(3)	8.7(4)	3.5(2)	-1.3(3)	1.2(2)	.3(2)
N9	3.9(2)	3.2(2)	3.2(2)	-.2(2)	1.8(2)	.1(2)
O3	11.0(4)	9.3(3)	4.8(2)	-3.3(3)	1.2(2)	1.2(2)
O4	12.5(4)	17.3(6)	5.4(3)	-2.1(4)	4.5(3)	-2.5(3)

Table 4-6 (cont.).

	U11(σ)	U22	U33	U12	U13	U23
O5	11.6(5)	7.9(4)	17.0(6)	.6(3)	3.2(4)	1.5(4)
O6	6.3(2)	3.8(2)	6.6(2)	1.5(2)	3.2(2)	1.4(2)
O7	9.2(3)	6.8(3)	7.4(3)	2.6(2)	5.7(3)	2.0(2)
O8	7.2(2)	3.9(2)	5.4(2)	.8(2)	3.5(2)	1.6(2)
W3	5.8(3)	9.3(3)	7.8(3)	-1.1(2)	3.1(2)	-.6(2)

Anisotropic Temperature Factors are of the form --
temp=-2*Pi*Pi*(h*h*u11*astar*astar+-
--+2*h*k*u12*astar*bstar+---)

Table 4-7. U values *100 for II.
E.S.Ds. refer to the last digit printed

	U11(σ)	U22	U33	U12	U13	U23
Cr1	4.2(2)	2.4(2)	1.8(2)	-.6(1)	-.1(1)	-.8(1)
Cr2	4.4(2)	1.6(1)	1.6(2)	-.7(1)	.3(1)	-.5(1)
C11	7.0(4)	4.6(3)	5.1(3)	-.6(3)	-1.7(3)	-1.1(3)
C12	6.6(4)	4.9(3)	5.6(3)	-3.0(3)	1.3(3)	-1.8(3)
C13	7.2(4)	5.0(3)	5.3(3)	-1.1(3)	.6(3)	-2.7(3)
C14	9.1(5)	4.2(3)	6.6(4)	.5(3)	.6(3)	-2.5(3)
O1	5.5(9)	2.7(7)	3.2(7)	-1.8(6)	-.3(6)	-1.0(6)
O2	5.2(9)	2.4(6)	1.1(6)	-1.8(5)	.3(5)	-.4(5)
O3	4.2(8)	3.0(6)	1.3(6)	-1.4(5)	-.4(5)	-1.4(5)
O4	6.4(9)	1.2(6)	1.9(6)	-1.1(5)	-.4(6)	-.1(5)
W1	8.9(11)	2.7(7)	2.4(7)	-.0(7)	-1.2(7)	-.8(6)
W2	2.8(8)	3.0(7)	4.3(7)	-.5(6)	.9(6)	-1.0(6)
W3	5.2(9)	2.5(6)	2.4(6)	-.2(6)	-.3(6)	-.4(5)
W4	6.6(10)	1.7(6)	2.7(7)	-2.1(6)	2.8(6)	-.8(5)
N1	4.6(10)	.9(7)	1.1(7)	-.8(6)	-1.1(6)	.5(6)
N2	5.7(12)	1.5(7)	2.7(8)	-.8(7)	-.3(7)	-.7(6)
N3	5.2(11)	2.1(8)	1.2(7)	-1.3(7)	.3(7)	-.5(6)
N4	6.0(12)	1.7(7)	3.0(8)	-.5(7)	-.5(7)	-1.8(7)
N5	5.9(11)	3.0(8)	2.6(8)	-.9(7)	-1.1(7)	-2.1(7)
N6	1.9(9)	1.5(7)	3.1(8)	-.2(6)	-.7(6)	-.7(6)
N7	5.2(11)	3.7(8)	.2(7)	-1.5(7)	.6(6)	-.6(6)
N8	5.8(12)	2.6(8)	3.2(8)	-2.3(7)	-1.0(7)	-.8(7)
N9	6.6(12)	1.1(7)	2.4(8)	-.1(7)	-.4(7)	-.8(6)
N10	7.7(12)	1.9(8)	1.7(8)	-1.6(7)	-.2(7)	-.7(6)
C1	3.9(13)	2.3(9)	1.5(9)	-.7(8)	-1.8(8)	.9(8)
C2	5.4(14)	4.2(11)	1.3(9)	-1.2(9)	.8(9)	-1.1(9)
C3	7.5(16)	1.0(9)	2.7(10)	.3(9)	-1.9(10)	.4(8)
C4	7.3(16)	2.0(10)	3.8(11)	-.6(9)	-.9(10)	-1.7(9)

Table 4-7 (cont.).

	U11(σ)	U22	U33	U12	U13	U23
C5	6.7(16)	1.0(9)	4.1(12)	.1(9)	-2.5(10)	.3(9)
C6	3.4(12)	1.8(9)	1.0(9)	.2(8)	-.8(8)	-.0(7)
C7	7.1(17)	6.8(14)	1.5(10)	-2.1(12)	-1.3(10)	-1.0(10)
C8	1.4(11)	4.2(11)	3.2(10)	-1.0(8)	.4(8)	-2.2(9)
C9	6.5(15)	.5(9)	3.3(11)	-1.2(8)	-.3(9)	.5(8)
C10	6.8(16)	2.9(11)	4.6(12)	-.4(10)	-1.6(10)	-1.8(9)
C11	5.6(15)	3.9(11)	3.1(11)	-1.2(9)	-.1(9)	-2.3(9)
C12	1.2(10)	2.3(9)	1.9(9)	.0(7)	-.7(7)	-.4(7)
C13	4.8(14)	1.7(10)	3.5(11)	-.1(8)	-1.2(9)	.3(8)
C14	5.9(14)	2.3(10)	1.4(10)	-1.3(9)	.2(9)	.8(8)
C15	7.5(16)	2.9(11)	2.2(10)	-.5(10)	-2.2(10)	-.6(8)
C16	4.5(13)	2.6(10)	2.4(10)	-2.0(9)	.5(8)	-.7(8)
C17	5.9(14)	2.1(10)	1.3(9)	-1.2(9)	.1(8)	-.1(8)
C18	9.0(20)	2.7(11)	4.1(12	-2.4(11)	-1.0(12)	-1.2(9)
C19	4.7(14)	4.1(11)	2.0(10)	-.9(9)	-1.0(8)	-1.9(9)
C20	8.1(17)	1.7(10)	2.6(11)	-.4(9)	-1.1(10)	-.1(8)
C21	7.4(17)	3.5(11)	2.9(11)	-1.6(10)	-1.1(10)	-.7(9)
C22	5.3(14)	2.6(10)	2.1(10)	-1.0(9)	.0(8)	-1.9(8)
C81	6.3(15)	1.3(9)	3.3(10)	.8(8)	-1.3(9)	-1.4(8)
C82	9.9(18)	2.3(10)	2.2(10)	-1.5(10)	.4(10)	-1.2(9)
C83	8.5(18)	3.0(11)	1.6(10)	-.4(10)	-.1(10)	.5(9)
C84	6.1(16)	2.7(11)	5.7(13)	.1(10)	-.5(11)	-1.8(10)
C85	10.1(19)	5.4(13)	3.5(11)	-3.8(12)	1.6(11)	-3.4(10)
C86	7.0(15)	1.8(10)	2.7(10)	-2.1(9)	-1.1(9)	-.2(8)
C111	4.6(13)	2.1(9)	2.2(9)	-.6(8)	.0(8)	-1.8 (8)
C112	3.4(13)	4.3(11)	3.0(10)	-1.3(9)	-.6(9)	-1.6 (9)
C113	8.2(18)	3.7(12)	3.9(12)	-1.3(11)	-.4(11)	-2.6 (10)

Table 4-7 (cont.).

	U11(σ)	U22	U33	U12	U13	U23
C114	7.6(18)	5.0(13)	3.4(11)	-.2(11)	-1.0(11)	-1.8(10)
C115	9.3(19)	3.9(12)	2.5(11)	-2.0(11)	-1.6(11)	.1(9)
C116	9.9(18)	2.4(10)	1.0(9)	-1.3(10)	1.0(10)	-.7(8)
C191	9.9(18)	3.1(11)	1.3(10)	-1.1(10)	.4(10)	-1.6(8)
C192	8.4(17)	3.1(11)	2.6(11)	.5(10)	-.1(10)	-1.4(9)
C193	3.3(13)	4.4(12)	2.8(11)	.5(9)	-.3(9)	-.9(9)
C194	5.4(15)	2.9(10)	3.3(11)	.8(9)	-1.6(10)	-.8(9)
C195	9.2(20)	5.6(14)	6.9(15)	-.8(13)	-.6(13)	-4.0(12)
C196	8.7(18)	4.5(12)	2.9(11)	-.3(11)	-.8(11)	-.8(10)
C221	6.4(15)	1.8(10)	2.7(10)	-.6(9)	.7(9)	-.9(8)
C222	8.5(17)	2.7(11)	3.7(11)	-2.7(10)	-.8(10)	-1.2(9)
C223	8.4(18)	4.1(12)	4.9(13)	-3.6(11)	1.9(12)	-2.3(10)
C224	8.5(18)	1.4(10)	5.0(13)	-2.7(10)	1.7(12)	-.1(9)
C225	7.6(17)	2.8(11)	5.3(13)	-2.7(10)	-.7(11)	-1.4(10)
C226	7.4(16)	3.8(11)	2.2(10)	-.5(10)	-1.1(10)	-.9(9)
W5	8.0(11)	3.6(7)	3.1(7)	.1(7)	.1(7)	-1.6(6)
W6	14.2(16)	6.1(10)	6.6(10)	-1.4(10)	-5.3(10)	-2.1(8)
W7	17.5(19)	7.4(11)	4.6(9)	-5.0(11)	-1.6(10)	-1.3(8)
W8	20.4(28)	14.2(19)	16.1(20)	.3(17)	-7.9(18)	-8.4(17)
W9	10.6(15)	7.5(11)	7.3(11)	-3.6(10)	1.1(10)	-1.3(9)

Anisotropic Temperature Factors are of the form --
Temp=-2*Pi*Pi*(h*h*u11*astar*astar+--
-+2*h*k*u12*astar*bstar+---)

Table 4-8. Hydrogen Atomic Parameters x,y,z and Biso for I. E.S.Ds. refer to the last digit printed.

	x	y	z	Biso
H1(N4)	-.029(4)	.559(3)	.566(4)	3.6(12)
H2(N4)	-.048(4)	.648(3)	.582(4)	2.2(10)
H3(N3)	.006(4)	.755(3)	.478(4)	3.8(11)
H4(C7)	-.023(5)	.904(4)	.399(5)	9.0(16)
H5(C7)	.108(6)	.913(5)	.426(6)	8.8(21)
H6(C7)	.030(6)	.943(4)	.328(6)	7.4(19)
H7(C4)	.092(4)	.955(3)	.154(4)	3.8(11)
H8(C3)	.150(4)	.945(4)	-.017(4)	4.8(12)
H9(C2)	.182(4)	.802(3)	-.080(4)	3.3(10)
H10(C10)	.252(5)	.570(4)	-.074(4)	5.6(14)
H12(C10)	.247(5)	.661(4)	-.109(5)	6.0(15)
H13(C10)	.146(5)	.605(4)	-.143(5)	5.4(18)
H14(N7)	.153(4)	.327(3)	.085(4)	3.5(10)
H15(N7)	.127(3)	.316(3)	.188(4)	1.8(19)
H16(W1)	-.103(5)	.574(4)	.088(5)	5.8(19)
H17(W1)	-.126(5)	.598(4)	.173(5)	3.3(16)
H18(W2)	.301(4)	.623(3)	.304(4)	3.9(13)
H19(W2)	.262(6)	.634(5)	.389(6)	6.8(21)
H20(W3)	.266(7)	.846(6)	.755(7)	15.2(22)
H21(W3)	.183(7)	.930(5)	.726(6)	10.9(23)

Table 4-9. Hydrogen Atomic Parameters x,y,z and Biso for II. E.S.Ds. refer to the last digit printed.

	x	y	z	Biso
H1(C7)	.690	.855	.394	3.9
H2(C7)	.659	.805	.462	3.9
H3(C7)	.560	.847	.453	3.9
H4(C2)	.618	.654	.491	3.6
H5(C3)	.619	.485	.495	3.6
H6(C4)	.622	.473	.338	4.3
H7(C10)	.572	.502	.198	3.9
H8(C10)	.699	.511	.160	3.9
H9(C10)	.608	.529	.081	3.9
H10(C18)	.944	.062	.658	6.0
H11(C18)	.835	.128	.607	3.9
H12(C18)	.817	.067	.704	3.9
H13(C13)	.859	.014	.871	3.8
H14(C14)	.875	.015	1.029	3.6
H15(C15)	.881	.183	1.033	4.5
H16(C21)	.875	.460	.946	3.9
H17(C21)	.806	.372	1.009	3.9
H18(C21)	.933	.331	.989	4.6
H19(C112)	.635	.736	-.185	3.7
H20(C113)	.624	.803	-.365	4.6
H21(C114)	.622	.990	-.474	5.0
H22(C115)	.624	1.108	-.406	5.2
H23(C116)	.662	1.035	-.230	4.0
H24(C222)	.884	.723	.744	4.6
H25(C223)	.907	.908	.660	5.2
H26(C224)	.891	1.011	.477	4.7
H27(C225)	.869	.928	.383	5.1
H28(C226)	.845	.745	.463	4.6
H29(C82)	.642	1.204	-.095	4.6
H30(C83)	.637	1.392	-.166	4.4
H31(C84)	.590	1.481	-.053	4.6
H32(C85)	.562	1.379	.134	5.8
H33(C86)	.583	1.186	.204	3.9
H34(C192)	.855	.601	.302	4.2
H35(C193)	.873	.650	.120	3.6
H36(C194)	.921	.516	.056	4.1
H37(C195)	.915	.336	.173	6.7
H38(C196)	.894	.278	.359	4.9
H39(W1)	.458	.914	.062	3.9
H40(W1)	.507	.900	.164	3.9
H41(W2)	.806	.885	.084	3.9
H42(W2)	.834	.819	.056	3.9
H43(W3)	.668	.477	.676	3.9

Table 4-9 (cont.).

	x	y	z	Biso
H44(W3)	.769	.416	.682	3.9
H45(W4)	1.049	.442	.597	3.9
H46(W4)	1.078	.383	.577	3.9
H47(W5)	.780	.669	.915	3.9
H48(W5)	.859	.674	.887	3.9
H49(W6)	.679	1.043	.259	3.9
H50(W6)	.705	1.105	.264	3.9
H51(W7)	.336	.718	.467	3.9
H52(W8)	.633	.282	.314	3.9
H53(W8)	.582	.198	.388	3.9
H54(W9)	.947	.093	.195	3.9
H55(W9)	.920	-.005	.198	3.9

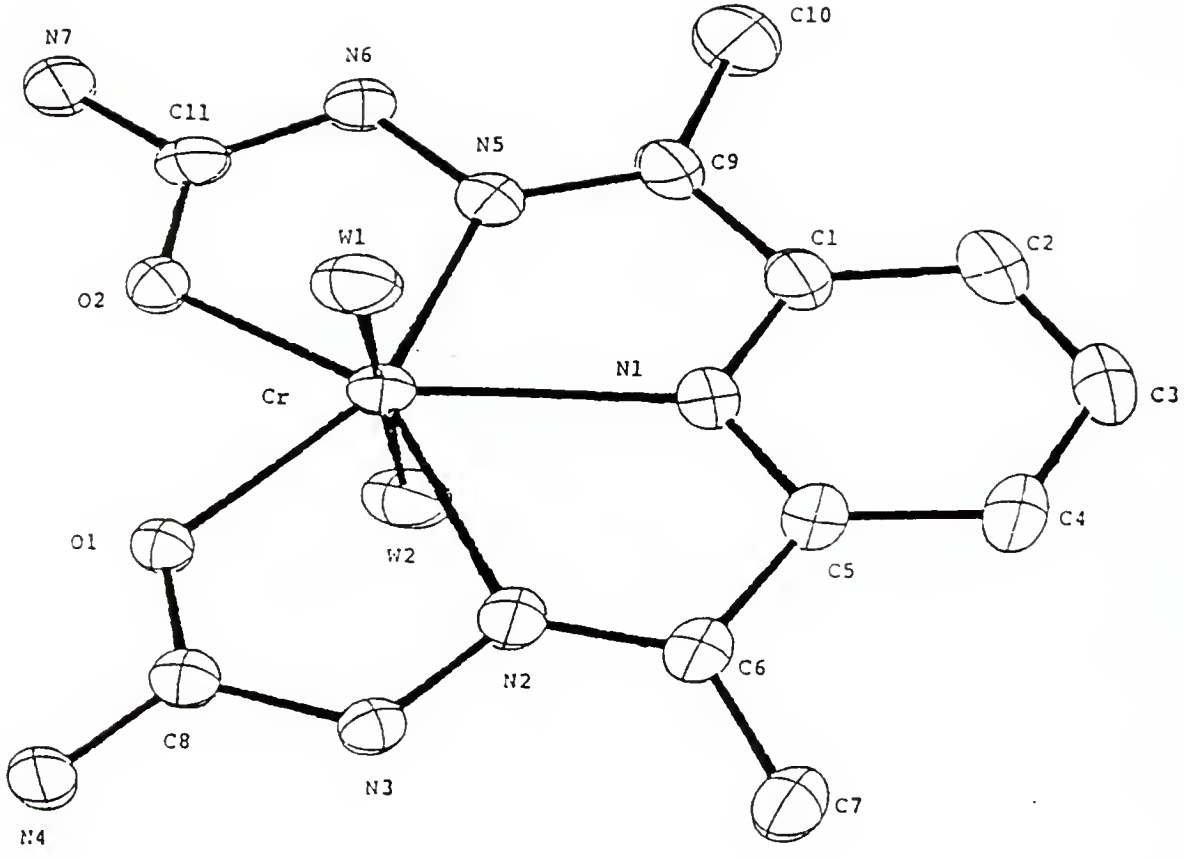

Figure 4-1. An ORTEP representation of Compound I.

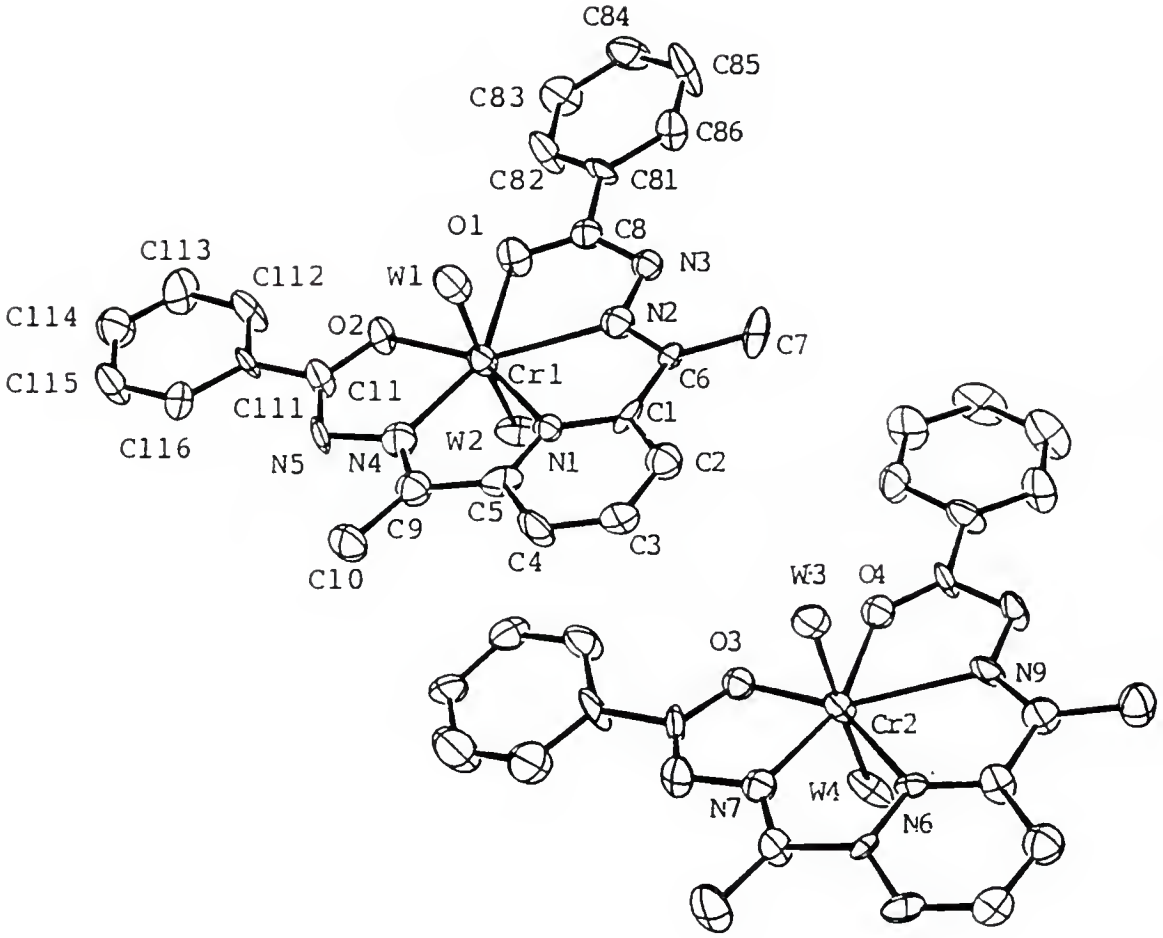

Figure 4-2. An ORTEP representation of compound II.

Table 4-10. Bond Distances in Å Within the Coordination Sphere

	I	II	
Cr - W1 =	1.955	1.984	2.027
- W2 =	1.962	1.992	1.993
- O1 =	2.112	2.203	1.987
- O2 =	1.970	1.974	2.094
- N1 =	2.258	2.181	2.231
- N2 =	2.396	2.330	1.996
- N5 =	2.043	2.034	2.440

Jahn - Teller Effect. Previously it was suggested[8] that the asymmetry observed in PBP Cr(III) complexes was due to a Jahn-Teller distortion[31] which occurs to remove the orbital degeneracy. Since both compounds exhibit solution magnetic moments corresponding to 3 unpaired electrons, the central Cr ion can be described as a d^3 system. The energy level diagrams, Figure 4-3, for the d-orbitals in PBP geometry[33,34] require placing one electron in either the antibonding $d_{x^2-y^2}$ or d_{xy} orbital. Assuming regular D_{5h} geometry, the imposed crystal field would lead to an orbital degeneracy which may be removable by a Jahn-Teller vibronic distortion.

With three unpaired electrons, an electron configuration of $e''_1{}^2$, e'_2 is obtained for Cr(III) in a PBP field. Upon coupling the two e''_1 electrons, a triplet spin function is obtained which is symmetric, consequently the antisymmetric direct product of the two electrons must be taken as required by the Pauli principal to produce an overall spin function which is antisymmetric.

$$[e''_1 \times e''_1]_{anti} = {}^3A'_2$$

Now coupling in the e'_2 electron and taking the symmetric direct product the ground state term symbol

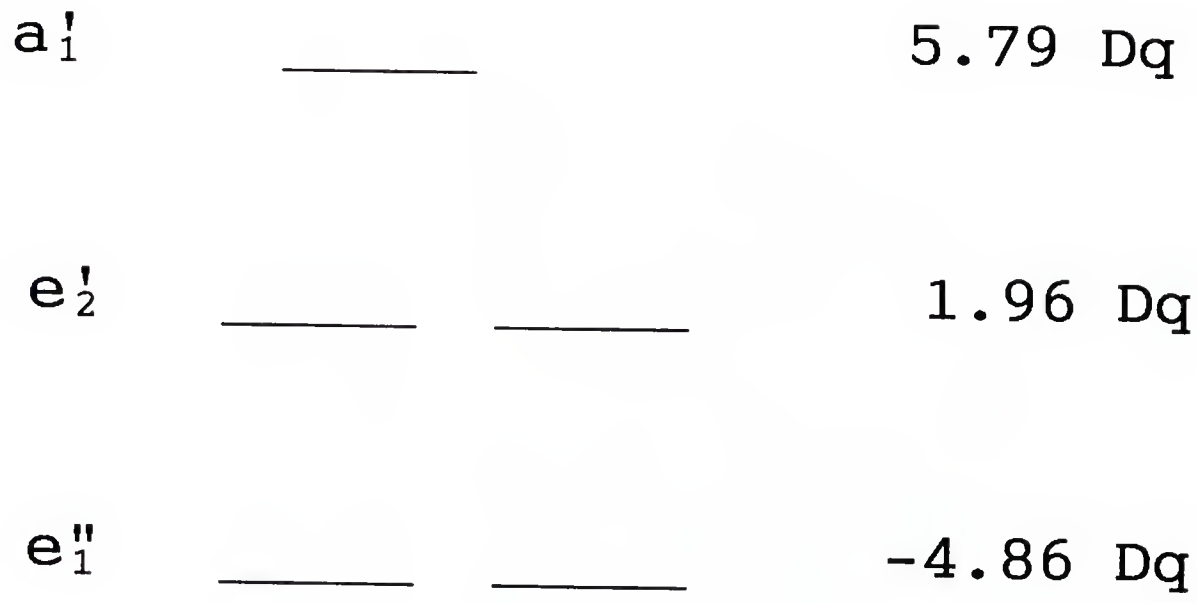

Figure 4-3. Crystal Field Splitting for a Pentagonal Bipyramidal Field (D_{5h})

$$[A'_2 \times e'_2]_{sym} = {}^4E'_2$$

is obtained. Attention must now be given to how the spin portion of the wave function transforms in the point group symmetry by looking at the spin-orbit coupling effects. If there is strong spin-orbit coupling, four states arise as shown below but all are Kramers doublets and thus not Jahn-Teller active.

Spin = 3/2

(i.e. quartet ground state)

$$3/2 = E_{1/2} + E_{3/2}$$

$$[E_{1/2} + E_{3/2}] \times E'_2 = E_{3/2} + E_{5/2} + E_{1/2} + E_{3/2}$$

In the case of Cr(III) the spin-orbit coupling can be considered weak[35]. In consequence upon taking the symmetric direct product of the E'_2 vibronic state only

$$[E'_2 \times E'_2] = A'_1 + E'_1$$

is obtained.

Although the A'_1 state is totally symmetric and not Jahn-Teller active, the E'_1 state is a two fold degenerate vibration and could indeed give rise to a Jahn-Teller vibronic distortion.

Although it is not our purpose to make any quantitative calculation on the magnitude of this distortion, the Jahn-Teller effect for a d^3 metal ion in a PBP field is important

since the orbital degeneracy involves an electron in either a $d_{x^2-y^2}$ or a d_{xy} orbital both of which participate strongly in bonding in the equatorial plane.

Deprotonation of the Ligand. A second contribution to the observed distortion in both PBP - Cr(III) complexes arises from the formation of a half-conjugated monoanion which results from the deprotonation of one of the NH functions of the respective ligand "arm" as shown in Figure 4-4. In complex I the hydrogen atom on N6 was not located; consequently, the ligand becomes a half-conjugated monoanion and as a result the overall charge on the complex has a 2+ which is balanced by two NO_3^- ions. Behavior of this type is not unusual as has been pointed out previously[29,36,37]. The bond lengths from the deprotonated arm to the Cr(III) ion are shorter than those on the opposite side as might be expected from electrostatic arguments.

The quality of the final difference map for complex I was not of sufficient quality to locate all hydrogens with certainty. It is likely that both molecules have lost one proton since each molecule has two chloride ions associated with it and requires a third negative charge to balance the 3+ state of the metal. Since the complex was obtained from a highly acidic solution, the existence of a OH^- ion rather than a water molecule in the unit cell is unlikely.

Deprotonation of either DAPSC or DAPBAH leads to the delocalization of the π-electrons in the ligand arm.

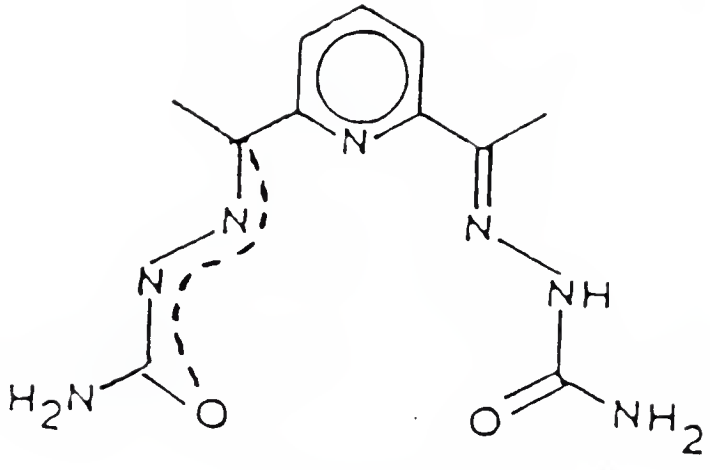

Figure 4-4. A representation of the half-conjugated monoanion which results from the deprotonation of the ligand.

Lengthening of the C=O and N=C bonds and a shortening of the N-C bond is observed in both 1 and 2 as would be expected. The N-N bond would also be expected to shorten though we find the bond actually lengthens which is in accord with previous reports[9,29]. This lengthening may be due to the presence of a π-nodal plane perpendicular to the equatorial plane of the pentagonal bipyramid which bisects the N-N bond. Deprotonation of the ligand puts an additional electron into the delocalized π-orbital which would in turn cause greater repulsion at the nodal plane. Hence π-orbital antibonding interactions are a more likely cause of this anomaly than ring stress in the five membered ring resulting from the strong attraction of the negatively charged portion of the ligand to the metal as has been suggested[29].

In conclusion, we see that PBP complexes of Cr(III) with either DAPSC or DAPBAH are readily obtained from aqueous media. Moreover, these two complexes provide additional examples of static Jahn-Teller distortions in PBP complexes. Furthermore, the distortions observed cannot be accounted for totally in terms of either a Jahn-Teller distortion or the formation of a half-conjugated monoanion but rather by a combination of both effects.

CHAPTER 5

SYNTHESIS AND CRYSTAL STRUCTURE OF A WATER SOLUBLE CATIONIC (η^3,η^3-$C_{10}H_{16}$)Ru(IV) COMPLEX: CHLORO[(1-3-η:6-8-η)-2,7-DIMETHYLOCTADIENEDIYL]SEMICARBAZIDE RUTHENIUM(IV) CHLORIDE DIHYDRATE.

Introduction

There is current interest in high formal oxidation state Ru complexes as models for the heme protein system, as well as for their relevance in catalytic processes[38-43] and for their use as oxidizing agents for organic synthesis[44]. Although stable bis(π-allyl)ruthenium complexes have been prepared[41], the reactions of the chloro-bridged dimer di-u-chloro-bis[(2,7,-dimethyl-octa-2,6-diene-1,8-diyl)ruthenium(IV)] chloride,I, has not been extensively studied. We chose to study the reaction of DAPSC with I[45-47] in an attempt to prepare a PBP Ru(IV) complex.

One problem encountered in preparing PBP complexes of the second and third transition series is that the spin-orbit coupling effect has a major influence on the splitting of the d-orbitals. This effect magnifies the energy differences between the d-orbitals which are initially produced by the PBP ligand field encountered by the metal-cation. The greatest difference in energy for second and third row metals comes between the e'_2 and e''_1 orbitals (Figure 4-3) with the e'_2

orbitals increasing dramatically in energy as compared to the $e"_1$ orbitals. Thus, it is reasonable to expect that metal cations with electron configurations of d^4 or lower[4] would be easier to isolate since it would not require the placement of one or more electrons into the higher energy orbitals.

Since a Ru(IV) complex had been reported[48] where bidentate ligands had been used to achieve PBP geometry, we were interested in exploring whether a pentadentate ligand could also be used to isolate Ru in a high formal oxidation state. The reported oxidation state of I suggested that the metal was d^4. Furthermore, this compound was known to be air stable and relatively uncomplicated to prepare. Consequently we decided to use I as a source of Ru(IV) in our study.

Rather than the expected PBP complex, a novel 5-coordinate species was isolated with an unusual trigonal bipyramidal, TBP, geometry around the Ru center resulting from a disruption of the chlorine bridges in the dimeric Ru starting material and the solvolysis of the DAPSC ligand. The new complex is the first example of a Ru(IV) ion chelated by both two (η^3-allyl) functions and a semicarbazide ligand.

Recently, the isomerism and solution equilibria for the chloro-bridged dimer, I, was reported and the possible existence of cationic species was postulated[49]. Indeed, this is the first report of the isolation and structural characterization of such a species.

Experimental

Materials. All solvents and chemicals were reagent grade and were used as supplied.

Synthesis. Dichloro(2,7-dimethyl-octa-2,6-diene-1,8-diyl)ruthenium chloride, I,[50] and DAPSC[9] were synthesized by methods previously described. Into 35 mL of deionized H_2O, DAPSC (0.045g, 0.2 mmole) was slurried together with I (0.050g, 0.1 mmole). This mixture was stirred and heated to 55°C for two hours. A clear yellow/brown solution was obtained which was filtered through a fine glass frit while warm. Upon reaching room temperature (23°C), the pH of the solution was adjusted to 1.45 with HCl. Brown, air stable single crystals were obtained from the above solution in 10 days by the slow evaporation of the solvent. The compound was found to be quite soluble in H_2O and decomposed at 180°C.

The yield of this compound can be increased dramatically by the reaction of I with semicarbazide directly. For example, 0.050g (0.1 mmole) of I was combined with 0.0181g (0.2 mmole) semicarbazide hydrochloride in 35 mL deionized water (pH = 1.50) and heated to 55°C for 2 hrs.. A clear yellow-brown solution formed which was filtered and allowed to cool to room temperature(25°C). Slow evaporation of this solution produced, after 12 days, brown crystals of the title complex (yield 77%). Elemental analysis: Calc. C = 31.50%, H = 6.01%, N = 10.02%, Found C = 31.30%, H = 6.20%, N = 9.91%.

X-ray Crystallography. A crystal 0.05 x 0.07 x 0.13 mm suitable for diffraction studies was mounted on the end of a glass fiber and all subsequent measurements were made using a Nicolet R3m diffractometer with graphite-monochromated Mo-Kα radiation (λ = 0.71069Å). The cell dimensions were determined by a least squares refinement of 25 automatically centered reflections. A variable-speed (1° - 29.3°) 2θ scan technique was used to measure the intensity data from 0° to 45° degrees in 2θ. Two standard reflections were measured every 98 reflections to monitor for any decomposition during the x-ray analysis. No absorption correction was made. The pertinent crystal data is given in Table 5-1.

Structure Refinement. The data reduction, structure solution and final refinement were performed using the NRCVAX (PC-Version)[18] package of programs. The Ru atom and all non-hydrogen atoms were located by the heavy-atom method (Patterson and Fourier syntheses) and refined anisotropically by full-matrix least squares. The hydrogen atoms were located by the calculation of a difference Fourier map and refined isotropically. The model converged to an R of 0.027 and a Rw of 0.034. The final positional parameters are given in Table 5-2. The final bond distances involving the non-hydrogen atoms and bond angles are listed in Table 5-3. Table 5-4 lists the anisotropic thermal parameters and Table 5-5 lists the hydrogen positional parameters.

Table 4-1. Crystal Data

formula	$RuC_{11}N_3O_3H_{25}Cl_2$
MW	419.31
a, Å	7.1907(12)
b, Å	15.280(4)
c, Å	7.8244(21)
α, deg	90.305(22)
β, deg	102.154(18)
γ, deg	89.895(18)
Vol., $Å^3$	840.4
Z	2
ϱ_{calc}, g/cm^3	1.66
space group	P 1bar
μ, cm^{-1}	26.1
no. of data used (Inet>2.5σInet)	2603
R^a	2.7
$R_w{}^b$	3.4

$$R=\sum \frac{|F_o|-|F_c|}{|F_c|}$$

$$R_w=\left[\frac{\sum w(|F_o|-|F_c|)^2}{\sum w|F_o|^2}\right]^{1/2}$$

Table 5-2. Atomic Parameters x,y,z and Biso.

	x/a	y/b	z/c	Biso
Ru	.21704(4)	.22152(2)	.29801(4)	1.765(12)
Cl1	.4133 (2)	.1624 (1)	.5579 (1)	3.05 (4)
O1	.0130 (4)	.3004 (2)	.1373 (3)	2.54 (11)
N3	.1059 (5)	.2994 (2)	.4855 (4)	2.27 (13)
C2	.4176 (6)	.2803 (3)	.1500 (5)	2.56 (17)
C8	.1037 (6)	.0868 (3)	.2342 (6)	2.88 (18)
CL2	-.2225 (2)	.4335 (1)	.7044 (1)	3.31 (5)
C1	.4176 (6)	.3321 (3)	.3017 (6)	2.79 (17)
C3	.3422 (8)	.3153 (3)	-.0332 (6)	3.83 (23)
C4	.4720 (6)	.1922 (3)	.1874 (6)	2.60 (17)
C5	.4586 (7)	.1207 (3)	.0508 (6)	3.51 (20)
C6	.2511 (7)	.1021 (3)	-.0383 (6)	3.39 (20)
C7	.1166 (6)	.1292 (3)	.0776 (6)	2.63 (17)
C9	.2157 (8)	.0059 (3)	.3003 (7)	4.08 (23)
C10	-.0126 (7)	.1303 (3)	.3309 (6)	3.17 (19)
C11	-.0655 (6)	.3574 (3)	.2169 (5)	2.28 (16)
N1	-.1857 (5)	.4155 (2)	.1310 (5)	2.91 (15)
N2	-.0314 (5)	.3589 (3)	.3926 (5)	3.01 (15)
W1	-.6733 (4)	.4531 (2)	.6394 (4)	3.13 (13)
W2	.8546 (5)	.2259 (2)	.7018 (5)	3.84 (16)

Table 5-3. Bond Distances(Å) and Angles(°)

Ru - C11	2.3976(12)	C2 - C1	1.423(6)
Ru - O1	2.102(3)	C2 - C3	1.521(6)
Ru - N3	2.162(3)	C2 - C4	1.417(6)
Ru - C1	2.219(4)	C8 - C7	1.409(7)
Ru - C2	2.224(4)	C8 - C9	1.508(7)
Ru - C4	2.230(4)	C8 - C10	1.404(6)
Ru - C7	2.223(4)	C4 - C5	1.514(6)
Ru - C8	2.230(4)	C5 - C6	1.534(7)
Ru - C10	2.220(5)	C6 - C7	1.514(6)
O1 - C11	1.267(5)	C11 - N1	1.319(5)
N3 - N2	1.426(5)	C11 - N2	1.345(5)

C11-Ru-O1	159.70(8)	C11-Ru-N3	82.39(9)
C11-Ru-C2	105.45(12)	C4-Ru-C10	127.80(17)
C11-Ru-C8	87.80(12)	C7-Ru-C10	64.14(17)
Ru-O1-C11	115.24(24)	Ru-N3-N2	108.58(22)
Ru-C2-C1	71.15(24)	Ru-C2-C3	119.6(3)
O1-Ru-N3	77.33(11)	Ru-C2-C4	71.67(23)
O1-Ru-C2	84.35(14)	C1-C2-C3	121.8(4)
O1-Ru-C8	102.72(14)	C1-C2-C4	113.6(4)
C3-C2-C4	124.1(4)	Ru-C8-C7	71.27(24)
Ru-C8-C9	122.5(3)	Ru-C8-C10	71.21(25)
N3-Ru-C2	120.20(15)	C7-C8-C9	123.4(4)
N3-Ru-C8	119.04(15)	C7-C8-C10	114.0(4)
C9-C8-C10	122.4(4)	C2-Ru-C8	120.42(17)
C2-C4-C5	124.3(4)	C4-C5-C6	111.4(4)
C5-C6-C7	111.2(4)	C8-C7-C6	124.3(4)
O1-C11-N1	121.4(4)	O1-C11-N2	120.4(4)
N1-C11-N2	118.2(4)	N3-N2-C11	118.1(3)

Table 5-4. U values *100.
E.S.Ds. refer to the last digit printed

	U11(σ)	U22	U33	U12	U13	U23
Ru	2.189(17)	2.385(16)	2.194(16)	.345(12)	.604(12)	.002(11)
Cl1	3.68 (6)	4.67 (6)	3.04 (5)	.82 (5)	.22 (4)	.78 (5)
O1	3.77 (17)	3.44 (16)	2.41 (14)	1.26 (13)	.64 (12)	-.26 (12)
N3	3.19 (19)	3.08 (18)	2.46 (17)	.71 (15)	.84 (14)	.09 (14)
C2	2.89 (22)	3.98 (24)	3.22 (22)	-.55 (18)	1.45 (18)	.12 (18)
C8	3.33 (24)	2.77 (22)	4.8 (3)	-.70 (18)	.78 (20)	-.55 (19)
C12	5.16 (7)	4.39 (6)	3.13 (5)	1.20 (5)	1.10 (5)	.21 (5)
C1	4.0 (3)	3.44 (23)	3.41 (23)	-.75 (19)	1.22 (19)	-.38 (18)
C3	6.7 (4)	5.1 (3)	3.30 (25)	.1 (3)	2.09 (24)	1.11 (22)
C4	2.34 (21)	4.04 (24)	3.82 (23)	.32 (18)	1.39 (18)	-.36 (19)
C5	4.2 (3)	4.8 (3)	4.8 (3)	.85 (22)	1.99 (22)	-1.04 (22)
C6	4.8 (3)	4.3 (3)	3.9 (3)	.21 (22)	1.13 (22)	-1.58 (21)
C7	3.40 (23)	2.78 (21)	3.66 (23)	-.01 (18)	.42 (18)	-.94 (18)
C9	6.1 (3)	2.72 (24)	6.4 (3)	.21 (22)	.6 (3)	.47 (23)
C10	3.34 (25)	3.9 (3)	5.1 (3)	-.77 (20)	1.50 (21)	-.36 (21)
C11	2.69 (21)	3.12 (21)	2.92 (21)	.41 (17)	.75 (17)	.01 (17)
N1	4.16 (22)	3.81 (20)	2.99 (19)	1.62 (17)	.54 (16)	.28 (16)
N2	4.47 (22)	4.42 (22)	2.67 (18)	2.15 (18)	1.08 (16)	.12 (16)
W1	4.24 (19)	4.25 (18)	3.71 (17)	.25 (14)	1.55 (14)	.19 (14)
W2	4.59 (20)	4.47 (19)	5.68 (22)	.02 (16)	1.44 (17)	.02 (16)

Anisotropic Temperature Factors are of the form --
Temp=-2*Pi*Pi*(h*h*u11*astar*astar+---+2*h*k*u12*astar*bstar+---)

Table 5-5. Hydrogen Atomic Parameters x,y,z and Biso. E.S.Ds. refer to the last digit printed.

	x/a		y/b		z/c		Biso	
H1(N1)	-.230	(7)	.472	(3)	.196	(7)	5.1	(12)
H2(N1)	-.196	(8)	.423	(3)	-.008	(7)	5.7	(13)
H3(N2)	-.104	(7)	.400	(3)	.472	(7)	5.1	(13)
H4(N3)	.213	(7)	.343	(3)	.555	(6)	4.4	(12)
H5(N3)	.032	(7)	.259	(3)	.562	(6)	3.9	(11)
H6(C1)	.357	(7)	.397	(3)	.283	(6)	3.6	(11)
H7(C1)	.520	(7)	.316	(3)	.419	(6)	4.1	(12)
H8(C3)	.448	(8)	.344	(4)	-.097	(7)	6.5	(14)
H9(C3)	.325	(7)	.385	(3)	-.016	(7)	5.5	(13)
H10(C3)	.249	(8)	.273	(3)	-.113	(7)	3.9	(13)
H11(C4)	.582	(7)	.175	(3)	.299	(6)	3.2	(11)
H12(C5)	.522	(7)	.061	(3)	.111	(7)	4.5	(12)
H13(C5)	.543	(7)	.139	(3)	-.043	(7)	4.8	(12)
H14(C6)	.210	(7)	.140	(3)	-.157	(6)	4.3	(12)
H15(C6)	.239	(7)	.032	(3)	-.063	(6)	4.1	(12)
H16(C7)	-.005	(7)	.166	(3)	.009	(6)	3.8	(11)
H17(C9)	.133	(7)	-.052	(3)	.254	(7)	5.4	(13)
H18(C9)	.222	(7)	.003	(3)	.440	(7)	5.5	(13)
H19(C9)	.368	(8)	.013	(3)	.314	(7)	5.8	(13)
H20(C10)	-.136	(7)	.166	(3)	.264	(6)	4.0	(11)
H21(C10)	-.020	(7)	.107	(3)	.459	(7)	4.9	(12)
H22(W1)	-.559	(9)	.475	(4)	.579	(8)	3.9	(17)
H23(W1)	-.525	(8)	.434	(4)	.681	(7)	7.0	(14)
H24(W2)	.717	(7)	.199	(3)	.642	(7)	5.2	(13)
H25(W2)	.817	(8)	.292	(3)	.729	(7)	5.8	(13)

Where Biso is the mean of the principal axes of the thermal ellipsoid.

Results and Discussion

Structure of the Compound. An ORTEP representation of the title compound along with the labeling scheme is given in Fig. 5-1.

The geometry of the complex can be described as a distorted TBP which is similar to the triflurophosphine Ru(IV) complex[47] previously reported with the Ru atom located at the center. The Ru ion along with C(2), C(8), and N(3) define the equatorial plane of the TBP with O(1) and Cl(1), the two most electronegative species, residing in off-axial positions as might be expected.

Within the Ru coordination sphere there is significant distortion from true TBP geometry exemplified by the O1-Ru-N3 angle of 77.3°. The constraint imposed by the formation of a 5-membered chelate ring where the semicarbazide spans an axial-equatorial position is a likely contributor to this distortion. The O1-Ru-N3 angle along with the other dimensions within the semicarbazide portion of the complex are similar to those we have previously reported[7-9] where it is part of the DAPSC ligand.

The dimeric nature of the starting material has been broken and a semicarbazide has replaced the two bridging chlorides of the starting material. This is a result of the Schiff base function of DAPSC being hydrolyzed which is essentially the reverse of the reaction used to form the ligand. Upon coordination of the Schiff base nitrogen to the

Ru, the dative bond formed is strongly polar towards the Ru resulting in electron density being directed away from the C adjacent to the N. This C then becomes susceptible to nucleophilic attack by H_2O which breaks up the Schiff base function. This is the first time this type of reaction has been observed to take place with DAPSC.

The Organo-metallic Interaction. The C2-C1 and C2-C4 bond lengths together with the C8-C7 and C8-C10 bond lengths provide clear evidence that the electron density for the allyl functions are delocalized over atoms (C1,C2 & C4) and (C7,C8 & C10) at opposite ends of the carbon skeleton respectively. Thus, both η^3-allyl groups may then be considered 3-electron donors following the convention suggested by Powell[51]. In addition the axial O and equatorial N are 2 electron donors and the remaining Cl donates a single electron to the metal center. Since the complex is known to be a cation from the structural results, the Ru center is assigned 7-electrons and an EAN of 18 is attained by the Ru center. This is in agreement with similar assignments of electrons for Ru-allyl interactions of this type[45,46,52].

Spanning two equatorial sites, the 2,7-dimethyl-octa 2,6-diene-1,8-diyl has dimensions quite similar to those previously reported[46]; however, a striking feature of the organic portion is the small angle made by C1-C2-C4 (113.6°) and C7-C8-C10 (114.0°) both of which are significantly less than 120° expected for a sp^2 type carbon atom.

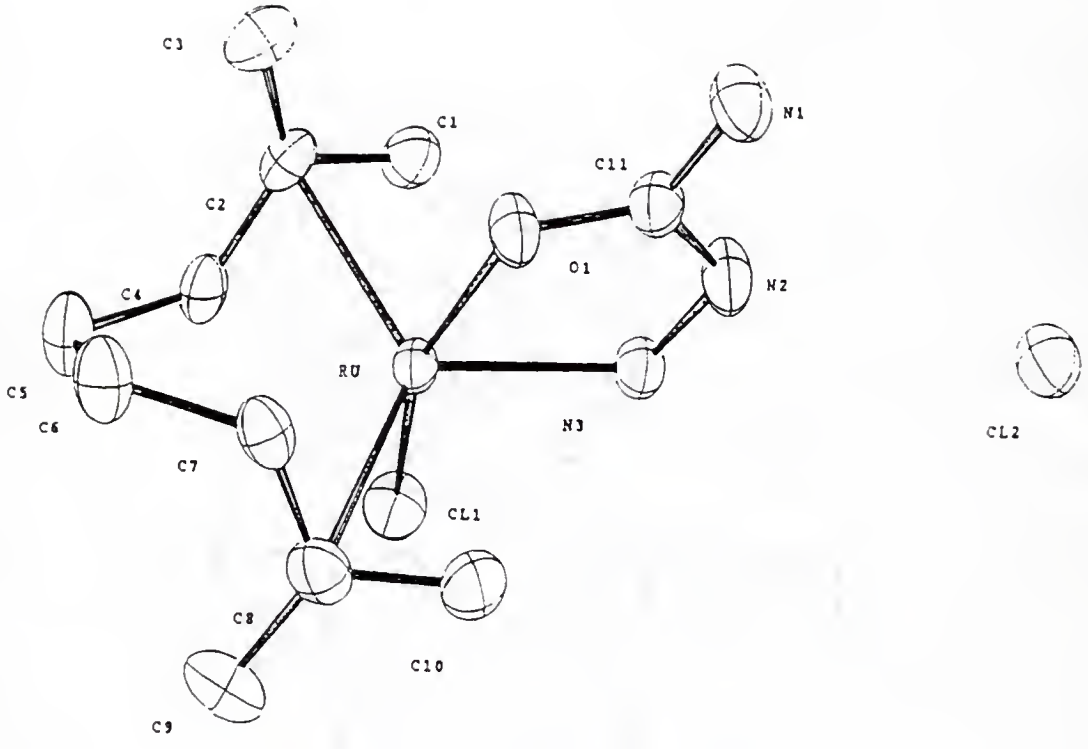

Figure 5-1. An ORTEP Representation of Chloro[(1-3-η:6-8-η)-2,7-dimethyloctadienediyl]semicarbazide-ruthenium(IV) Chloride Dihydrate.

As 3-electron donors, the $\eta 3$-allyl functions have three delocalized electrons in the pπ orbital. As electrons fill the three molecular orbitals, the pi-bonding orbital is filled first and the non-bonding orbital is singly occupied. Since the bonding orbital is bonding overall, it can be seen from Figure 5-2 where the bonding, nonbonding, and antibonding molecular orbitals are shown a - c respectively, that there will be a slight attraction of the terminal allyl carbons which in turn would lead to a decrease of the C-C-C angle from 120°. There will however be a second force counter to the one just described resulting from the singly occupied allyl non-bonding orbital which is directed at minimizing the antiaromatic character of the terminal pπ orbitals of the η^3-allyl function. It would be expected that a decrease in the C-C-C angle would most likely be exhibited since the bonding orbital is filled where the non-bonding orbital is singly occupied.

This qualitative bonding description is supported as a first approximation by geometry optimization calculations[53-55] involving η^3-allyl molecules in isolated states. The calculations show that with the addition of electons to the delocalized π-orbital, the C-C-C angle increases significantly, 120° - 132°, from the π-allyl cation to the anion respectively.

Formal Oxidation State Assignment. It is clear that the title complex is ionic due to the presence of the Cl- in the

A

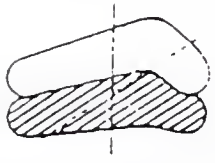

B

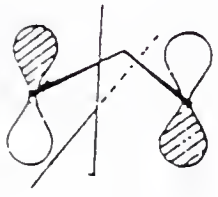

C

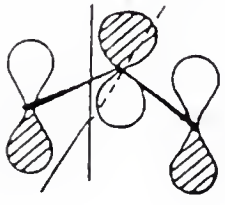

Figure 5-2. A representation of the bonding (A), non-bonding (B), and anti-bonding (C) molecular orbitals for a 3-electron η^3-allyl function.

lattice. A second Cl- resident in the coordination sphere and the two η^3-allyl functions, each assigned as -1 donors, brings the anionic charge to -4 and hence the Ru is formally (IV) by accepted conventions[46,56]. The general tendency to observe spin-paired complexes and high spin orbit coupling constants for second and third row transition metals makes the direct determination of the formal oxidation state for a Ru center difficult at best. Hence we stress that it is highly unlikely that a Ru center in the described chemical environment would resemble a Ru 4+ cation. As Seddon and Seddon[57] point out, whenever ligands are strong π-donors or π-acceptors (i.e. allyl), traditional oxidation formalism no longer holds. Moreover, long accepted tenets such as the Principle of Electroneutrality[58] and the Principal of Electronegativity Equalization[59] would not support the existence a high oxidation state as 4+ in any real sense.

Cambridge Crystallographic Database Results. Since Ru(IV) complexes are of current interest, we felt some insight could be gained concerning the nature of the Ru(IV) cation in the title compound by comparing it with other Ru structural data cataloged in the Cambridge Crystallographic Database.

Since it is generally accepted for transition metals that with an increasing oxidation state there is a corresponding decrease in the bond lengths within the coordination sphere, we decided to investigate the relation of the Ru - Cl bond length of known complexes as a function of

the formal oxidation state. Structures with an Rfact > 9.1% or containing bridging Cl atoms were discarded to narrow a search of the Cambridge Database[60] which provided 289 structures containing Ru - Cl bonds. Furthermore, we were able to search the file in a narrower fashion and correlate the Ru - Cl bond lengths in relation to the species trans to Cl (defined as species coordinated to Ru and making an angle of 160 to 180 with the Cl of the Ru - Cl of interest) and the oxidation state of the Ru in the complex as determined from the literature.

Several interesting trends were observed and the results of these searches are summarized in Table 5-6.

These results suggest that if hard donors such as N, O, and Cl are trans to Cl, there is noticeable variation in the Ru - Cl bond length with changing oxidation state. In complexes where Ru is formally (II) the Ru - Cl bond length is somewhat longer (ca. 0.05Å) than where Ru is formally (III). Since hard donors tend to be more ionic in nature, shorter bond lengths with an increase in oxidation state from (II) to (III) is not a surprise though the behavior is not as pronounced as with the first row metals which are more ionic in nature.

There is a dramatic change in the Ru - Cl bond lengths observed when soft donors such as C, P, and S are trans relative to Cl. In these complexes Ru is formally (II) and the Ru - Cl bond lengths are longer on average than those

Table 5-6. Summary of the Ru-Cl Bond Distances

OX State of Ru	Trans Species (X)	Ru - Cl dist.	No. Averaged	Ref.§
II	N	2.399	14	1 - 14
III	N	2.358	8	15 - 22
IV	N	2.397	1	23
II	O	2.397	1	24
III	O	2.348	5	25 - 29
IV	O	2.505	1	30
II	Cl	2.407	24	31 - 54
III	Cl	2.351	10	55 - 64
IV	Cl	2.389	6	65 - 70
II	C	2.445	28	71 - 98
II	P	2.479	4	99 - 102
II	S	2.441	7	103 - 109
IV	S	2.448	1	110

§ The complete reference for each structure can be found in Appendix 1.

found for Ru(II) with the harder donors by ca. 0.05A. This increase in the Ru -Cl bond length suggests a trans influence.

Finally, it is interesting to note that where Ru is formally (IV), the Ru - Cl bond length mimics that observed for Ru when it is formally (II) in each case where data is available.

Conclusion

The growing interest in the organometallic chemistry of the Ru(IV) formal oxidation state centers around the cations role in bond activation and redox reactions. We have shown that the Ru-Cl bond lengths exhibited for the title compound and those of similar structures are quite analogous to those found for Ru(II) complexes. We were able to detect a difference from structural data in the Ru-Cl bond length for Ru(II) and Ru(III) but not for Ru(IV) which suggests that the oxidation state formalism used, in relation to ionic character, breaks down at (IV) and may be at its limit for (II) and (III).

There is great potential for reactivity at the Ru center of the dimer as evidenced by the hydrolysis reaction which lead to the formation of the title complex. The ability to obtain this complex by the direct reaction of semicarbazide hydrochloride with I will provide access to a large number of cationic Ru(IV) complexes. Since this compound is water soluble there exists the potential for the development of a water-based organometallic chemistry.

CHAPTER 6

A THEORETICAL INVESTIGATION OF THE ELECTRONIC AND STRUCTURAL PROPERTIES OF THE LIGAND DAPSC AND THE PENTAGONAL BIPYRAMIDAL COMPLEX DIAQUA(2,6-DIACETYLPYRIDINEBIS(SEMICARBAZONE))IRON(II).

Introduction

Throughout our investigations involving DAPSC we have not been able to obtain any structural information regarding the ligand as an isolated molecule. Our data, in terms of conformation, bond distances and bond angles, has come exclusively from X-ray structural measurements where DAPSC is coordinated to a transition metal-cation. In each instance where we have observed this ligand as part of a PBP complex, we have also noted the ligand to be planar though in some cases there appears to be a slight distortion similar to the type described for the [Ti(DAPBAH)Cl_2] complex in chapter 2. The conformation DAPSC has adopted repeatedly in each of the PBP complexes is one where both semicarbazone "arms" of the ligand are directed outwards, identical to the conformation shown in Figure 1-1. It became clear during the course of this project that if a plausible model of this molecule was to be developed, the question of conformation had to be addressed; particularly which ones were favored energetically and sterically by this molecule.

Since the ligand DAPSC is not soluble in any common solvent or mixture of solvents, the possibility of obtaining single crystals for X-ray diffraction studies was remote. Furthermore, dissolving a large enough sample of this compound in an appropriate solvent to obtain NMR spectra has not been possible either. Recent reports[61,62] discussing how molecular mechanics (MM) calculations have become increasingly important in the study of coordination chemistry, particularly with regard to ligands, provided a hint as to how we might proceed with this investigation into the nature of DAPSC. Since organic chemists have been very successful in using MM calculations to predict bond lengths in organic molecules to within 0.01Å, and bond angles to within 1.2° of the experimentally observed values[63], performing this type of a calculation on DAPSC appeared to be an excellent place to begin work.

Consequently, we turned from physical methods to those of theory, specifically molecular mechanics and semi-empirical quantum mechanical methods of the INDO (Intermediate Neglect of Differential Overlap) type. Both of these methods are currently developed to levels where they are practical and can be used effectively in treating systems the size of a DAPSC molecule. Thus in an effort to learn more about the structural and conformational properties of the DAPSC molecule, a theoretical investigation was launched employing these tools.

Although the original intent of this endeavor was to gain insight into the structural aspects of DAPSC, it was found as the project progressed through the initial stages that a semi-empirical quantum mechanical method existed which could handle not only DAPSC but also an entire coordination complex of the type $[M(DAPSC)(H_2O)_2]$ where DAPSC is coordinated in a pentadentate fashion to a transition metal-cation (M). Accordingly, after the initial work where MM2[64] calculations were employed, we continued on using semi-empirical methods exclusively for the remainder of the work which allowed ultimately for perturbation of DAPSC by a transition metal-cation.

The ability to include transition metals in the calculations provided for a unique opportunity to compare theoretical results with those obtained experimentally. Do to the requirements of the semi-empirical method which was used, Fe^{2+} (d^6) appeared to be a good candidate to investigate since with this metal we could study a variety of electronic effects including the influence of the spin state multiplicity on the conformation of the complex. This metal was also a good choice from the standpoint of experimental evidence since a X-ray diffraction study of a $[Fe(DAPSC)(H_2O)Cl]^+$ complex had been reported. Semi-empirical calculations model molecules in the gas phase where there is no strain imposed externally on the molecule. Since the experimental data show the $[Fe(DAPSC)(H_2O)Cl]$ complex to be comparably free of external

strain, the structural results obtained from the theoretical work could be compared directly to those obtained via experiment.

Calculations

Initial Calculations on the Ligand DAPSC. The initial calculations performed on DAPSC were MM2[64] energy minimizations which were calculated for assorted conformations using a CAChe work station manufactured by Tektronics Inc. (1989). Three of the conformations which are illustrated in Figure 6-1 were found to exhibit relatively low total energy values and were selected for further study. Next ZDO (Zero Differential Overlap) calculations were preformed using MOPAC[65] (Molecular Orbital Package), with the AM1[66] (Austin Model 1) parameterization scheme on the CAChe work station which corroborated the three conformations as being minimum energy conformations.

At this juncture, the semi-empirical routine ZINDO was selected for the remainder of the calculations which were to be preformed for three reasons: first, this is the only method available that is parameterized to handle transition metal-cations; hence, as the work progressed we would be able to add a metal (Fe^{2+}) to the system and observe the effects of this perturbation. Second, though ZINDO may not be the method of choice for dealing with organic systems such as DAPSC, the method is known to give good results for rotational barriers

A.

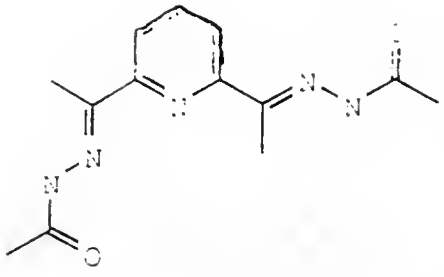

B.

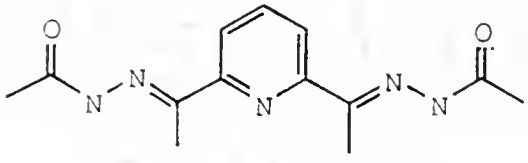

C.

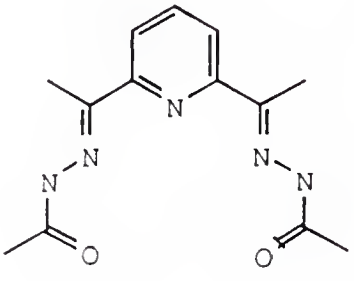

Figure 6-1. Representations of the DAPSC conformations which exhibited the lowest relative total energy.

around bonds and reasonable estimations of steric effects. This was critical for a credible determination of which conformations corresponded to energy minima. Third, by implementing this method and only this method, a consistent Hamiltonian employing the same parameterization would be used for all subsequent calculations.

Geometry Optimization of DAPSC Using ZINDO. Using the program ZINDO, a full geometry optimization was preformed on the ligand DAPSC again using the CAChe work station and the results of these calculations in terms of bond distances and angles are tabulated in Table 6-1. Accompanying the table is an illustration of the ligand, Figure 6-2, in the optimum conformation as determined by ZINDO.

Determination of the Rotation Barriers for the Semicarbazone "arm". To determine the energy of the rotation barrier for the semicarbazone "arms", the total energy of the molecule was calculated using ZINDO for a series of locked conformations which proceeded as follows:

i. one semicarbazone "arm" was locked forward as illustrated in A. of Figure 6-1.

ii. the second semicarbazone "arm" was rotated through 360° in increments of 20°.

iii. with each increment, the conformation of the molecule was locked and the total energy was determined for that exact conformation.

iv. the energy of each conformation was determined

Table 6-1. Bond Distances (Å) and Associated Angles(°)

N2-C7	1.360	C14-N4	1.388
C14-N20	1.386	C14-O18	1.285
C13-C11	1.458	C7-C8	1.402
C13-C17	1.470	C8-C9	1.392
C13-N5	1.321	C9-C10	1.392
N5-N6	1.331	C10-C11	1.401
C15-N6	1.389	C11-N2	1.360
C15-N21	1.386	C12-C7	1.458
C15-O19	1.285	C12-C16	1.470
C12-N3	1.322	N3-N4	1.330

C7-N2-C11	119.03	N2-C7-C8	121.70
C7-C8-C9	118.90	C8-C9-C10	119.73
C9-C10-C11	118.79	C10-C11-N2	121.84
C8-C7-C12	123.47	N2-C7-C12	114.81
C7-C12-C16	122.18	C7-C12-N3	114.70
N3-C12-C16	123.11	C12-N3-N4	117.29
N3-N4-C14	117.77	N4-C14-N20	115.38
N20-C14-O18	122.01	N4-C14-O18	122.39
C10-C11-C13	124.29	N2-C11-C13	113.86
C11-C13-N5	115.56	C11-C13-C17	120.37
N5-C13-C17	124.07	C13-N5-N6	117.31
N5-N6-C15	116.73	N6-C15-N21	115.71
N6-C15-O19	122.31	N21-C15-O19	121.98

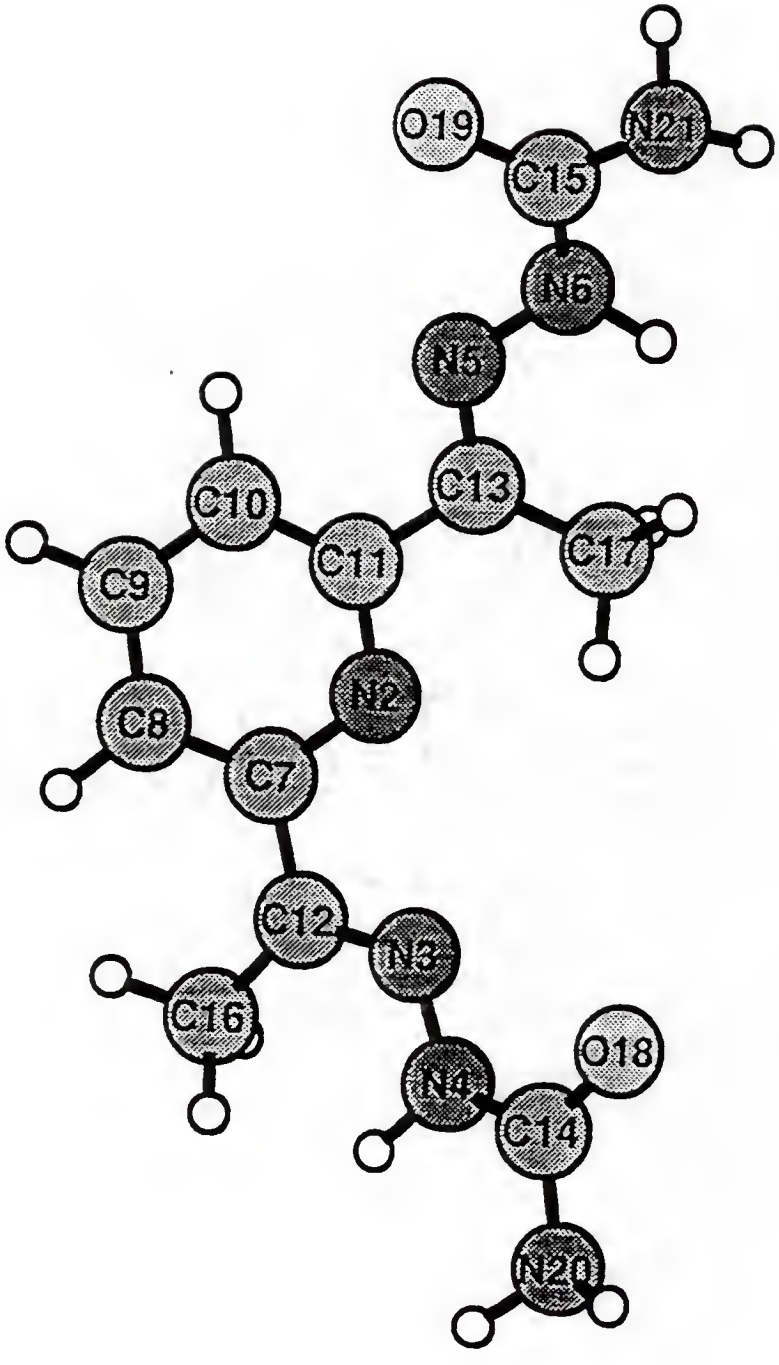

Figure 6-2. A representation of DAPSC in optimum conformation as determined by the program ZINDO.

relative to that of the starting conformation and a plot of the relative energy vs. angle of rotation is shown in Figure 6-3.

v. steps i through iv were then repeated this time starting with one of the semicarbazone "arms" locked back as illustrated in B. of Figure 6-1. A plot of the relative energy vs. angle of rotation for this series of conformations is shown in Figure 6-4.

Effects of Spin State Multiplicity and Geometry Optimizations on an Fe-DAPSC Complex. In order to determine the effect of a metal-cation and the associated spin multiplicity on the conformation of a DAPSC coordination complex having the formula $[Fe(DAPSC)(H_2O)_2]^{2+}$, separate geometry optimizations were performed on three separate spin states associated with a d^6 metal. If the molecule can be assumed to be low spin (i.e. high field with no degeneracy occuring in the d-orbitals) having psudo-C_{2v} symmetry, a closed shell singlet results. An open shell triplet can be obtained from the d-orbital splitting pattern expected from the point group D_{5h}. For a weak field, a high spin quintet is obtained. Each of these three states is depicted in Figure 6-5. For each minimum conformation, ΔSCF calculations were performed on the different spin states.

Due to previous success in dealing with transition metal compounds, the INDO model Hamiltonian[67], as implemented in

Figure 6-3. An illustration of the relative total energy vs. angle of rotation for DAPSC with one semicarbazone "arm" locked forward.

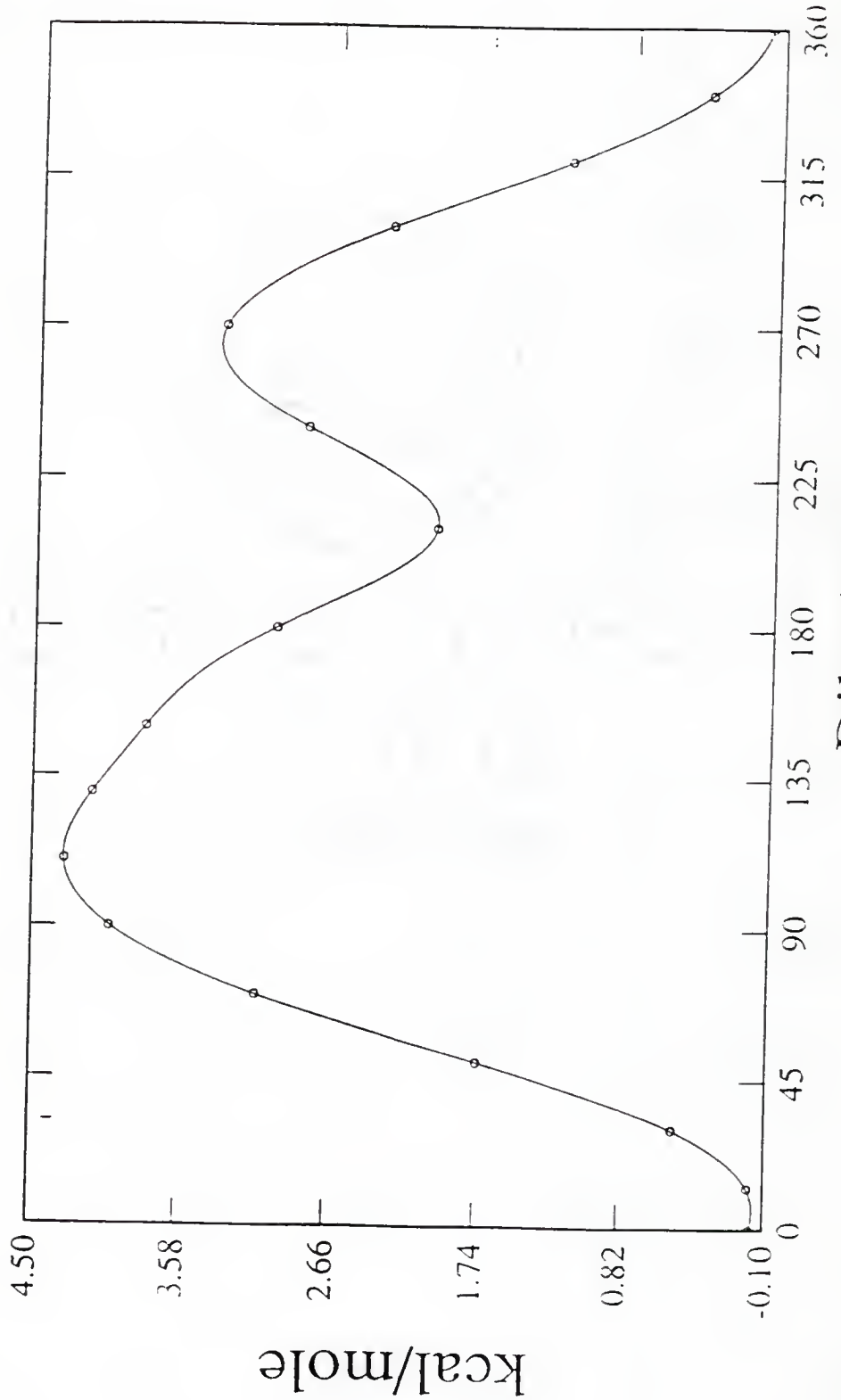
4.50
3.58
2.66
1.74
0.82
-0.10
kcal/mole
0
45
90
135
180
225
270
315
360
Dihedral

Figure 6-4. An illustration of the relative total energy vs. angle of rotation for DAPSC with one semicarbazone "arm" locked backward.

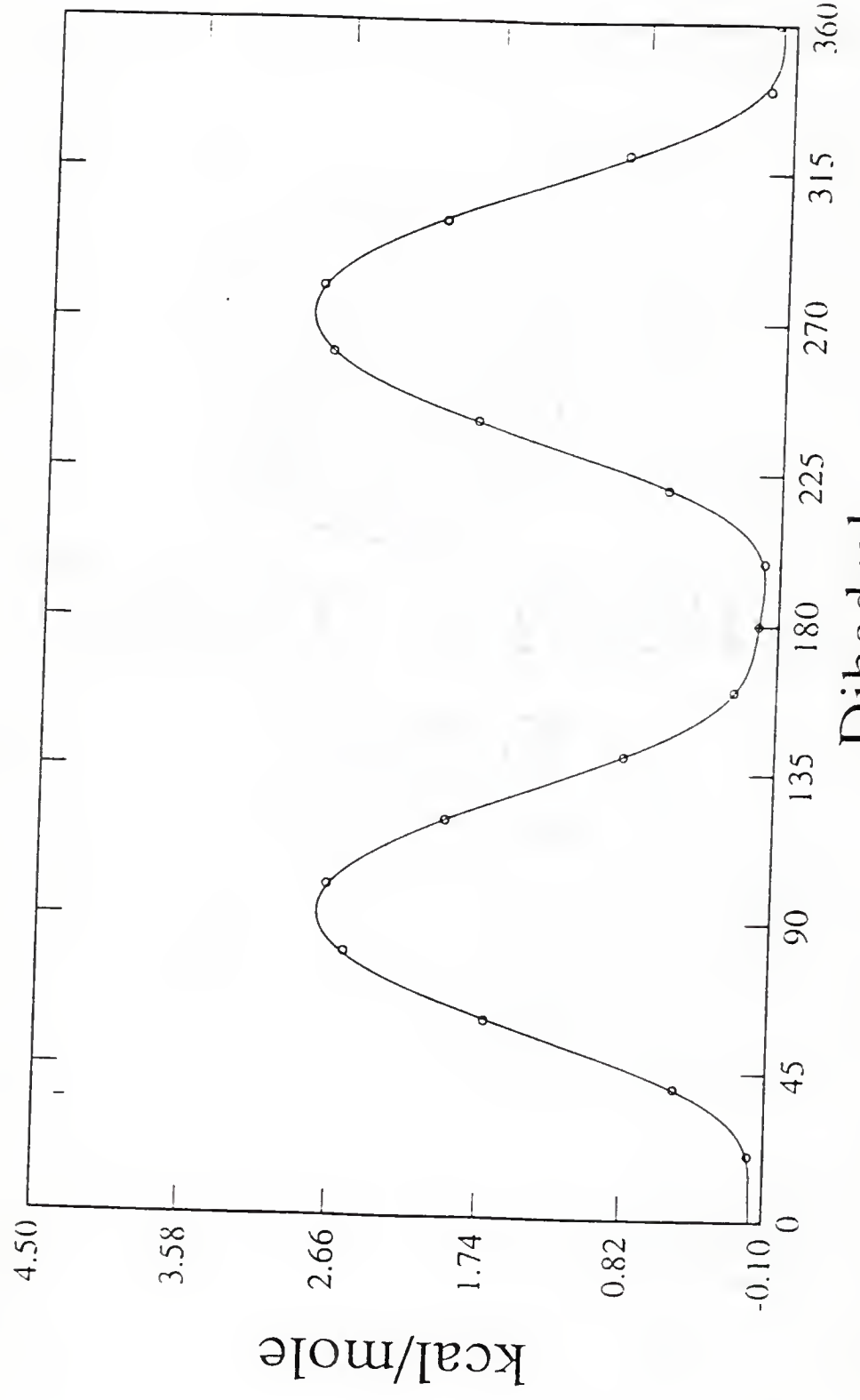
kcal/mole
4.50
3.58
2.66
1.74
0.82
-0.10
0
45
90
135
180
225
270
315
360
Dihedral

1. Singlet - closed shell

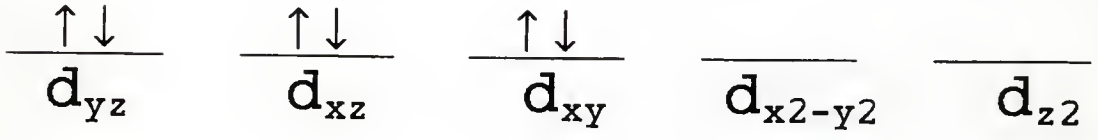

2. Triplet - open shell

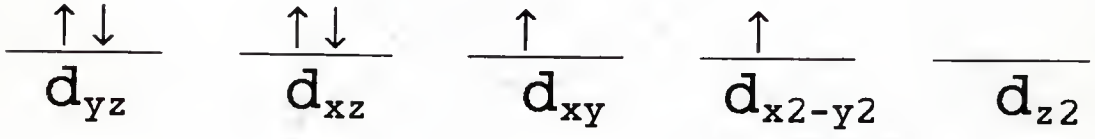

3. Quintet - open shell

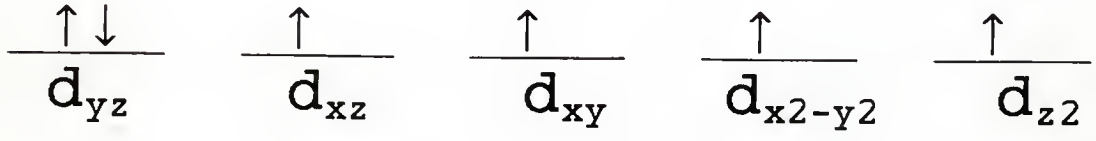

Figure 6-5. An illustration of the possible spin states for an Fe^{2+} (d^6) ion.

the program ZINDO[68,69], was used for all calculations. No refinement of the parameterization was found to be necessary in order to perform this study. The INDO model is appropriate for this investigation since all one-center two-electron integrals are retained. These integrals have been found to be necessary in order to properly differentiate between atomic state energies which is the primary concern of this section[70].

The geometry optimizations were performed on an IBM RS/6000 computer using the BFGS quasi-Newton update technique[71] for each spin state and were considered converged when the norm of the gradient was less than 1.0×10^{-3} atomic units. A restricted Hartree-Fock determinant (RHF) was used for the closed shell singlet. The open shells were also restricted (ROHF) in order to allow a direct comparison between pure spin states[72].

For all states the SCF was continued until successive cycles yielded differences in energy of less than 1.0×10^{-10} atomic units.

Discussion

The Ligand DAPSC. It is important not to underestimate the value of the initial MM calculations which showed three different conformations for DAPSC corresponding to energy minima. This information helped to dramatically reduce the computing time required for the full geometry optimization of DAPSC since we were able to begin with a good initial model

having a conformation quite close to the global minima determined by ZINDO. For this specific project we did not use MM beyond the initial calculations performed on this ligand since the intent was to ultimately investigate the electronic properties involving the spin state multiplicity of the [Fe(DAPSC)(H_2O)$_2$] complex which required the use of quantum mechanical methods. Even though MM were not used more in this project, the results were very helpful.

The use of MM calculations in coordination chemistry will likely increase in the future since there have been reports in which the method has been parameterized for a few transition metals yielding good results[73]. Attempts have also been made to use MM calculations to model metal-metal bonded systems[74]. Thus, MM[75] calculations should not be overlooked since they can provide insight into the conformation of ligands and are easily accessible on PC-computers using software packages such as ALCHEMY II[76].

The geometry optimization of this molecule shows clearly that the conformation which has been observed in the solid state, that is when DAPSC is coordinated to a transition metal-cation, is not the one of lowest energy. In fact, the energy calculations performed to determine the rotation barriers of the semicarbazone "arms" show this conformation (as illustrated in A of Figure 6-1) to be the highest in total energy of the three minima. Thus it appears that the presence of a metal-cation stabilizes this particular configuration.

It should be noted that the energy barrier between the three minimum configurations is not very large; nevertheless, it can generally be expected that the vast majority of the molecules will be in the lowest energy state available at any given instant. This is significant in terms of what has been observed experimentally since several of the reactions of DAPSC with first row transition metals have been observed to go to completion much more rapidly if the mixture is heated slightly. Applying heat may significantly increase the population of DAPSC molecules having the high energy configuration which is likely to favor complex formation.

The Complex $[Fe(DAPSC)(H_2O)_2)$. Our interest in this study was to determine the effect of spin multiplicity on the conformation of this Fe-DAPSC complex since several spin states can arise for a d^6 species such as Fe^{2+}. Specifically we were interested in the variation in bond distances between the metal-cation and the ligand donors as well as the geometry exhibited within the coordination sphere as a function of the spin state. Figure 6-6 displays the coordinate system used in this work as well as the atom numbering scheme for the donors in the immediate coordination sphere and Figure 6-7 illustrates the optimum geometry of the complex as determined by ZINDO for the quintet spin state. Table 6-2 is a listing of the bond distances and associated bond angles obtained from the optimization calculations for an Fe^{2+} (d^6) center in the quintet spin state. Table 6-3 summarizes the experimentally

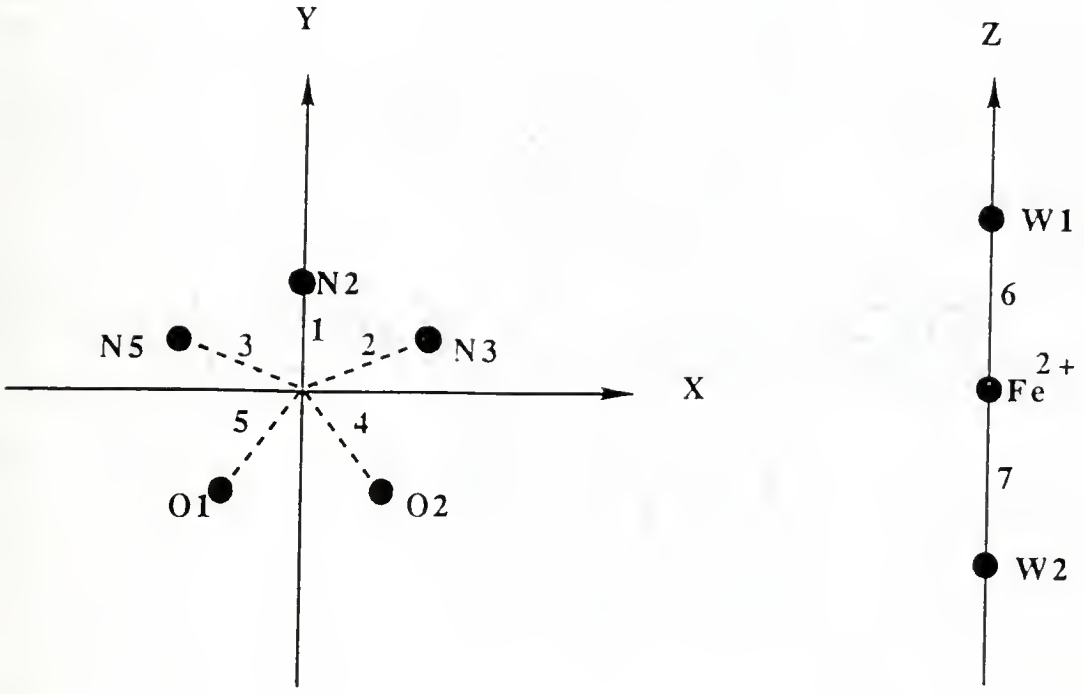

Figure 6-6. Coordinate system and atom numbering scheme.

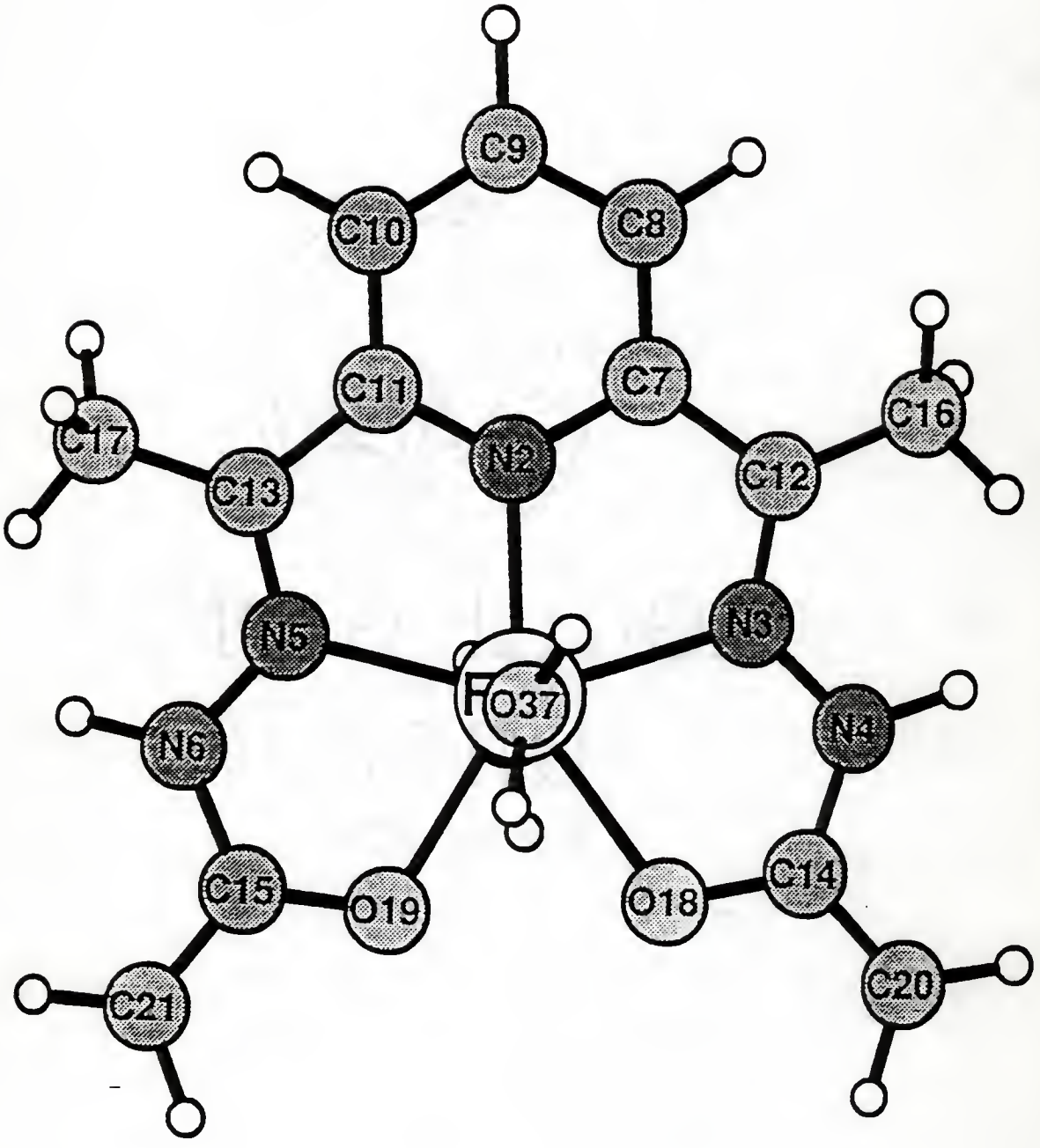

Figure 6-7. An illustration of the optimized geometry for the complex $[Fe(DAPSC)(H_2O)_2]^{2+}$ as determined by ZINDO.

Table 6-2 Bond Distances(Å) and Angles(°) for $[Fe(DAPSC)(H_2O)_2]^{2+}$

Fe-O37	2.214	N2-C7	1.365
Fe-O38	2.214	C7-C8	1.398
Fe-O18	2.184	C8-C9	1.393
Fe-O19	2.184	C9-C10	1.393
Fe-N3	2.229	C10-C11	1.398
Fe-N2	2.219	C11-N2	1.366
Fe-N5	2.229	C11-C13	1.463
O18-C14	1.308	C13-C17	1.462
C14-N20	1.359	C13-N5	1.325
C14-N4	1.385	N5-N6	1.337
N4-N3	1.337	N6-C15	1.385
N3-C12	1.325	C15-N21	1.359
C12-C16	1.462	C15-O19	1.308
C12-C7	1.463		

O37-Fe-O38	170.80	N2-C7-C8	120.19
O37-Fe-O18	85.40	C7-C8-C9	119.09
O37-Fe-O19	87.72	C8-C9-C10	120.30
O37-Fe-N3	93.52	C9-C10-C11	119.05
O37-Fe-N2	94.54	C10-C11-N2	120.22
O37-Fe-N5	89.53	C11-N2-C7	121.14
O38-Fe-O18	87.39	N2-C11-C13	114.82
O38-Fe-O19	84.95	C10-C11-C13	124.96
O38-Fe-N3	89.65	C11-C13-C17	123.31
O38-Fe-N2	94.66	C17-C13-N5	123.39
O38-Fe-N5	93.46	C11-C13-N5	113.29
O18-Fe-O19	75.48	C13-N5-N6	121.18
O18-Fe-N3	71.97	N5-N6-C15	113.51
N3-Fe-N2	70.38	N6-C15-N21	118.97
N2-Fe-N5	70.40	N6-C15-O19	119.96
N5-Fe-O19	71.94	N21-C15-O19	121.03
Fe-O18-C14	115.96	C15-O19-Fe	115.91
O18-C14-N20	121.02	C20-C14-N4	119.00
O18-C14-N4	119.95	C14-N4-N3	113.62
N4-N3-C12	121.26	N3-C12-C16	123.50
C16-C12-C7	123.22	N3-C12-C7	113.26
C12-C7-N2	114.85	C12-C7-C8	124.96

Table 6-3. Bond Distances Within the Immediate Coordination Sphere as Determined from the Optimization Calculations for an Fe^{2+} (d^6) Center in Singlet, Triplet and Quintet Spin States.

	Singlet	Triplet	Quintet	Observed
1	2.090	2.207	2.219	2.220
2	2.165	2.226	2.229	2.229
3	2.171	2.226	2.229	2.195
4	2.238	2.177	2.184	2.192
5	2.242	2.177	2.184	2.175
6	2.160	2.152	2.214	
7	2.160	2.152	2.214	

* All bond distances are given in Å. Bonds are in reference to Figure 6–6.

Table 6–4. Relative Total Energy (eV)

	Singlet	Triplet	Quintet
Singlet	2.686	2.855	2.915
Triplet	1.985	1.802	1.850
Quintet	0.255	0.066	0.0

observed bond distances for a complex similar in structure to the complex which was optimized which were obtained by X-ray diffraction studies together with those distances observed for the Fe^{2+} singlet, triplet and quintet spin states. Table 6-4 lists the relative energy (in eV) of each possible spin state for each of the three optimized spin states. These values have all been calculated relative to that which was determined for the constrained quintet state which was found to be the lowest in energy overall.

These results are in excellent agreement with what has been observed experimentally in three areas. First, the geometry optimizations show the open-shell quintet to have the lowest overall energy which says that the metal is high spin and the ligand is low field. This agrees well with what has been observed for the Cr^{3+}-DAPSC/DAPBAH complexes (as presented in Chapter 4) where both of the complexes were high-spin and with what has been reported for Fe^{3+}-DAPSC in aqueous solution. Second, the bond distances and associated angles determined in the geometry optimization between the atoms within the immediate coordination sphere of the $[Fe(DAPSC)(H_2O)_2]$ species are quite close to that which has been observed in the solid state for a closely related Fe^{2+}-DAPSC complex. Finally, the fact that the geometry optimization shows the ligand DAPSC to be planar is indeed significant.

The comparison of the bond distances in Table 6-2 is noteworthy and shows the reliability of the ZINDO method. It

is clear that as electron density is placed into the $d_{x^2-y^2}$ and d_{z^2} orbitals that two things happen. First, the bonds to the nitrogen donors become longer, most notably Fe-N2, since an electron is now in the $d_{x^2-y^2}$ orbital and hence there is now repulsion between the donor electrons and this electron resulting in a longer bond length. A similar effect is reflected in the axial bond lengths especially as an electron is placed into the d_{z^2} orbital which is aligned directly towards the water donors. Second, as an electron is removed from the d_{xy} orbital and placed into the $d_{x^2-y^2}$ orbital in going from a singlet to the triplet state, a notable decrease in bond length is observed for the Fe-O1 and Fe-O2 bonds which is due to the removal of an electron from the d_{xy} orbital directed towards both semicarbazone oxygens resulting in less repulsion and hence a decrease in bond length. Both of these results are reasonable and they match quite well with the behavior which would be expected.

A comparison of the bond lengths within the equatorial plane determined for the quintet spin state with those observed in the solid state is extremely good. Although the solid state complex used in the comparison differs in the axial donors, the five equatorial positions are identical. It is important to note that the ZINDO calculations performed on the $[Fe(DAPSC)(H_2O)_2]^{2+}$ complex assume that there are no external effects contributing to the conformation of the observed complex. In other words, the complex is treated as

an isolated system throughout the geometry optimization. This same condition is not true for the geometry of the Fe-DAPSC complex observed in crystalline form which is most certainly affected by near neighbors as well as other realities of our planet. Nonetheless, two points can certainly be made: first, the differences in bond lengths between the quintet spin state, determined to be the lowest in energy from geometry optimization calculations, and those observed via experiment are minor which suggests that effects such as packing forces in the solid state may actually be trivial in affecting the structure of these complexes. Second, though the method used to optimize the geometry was semi-empirical (i.e. experimental results used in the parameterization scheme), three different geometries were clearly distinguished which corresponded to the three different spin states. These results show that the spin state of the complex may in fact be one of the most important factors affecting the bond lengths, angles and geometry observed within the immediate coordination sphere of this type of complex.

Determining which spin state was the lowest in relative total energy required considerable amounts of computing time. It is interesting to see how the total relative energies (Table 6-4) of the various spin states relate to that of the quintet ground state which was found to be the lowest in energy. The geometry constraints are given across the table as column headings and the relative energies for the spin

states are listed down the left side as row headings. From Table 6-4 it is easy to determine the amount of energy required to go from one spin state to another in a particular geometry or from one spin state in a particular geometry to the same spin state in a different geometry. For instance if the geometry was that of a quintet and the spin state changed form a quintet to a triplet, this would require 1.850 eV or 14921 cm^{-1} of energy.

APPENDIX
COMPLETE REFERENCES FOR THE RUTHENIUM
COMPLEXES CITED IN CHAPTER 4

1. CIS-DICHLORO-BIS(2,7-DIMETHYL-3,6-DIAZA-3,5-OCTADIENE) RUTHENIUM(II)
   BASTAQ — V.PANK,J.KLAUS,K.VON DEUTEN,M.FEIGEL, H.BRUDER,H.TOM DIECK, TRANSITION MET.CHEM., 6,185,1981.

2. CIS,CIS-DICHLORO-BIS(2-(PHENYLAZO)-PYRIDINE)-RUTHENIUM
   BOYHAY — S.GOSWAMI,A.R.CHAKRAVARTY,A.CHAKRAVORTY, INORG.CHEM., 22,602,1983.

3. DICHLORO-BIS(2-PHENYLAZOPYRIDINE)-RUTHENIUM(II) (C-1-ISOMER)
   BOYHAY01 — A.SEAL,S.RAY, ACTA CRYST.,C (CR.STR.COMM.), 40,929,1984.

4. TRANS-CHLORO-NITROSYL-TETRAKIS(PYRIDINE)-RUTHENIUM(II) BIS(HEXAFLUOROPHOSPHATE) HEMIHYDRATE
   BUPPIL — T.KIMURA,T.SAKURAI,M.SHIMA,T.TOGANO, M.MUKAIDA,T.NOMURA, INORG.CHIM.ACTA, 69,135,1983.

5. DICHLORO-BIS(ALPHA-(PHENYLAZO)BENZALDOXIME)-RUTHENIUM(II)
   CAHGAT — A.R.CHAKRAVARTY,A.CHAKRAVORTY, F.A.COTTON,L.R.FALVELLO,B.K.GHOSH, M.TOMAS, INORG.CHEM., 22,1892,1983.

6. TRICHLORONITROSYL-BIS(METHYLDIPHENYLPHOSPHINE) RUTHENIUM(II)
   MPNCRU10 — A.J.SCHULTZ,R.L.HENRY,J.REED, R.EISENBERG, INORG.CHEM., 13,732,1974.

7. CHLORO-CARBONYL-(N-ISOPROPENYL-N'-ISOPROPYL-FORMAMIDINATO)-BIS-TRIPHENYLPHOSPHINE)-RUTHENIUM(II)
   PRFCRU — A.D.HARRIS,S.D.ROBINSON,A.SAHAJPAL, M.B.HURSTHOUSE, J.ORGANOMET.CHEM., 174,C11,1979.

8. CARBONYL-CHLORO-(N-ISOPROPENYL-N'-ISOPROPYLFORMAMIDINATO)-BIS (TRIPHENYLPHOSPHINE)-RUTHENIUM(II)
   PRFCRU10 A.D.HARRIS,S.D.ROBINSON,A.SAHAJPAL, M.B.HURSTHOUSE, J.CHEM.SOC.,DALTON, ,1327,1981.

9. CIS-CARBONYL-DICHLORO-(2,2'.6',2''-TERPYRIDYL)-RUTHENIUM(II)
   COXMUX G.B.DEACON,J.M.PATRICK,B.W.SKELTON, N.C.THOMAS,A.H.WHITE, AUST.J.CHEM., 37,929,1984.

10. CARBONYL-CHLORO-(CIS-2,7,12-TRIMETHYL-3,7,11,17-TETRA-AZABICYCLO(11.3.1)HEPTADECA-1,(17),13,15-TRIENE)-RUTHENIUM(II) TETRAPHENYLBORATE
   DIJKAI A.J.BLAKE,T.I.HYDE,R.S.E.SMITH, M.SCHRODER, J.CHEM.SOC.,CHEM.COMM., ,334,1986.

11. CIS-BIS(2,2'-BIPYRIDYL)-DICHLORO-RUTHENIUM(II) HYDRATE
   DOGMOB D.S.EGGLESTON,K.A.GOLDSBY,D.J.HODGSON, T.J.MEYER, INORG.CHEM., 24,4573,1985.

12. BIS(2-(BENZYLTHIO)-AZOBENZENE-N,S.C,N,S)-CHLORO-RUTHENIUM(II)
   DOWZEU A.K.MUKHERJEE,M.MUKHERJEE,P.K.DAS, A.K.MAHAPATRA,S.GOSWAMI,A.CHAKRAVORTY, ACTA CRYST.,C (CR.STR.COMM.), 42,793,1986.

13. TRICHLORO(P-TOLYLAZO)BIS(TRIPHENYLPHOSPHINE) RUTHENIUM(II) ACETONE SOLVATE
   CTZPRU J.V.MCARDLE,A.J.SCHULTZ,B.J.CORDEN, R.EISENBERG, INORG.CHEM.,12,1676,1973.

14. CIS-DICARBONYL-CIS-DICHLORO-(3,6-BIS(2-PYRIDYL)PYRIDAZINE-N,N') RUTHENIUM(II)
   GIDBOK G.DE MUNNO,G.DENTI,G.DE ROSA,G.BRUNO, ACTA CRYST.,C (CR.STR.COMM.), 44,1193,1988.

15. AMMINE-TRICHLORO-BIS(TRIMETHYLPHOSPHITE)-RUTHENIUM(III)
   AMCLRU M.I.BRUCE,D.A.KELLY,G.M.MCLAUGHLIN, G.B.ROBERTSON,I.B.TOMKINS,R.C.WALLIS, AUST.J.CHEM., 33,195,1980.

16. DICHLORO-TRIAMINE-(CAFFEINE-8-YL) RUTHENIUM(III) CHLORIDE MONOHYDRATE
CAFFRU H.J.KRENTZIEN,M.J.CLARKE,H.TAUBE, BIOINORG.CHEM., 4,143,1975.

17. CIS-DICHLORO-(N,N,N',N'-TETRAMETHYL-3,6-DIMETHYL-3,6-DIAZAOCTANE-1,8-DIAMINE-N,N',N'',N''')-RUTHENIUM(III) PERCHLORATE
SABCIH CHI-MING CHE,WAI-TONG TANG, MICHAEL HON-WAH LAM,T.C.W.MAK, J.CHEM.SOC.,DALTON, ,2885,1988.

18. CIS-AQUA-CHLORO-BIS(ETHANE-1,2-DIAMINE)-RUTHENIUM(III) BIS(TRIFLUOROMETHANESULFONATE) MONOHYDRATE
COLGUF T.W.HAMBLEY,G.A.LAWRANCE, AUST.J.CHEM., 37,435,1984.

19. CIS-BIS(2,2'-BIPYRIDYL)-DICHLORO-RUTHENIUM(III) CHLORIDE DIHYDRATE
DOGMIV D.S.EGGLESTON,K.A.GOLDSBY,D.J.HODGSON, T.J.MEYER, INORG.CHEM., 24,4573,1985.

20. BIS(IMIDAZOLIUM) PENTACHLORO-(IMIDAZOLE-N)-RUTHENIUM(III) (ANTI-TUMOR ACTIVITY)
FEGGED B.K.KEPPLER,D.WEHE,H.ENDRES,W.RUPP, INORG.CHEM., 26,844,1987.

21. CIS,CIS-CHLORO-BIS(2-METHYL-8-QUINOLINOLATO-O,N)-NITROSYL RUTHENIUM(III)
FISSAB Y.KAMATA,T.KIMURA,R.HIROTA,E.MIKI, K.MITZUMACHI,T.ISHIMORI, BULL.CHEM.SOC.JPN., 60,1343,1987.

22. MER-(ACETONITRILE-N)-TRICHLORO-(1-METHYL-3-(2-PYRIDYL)-1,2,4-TRIAZOLE-N(4),N(1'))-RUTHENIUM(III)
FUYPUK R.HAGE,R.PRINS,R.A.G.DE GRAAFF, J.G.HAASNOOT,J.REEDJIK,J.G.VOS, ACTA CRYST.,C (CR.STR.COMM.), 44,56,1988.

23. TRICHLORO-BIS(DIETHYLPHENYLPHOSPHINE) -(DIETHYLPHENYLPHOSPHINE-IMINATO) RUTHENIUM(IV)
CRUPIM10 F.L.PHILLIPS,A.C.SKAPSKI, J.CHEM.SOC.,DALTON, ,1448,1976.

24. (BENZOATO-O,O')-CHLORO-CARBONYL-BIS(TRIPHENYLPHOSPHINE) RUTHENIUM(II)
BZCPRU M.F.MCGUIGGAN,L.H.PIGNOLET, CRYST.STRUCT.COMMUN., 7,583,1978.

25. BENZOATO-DICHLORO-BIS(TRIPHENYLPHOSPHINE)-RUTHENIUM(III)
BAWZUU M.F.MCGUIGGAN,L.H.PIGNOLET, CRYST.STRUCT.COMMUN., 10,1227,1981.

26. MER,TRANS-TRICHLORO-(ETHYLDIPHENYLPHOSPHINOACETATE-P)-(ETHYLDIPHENYLPHOSPHINOACETATE-O,P)-RUTHENIUM(III)
DIDSEO P.BRAUNSTEIN,D.MATT,D.NOBEL, S.-E.BOUAOUD,B.CARLUER,D.GRANDJEAN, P.LEMOINE, J.CHEM.SOC.,DALTON, ,415,1986.

27. CIS,TRANS-CHLORO-BIS(2-METHYL-8-QUINOLINOLATO-O,N)-NITROSYL-RUTHENIUM(III)
FISRUU J.KAMATA,T.KIMURA,R.HIROTA,E.MIKI, K.MITZUMACHI,T.ISHIMORI, BULL.CHEM.SOC.JPN., 60,1343,1987.

28. TRANS-CHLORO-HYDROXO-TETRAKIS(PYRIDINE)-RUTHENIUM(III) HEXAFLUOROPHOSPHATE (EARLIER PUBLICATION IN CHEM LETT,2135,1986)
FUCGIT H.NAGAO,K.AOYAGI,Y.YUKAWA,F.S.HOWELL, M.MUKAIDA,H.KAKIHANA, BULL.CHEM.SOC.JPN., 60,3247,1987.

29. TRANS-CHLORO-METHOXO-TETRAKIS(PYRIDINE)-RUTHENIUM(III) PERCHLORATE (EARLIER PUBLICATION IN CHEM LETT,2135,1986)
FUCGUF H.NAGAO,K.AOYAGI,Y.YUKAWA,F.S.HOWELL, M.MUKAIDA,H.KAKIHANA, BULL.CHEM.SOC.JPN., 60,3247,1987.

30. TRANS-CHLORO-OXO-(1,4,8,11-TETRAMETHYL-1,4,8,11-TETRA-AZA-CYCLOTETRADECANE-N-1-,N-4-,N-8-,N-11-)-RUTHENIUM(IV) PERCHLORATE
DAGVIQ CHI-MING CHE,KWOK-YIN WONG,T.C.W.MAK, J.CHEM.SOC.,CHEM.COMM., ,988,1985.

31. CIS-DICHLORO-DICARBONYL-BIS(TRIBENZYLPHOSPHINE)-RUTHENIUM(II)
BEYGUH L.M.WILKES,J.H.NELSON,J.P.MITCHENER, M.W.BABICH,W.C.RILEY,B.J.HILLAND, R.A.JACOBSON ,M.Y.CHENG,K.SEFF, L.B.MCCUSKER, INORG.CHEM., 21,1376,1982.

32. CARBONYL-DICHLORO-BIS(TRICYCLOHEXYLPHOSPHINE)-RUTHENIUM(II)
BOMMEV F.G.MOERS,P.T.BEURSKENS,J.H.NOORDIK, CRYST.STRUCT.COMMUN.,11,1655,1982.

33. DICHLORO-TRIS(ETHYL-(DIPHENYLPHOSPHINO)-ACETATE-O-3-, P-2-,P-1-,P-3-) RUTHENIUM(II)
BUVGUU P.BRAUNSTEIN,D.MATT,Y.DUSAUSOY, INORG.CHEM., 22,2043,1983.

34. DICHLORO-CARBONYL-TRIS(1-PHENYL-3,4-DIMETHYLPHOSPHOLE) -RUTHENIUM(II)
CATRIY L.M.WILKES,J.H.NELSON,L.B.MCCUSKER, K.SEFF, INORG.CHEM., 22,2476,1983.

35. TRANS-DICHLORO-((+-)-O-PHENYLENE-BIS(METHYL (PHENYL)PHOSPHINE))-((+-)-O-PHENYLENE-BIS(METHYL (PHENYL)PHOSPHINE)-P-OXIDE)-RUTHENIUM(II)
CEGFEZ S.R.HALL,B.W.SKELTON,A.H.WHITE, AUST.J.CHEM., 36,267,1983.

36. TRANS-CARBONYL-DICHLORO-(2,2'.6',2''-TERPYRIDYL) -RUTHENIUM(II)
COXMOR G.B.DEACON,J.M.PATRICK,B.W.SKELTON, N.C.THOMAS,A.H.WHITE, AUST.J.CHEM., 37,929,1984.

37. DICHLORO-BIS(O-(DIPHENYLPHOSPHINO)ANISOLE)- RUTHENIUM(II) DICHLOROMETHANE SOLVATE
CPASRU J.C.JEFFERY,T.B.RAUCHFUSS, INORG.CHEM., 18,2658,1979.

38. TRICHLORO(P-TOLYLAZO)BIS(TRIPHENYLPHOSPHINE) RUTHENIUM(II) ACETONE SOLVATE
CTZPRU J.V.MCARDLE,A.J.SCHULTZ,B.J.CORDEN, R.EISENBERG, INORG.CHEM., 12,1676,1973.

39. TRANS-DICHLORO-(HEXAPHENYL-1,4,7,10-TETRAPHOSPHADECANE) -RUTHENIUM(II)
DAVDEJ A.V.RIVERA,E.R.DE GIL,B.FONTAL, INORG.CHIM.ACTA, 98,153,1985.

40. TRANS-DICHLORO-TETRAKIS(DIMETHYLPHOSPHINE) RUTHENIUM(II)
DCDMPR F.A.COTTON,B.A.FRENZ,D.L.HUNTER, INORG.CHIM.ACTA, 16,203,1976.

41. METHYLTRIPHENYLPHOSPHONIUM TRIS(MU-2--CHLORO) -DICARBONYL-DICHLORO-BIS-(TRIPHENYLPHOSPHINE)- DI-RUTHENIUM(II) DICHLOROMETHANE SOLVATE
DOSPUW R.A.SANCHEZ-DELGADO,U.THEWALT, N.VALENCIA,A.ANDRIOLLO, R.L.MARQUEZ-SILVA,J.PUGA, H.SCHOLLHORN,H.-P.KLEIN,B.FONTAL, INORG.CHEM., 25,1097,1986.

42. TRANS-DICHLORO-TETRAKIS(1,3-DIETHYLIMIDAZOLIN-2-YLIDENE) RUTHENIUM(II)-DI-N-BUTYL ETHER SOLVATE
EIMZRV P.B.HITCHCOCK,M.F.LAPPERT,P.L.PYE, J.CHEM.SOC.,DALTON, ,826,1978.

43. (R,R),(R,R)-DICHLORO-BIS(1,2-BIS-(METHYLPHENYLPHOSPHINO)ETHANE) RUTHENIUM(II) (ABSOLUTE CONFIGURATION)
EMPCRU R.WARTCHOW,H.J.BERTHOLD, Z.KRISTALLOGR., 145,240,1977.

44. DICHLORO-TRIS(DIPHENYL(TRIMETHYLSILYLMETHYL)PHOSPHINE)-RUTHENIUM(II)
FOJDIR F.A.COTTON,M.MATUSZ, INORG.CHIM.ACTA, 131,213,1987.

45. TRANS-DICHLORO-CIS-BIS((2-METHOXYETHYL) DIPHENYLPHOSPHINE-O,P) RUTHENIUM(II) ETHANOL SOLVATE
FOPDAP E.LINDNER,U.SCHOBER,R.FAWZI,W.HILLER, U.ENGLERT,P.WEGNER, CHEM.BER., 120,1621,1987.

46. CARBONYL-TRANS-DICHLORO-TRANS(((2-METHOXYETHYL) DIPHENYLPHOSPHINE-O,P)-(2-METHOXYETHYL) DIPHENYLPHOSPHINE-P)-RUTHENIUM(II) N-HEXANE SOLVATE
FOPDET E.LINDNER,U.SCHOBER,R.FAWZI,W.HILLER, U.ENGLERT,P.WEGNER, CHEM.BER., 120,1621,1987.

47. MER-TRANS-DICHLORO-CARBONYL-(5,6-DIMETHYL-7-PHENYL-2-DIPHENYLPHOSPHINO-7-PHOSPHABICYCLO(2.2.1)HEPT-5-ENE-P,P')-(VINYLIDENEPHENYLPHOSPHINE)- RUTHEIUM(II) (AT -100 DEG.C)
FUJMIG R.L.GREEN,J.H.NELSON,J.FISCHER, ORGANOMETALLICS, 6,2256,1987.

48. DICHLORO-(SIGMA-1-,ETA-4--2,6-DIALLYLPYRIDINE-N)-TRIPHENYLPHOSPHINE-RUTHENIUM(II)
GAZHOE G.VASAPOLLO,C.F.NOBILE,M.LATRONICO, M.LANFRANCHI,M.A.PELLINGHELLI, J.ORGANOMET.CHEM., 336,429,1987.

49. TRANS-DICHLORO-BIS(1,1-BIS(DIPHENYLPHOSPHINO) ETHENE-P,P')-RUTHENIUM(II) DICHLOROMETHANE SOLVATE
GEDCAT F.A.COTTON,M.P.DIEBOLD,M.MATUSZ, POLYHEDRON, 6,1131,1987.

50. (MU-2--2,4,6-TRIS(2-PYRIDYL)-2-METHOXY-1,3,5-TRIAZINE)-BIS(DICARBONYL-DICHLORO-RUTHENIUM(II)) METHANOL SOLVATE
GEYJID N.C.THOMAS,B.L.FOLEY,A.L.RHEINGOLD, INORG.CHEM., 27,3426,1988.

51. CIS-DICARBONYL-TRANS-DICHLORO-(3,6-BIS(2-PYRIDYL) PYRIDAZINE-N,N')-RUTHENIUM(II)
GIDBIE G.DE MUNNO,G.DENTI,G.DE ROSA,G.BRUNO, ACTA CRYST.,C (CR.STR.COMM.), 44,1193,1988.

52. TRANS-DICHLORO-TETRAKIS(DIMETHYL SULFOXIDE-S)-RUTHENIUM(II) (ANTI-TUMOUR AGENT)
KACNOR E.ALESSIO,G.MESTRONI,G.NARDIN,W.M.ATTIA, M.CALLIGARIS,G.SAVA,S.ZORZET, INORG.CHEM., 27,4099,1988.

53. TRICHLORONITROSYL-BIS(METHYLDIPHENYLPHOSPHINE) RUTHENIUM(II)
MPNCRU10 A.J.SCHULTZ,R.L.HENRY,J.REED, R.EISENBERG, INORG.CHEM., 13,732,1974.

54. TRANS-CARBONYL-DICHLORO-TRIS(DIPHENYLMETHYLPHOSPHINE)-RUTHENIUM(II)
SADPES D.W.KRASSOWSKI,J.H.NELSON,K.R.BROWER, D.HAUENSTEIN,R.A.JACOBSON, INORG.CHEM., 27,4294,1988.

55. AMMINE-TRICHLORO-BIS(TRIMETHYLPHOSPHIT) -RUTHENIUM(III)
AMCLRU M.I.BRUCE,D.A.KELLY,G.M.MCLAUGHLIN, G.B.ROBERTSON,I.B.TOMKINS, R.C.WALLIS, AUST.J.CHEM., 33,195,1980.

56. (1,4,8,11-TETRA-AZACYCLOTETRADECANE)-DICHLORO-RUTHENIUM (III) BROMIDE
BANRAJ D.D.WALKER,H.TAUBE, INORG.CHEM., 20,2828,1981.

57. BENZYLTRIPHENYLPHOSPHONIUM CARBONYL-PENTACHLORO -RUTHENIUM(III) DICHLOROMETHANE SOLVATE
BZPPRU R.O.GOULD,L.RUIZ-RAMIREZ,T.A.STEPHENSON, M.A.THOMSON, J.CHEM.RES., 254,3301,1978.

58. MER,TRANS-TRICHLORO-(ETHYLDIPHENYLPHOSPHINOACETATE-P) -(ETHYLDIPHENYLPHOSPHINOACETATE-O,P)- RUTHENIUM(III)
DIDSEO P.BRAUNSTEIN,D.MATT,D.NOBEL, S.-E.BOUAOUD,B.CARLUER,D.GRANDJEAN, P.LEMOINE, J.CHEM.SOC.,DALTON, ,415,1986.

59. TETRAPHENYLARSONIUM TETRACHLORO
-(DL-2,5-DISELENAHEXANE-SE,SE') RUTHENIUM(III)
DUVTAP E.G.HOPE,H.C.JEWISS,W.LEVASON,M.WEBSTER,
J.CHEM.SOC.,DALTON, ,1479,1986.

60. DI-SODIUM DICHLORO-HYDROGEN-BIS(OXALATO-O,O)-
RUTHENIUM(III) OCTAHYDRATE
FADTUZ J.P.DELOUME,G.DUC,R.FAURE,
G.THOMAS-DAVID,
REV.CHIM.MINER.,22,728,1985.

61. BIS(IMIDAZOLIUM) PENTACHLORO-(IMIDAZOLE-N)-
RUTHENIUM(III) (ANTI-TUMOR ACTIVITY)
FEGGED B.K.KEPPLER,D.WEHE,H.ENDRES,W.RUPP,
INORG.CHEM., 26,844,1987.

62. IMIDAZOLIUM TRANS-BIS(IMIDAZOLE-N)-TETRACHLORO
-RUTHENIUM(III) (ANTI-TUMOUR ACTIVITY)
FUMWIT B.K.KEPPLER,W.RUPP,U.M.JUHL,
H.ENDRES,R.NIEBL,W.BALZER,
INORG.CHEM., 26,4366,1987.

63. 4-METHYLIMIDAZOLIUM TRANS-BIS(4-METHYLIMIDAZOLE)
-TETRACHLORO-RUTHENIUM(III) (ANTI-TUMOUR ACTIVITY)
FUMWOZ B.K.KEPPLER,W.RUPP,U.M.JUHL,
H.ENDRES,R.NIEBL,W.BALZER,
INORG.CHEM., 26,4366,1987.

64. MER-(ACETONITRILE-N)-TRICHLORO-(1-METHYL-3-
(2-PYRIDYL)-1,2,4-TRIAZOLE-N(4),N(1'))-RUTHENIUM(III)
FUYPUK R.HAGE,R.PRINS,R.A.G.DE GRAAFF,
J.G.HAASNOOT,J.REEDJIK,J.G.VOS,
ACTA CRYST.,C (CR.STR.COMM.),
44,56,1988.

65. DICHLORO-BIS(1-ETHYL-3-P-TOLYLTRIAZENE-1-OXIDATO)
-RUTHENIUM(IV) (AT 5 DEG.C)
CIMWEA S.BHATTACHARYA,A.CHAKRAVORTY,F.A.COTTON,
R.MUKHERJEE,W.SCHWOTZER,
INORG.CHEM., 23,1709,1984.

66. TRICHLORO-BIS(DIETHYLPHENYLPHOSPHINE)-
(DIETHYLPHENYLPHOSPHINE-IMINATO) RUTHENIUM(IV)
CRUPIM10 F.L.PHILLIPS,A.C.SKAPSKI,
J.CHEM.SOC.,DALTON, ,1448,1976.

67. DICHLORO(DODECA-2,6,10-TRIENE-1,12-DIYL) RUTHENIUM(IV)
CTRDRU10 J.E.LYDON,M.R.TRUTER,
J.CHEM.SOC.A, ,362,1968.

68. BIS(BIS(TRIPHENYLPHOSPHINE)IMINIUM) TRANS-TETRACHLORO-DIOXO-RUTHENIUM(VI) BENZENE SOLVATE
VADNIX S.PERRIER,J.K.KOCHI,
INORG.CHEM., 27,4165,1988.

69. BIS(TRIPHENYLPHOSPHINE)IMINIUM CIS-TRICHLORO-DIOXO-RUTHENIUM(VI)
VADNOD S.PERRIER,J.K.KOCHI,
INORG.CHEM., 27,4165,1988.

70. TETRAPHENYLPHOSPHONIUM TRANS-TRICHLORO-DIOXO-RUTHENIUM(VI)
VADNUJ S.PERRIER,J.K.KOCHI,
INORG.CHEM., 27,4165,1988.

71. CHLORO-(ETA-4--CYCLO-OCTADIENE)-METHYL-TRIS(O-METHOXYPHENYLPHOSPHINE) RUTHENIUM(II) DICHLOROMETHANE SOLVATE
BAKYOB M.M.DE V.STEYN,R.B.ENGLISH,T.V.ASHWORTH,
E.SINGLETON,
J.CHEM.RES., 267,3149,1981.

72. DICHLORO-DICARBONYL-(2-(DIPHENYLPHOSPHINO)-PYRIDINE)-RUTHENIUM(II) (AT 140 DEG.K)
BEFBUJ M.M.OLMSTEAD,A.MAISONNAT,J.P.FARR,
A.L.BALCH,
INORG.CHEM., 20,4060,1981.

73. CIS-DICHLORO-DICARBONYL-BIS(BENZYLDIPHENYLPHOSPHINE)-RUTHENIUM(II)
BEYHAO L.M.WILKES,J.H.NELSON,J.P.MITCHENER,
M.W.BABICH,W.C.RILEY,B.J.HELLAND,
R.A.JACOBSON,M.Y.CHENG,
K.SEFF,L.B.MCCUSKER,
INORG.CHEM., 21,1376,1982.

74. CARBONYL-DICHLORO-(P-CHLOROPHENYLISOCYANIDE)-BIS(TRIPHENYLPHOSPHINE)-RUTHENIUM(II) ETHANOL SOLVATE
BIDHOL G.R.CLARK,
ACTA CRYSTALLOGR.,SECT.B, 38,2256,1982.

75. DICHLORO-CARBONYL-(DIMETHYLSULFOXIDE)-(O-PHENYLENE-BIS(METHYLPHENYLPHOSPHINE))-RUTHENIUM(II)
BUXMUC S.R.HALL,B.W.SKELTON,A.H.WHITE,
AUST.J.CHEM., 36,271,1983.

76. CIS-DICARBONYL-DICHLORO-((+-)-O-PHENYLENE-BIS(METHYLPHENYLARSINE))-RUTHIUM(II)
BUXNAJ S.R.HALL,B.W.SKELTON,A.H.WHITE,
AUST.J.CHEM., 36,271,1983.

77. BENZYLTRIPHENYLPHOSPHONIUM BICYCLO(2.2.1)HEPTA-2,5-DIENE-(CARBONYL)-TRICHLORO-RUTHENIUM(II)
BZPHRU R.O.GOULD,L.RUIZ-RAMIREZ,T.A.STEPHENSON, M.A.THOMSON, J.CHEM.RES., 254,3301,1978.

78. CHLORO-(1-6-ETA-P-CYMENE)-BIS(PYRAZINE)-RUTHENIUM(II) HEXAFLUOROPHOSPHATE
CABYIN D.A.TOCHER,R.O.GOULD,T.A.STEPHENSON, M.A.BENNETT,J.P.ENNETT, T.W.MATHESON, L.SAWYER,V.K.SHAH, J.CHEM.SOC.,DALTON, ,1571,1983.

79. DICHLORO-TRIAMINE-(CAFFEINE-8-YL) RUTHENIUM(III) CHLORIDE MONOHYDRATE
CAFFRU H.J.KRENTZIEN,M.J.CLARKE,H.TAUBE, BIOINORG.CHEM., 4,143,1975.

80. T-BUTYLISOCYANIDE-CARBONYL-CHLORO-BIS (DIMETHYLPHENYLPHOSPHINE)-PHENYL-RUTHENIUM(II)
CAFTAE Z.DAUTER,R.J.MAWBY,C.D.REYNOLDS, D.R.SAUNDERS, ACTA CRYST.,C(CR.STR.COMM.), 39,1194,1983.

81. CARBONYL-CHLORO-BIS(TRIETHYLPHOSPHINE)-(N,N'-BIS(P-TOLYL)-IMIDAZOLIDIN-2-YLIDENE)-RUTHENIUM(II)
CCTIMR P.B.HITCHCOCK,M.F.LAPPERT,P.L.PYE, S.THOMAS, J.CHEM.SOC.,DALTON, ,1929,1979.

82. CHLORO-METHYL-(ETA-4--CYCLO-OCTA-1,5-DIENE)-(O-METHOXYPHENYLDIPHENYLPHOSPHINE-O,P)-RUTHENIUM(II)
CEFNOQ T.V.ASHWORTH,E.SINGLETON,R.B.ENGLISH, M.M.DEV.STEYN, S.AFR.J.CHEM., 36,97,1983.

83. BIS(DIMETHYLPHENYLPHOSPHINE)(ETHYLENE)(CARBONYL) DICHLORO-RUTHENIUM(II)
CEYMRU L.D.BROWN,C.F.J.BARNARD,J.A.DANIELS, R.J.MAWBY,J.A.IBERS, INORG.CHEM., 17,2932,1978.

84. DICHLORO-CARBONYL-1,6-BIS(DIPHENYLPHOSPHINO)-TRANS-HEX-3-ENE RUTHENIUM(II)
CILXUQ G.R.CLARK,K.MARSDEN, J.ORGANOMET.CHEM., 265,215,1984.

85. TETRAKIS(DIETHYLDITHIOCARBAMATO)-DICHLORO-TRICARBONYL-TRIRUTHENIUM(II)
CLECRU C.L.RASTON,A.H.WHITE, J.CHEM.SOC.,DALTON, ,2422,1975.

86. CIS-CARBONYL-DICHLORO-(2,2'.6',2''-TERPYRIDYL)-RUTHENIUM(II)
COXMUX J.B.DEACON,J.M.PATRICK,B.W.SKELTON, N.C.THOMAS,A.H.WHITE, AUST.J.CHEM., 37,929,1984.

87. CHLORO-DICARBONYL-(CIS-PHENYLDIAZENE)-BIS (TRIPHENYLPHOSPHINE) RUTHENIUM(II) PERCHLORATE METHYLENE DICHLORIDE SOLVATE
CPDZRU B.L.HAYMORE,J.A.IBERS, J.AM.CHEM.SOC., 97,5369,1975.

88. CHLORO-DICARBONYL-(3-BENZYLIDYNE-1-CHLORO-MERCURY-1-PHENYL-PROP-1-EN-2-YL)- BIS(DIMETHYLPHENYLPHOSPHINE)-RUTHENIUM(II)
DIDTAL Z.DAUTER,R.J.MAWBY,C.D.REYNOLDS, D.R.SAUNDERS, J.CHEM.SOC.,DALTON, ,433,1986.

89. METHYLTRIPHENYLPHOSPHONIUMTRIS(MU-2--CHLORO)-DICARBONYL-DICHLORO-BIS-(TRIPHENYLPHOSPHINE)-DI-RUTHENIUM(II) DICHLOROMETHANE SOLVATE
DOSPUW R.A.SANCHEZ-DELGADO,U.THEWALT, N.VALENCIA,A.ANDRIOLLO,R.L.MARQUEZ-SILVA,J.PUGA,H.SCHOLLHORN, H.-P.KLEIN,B.FONTAL, INORG.CHEM., 25,1097,1986.

90. CARBONYL-CHLORO-HYDRIDO-TRIS(METHYLDIPHENYLPHOSPHINE)-RUTHENIUM(II)
FEGXIY M.MOTEVALLI,M.B.HURSTHOUSE,A.R.BARRON, G.WILKINSON, ACTA CRYST.,C (CR.STR.COMM.), 43,214,1987.

91. CARBONYL-CHLORO-BIS(TRIPHENYLPHOSPHINE)-(DITHIOFORMATO-S,S')RUTHENIUM(II) TETRAHYDROFURAN SOLVATE
FUMKED S.GOPINATHAN,I.R.UNNI,C.GOPINATHAN, V.G.PURANIK,S.S.TAVALE,T.N.G.ROW, POLYHEDRON, 6,1859,1987.

92. (ETA-4--CYCLO-OCTA-1,5-DIENE)-BIS(ACETONITRILE-N)-DICHLORO-RUTHENIUM(II) MONOHYDRATE
GAYBAJ T.V.ASHWORTH,D.C.LILES,D.J.ROBINSON, E.SINGLETON,N.J.COVILLE,E.DARLING, A.J.MARKWELL, S.AFR.J.CHEM., 40,183,1987.

93. CIS-DICARBONYL-CIS-DICHLORO-(3,6-BIS(2-PYRIDYL) PYRIDAZINE-N,N') RUTHENIUM(II)
GIDBOK G.DE MUNNO,G.DENTI,G.DE ROSA,G.BRUNO, ACTA CRYST.,C (CR.STR.COMM.), 44,1193,1988.

94. (ETA-6--BENZENE)-CHLORO-(6-METHYL-2-HYDROXYPYRIDINATO-N,O)-RUTHENIUM(II)
GIDXUM E.C.MORRISON,C.A.PALMER,D.A.TOCHER, J.ORGANOMET.CHEM., 349,455,1988.

95. CIS-CARBONYL-DICHLORO-TRIS(DIPHENYLMETHYLPHOSPHINE)-RUTHENIUM(II)
SADPAO D.W.KRASSOWSKI,J.H.NELSON,K.R.BROWER, D.HAUENSTEIN,R.A.JACOBSON, INORG.CHEM., 27,4294,1988.

96. DICHLORO-CARBONYL-SELENOCARBONYL-BIS(TRIPHENYLPHOSPHINE)RUTHENIUM(II)
SELCRU G.R.CLARK,S.M.JAMES, J.ORGANOMET.CHEM., 134,229,1977.

97. (1,3-BIS(4-TOLYL)-IMIDAZOLIDIN-2-YLIDENE)-CHLORO-BIS(TRIETHYLPHOSPHINE)-RUTHENIUM(II)
TZLPRU P.B.HITCHCOCK,M.F.LAPPERT, P.L.PYE,S.THOMAS, J.CHEM.SOC.,DALTON, ,1929,1979.

98. DICHLORO-DICARBONYL-(2-(DIPHENYLPHOSPHINO)-PYRIDINE)-RUTHENIUM(II) (AT 140 DEG.K)
BEFBUJ M.M.OLMSTEAD,A.MAISONNAT, J.P.FARR,A.L.BALCH, INORG.CHEM., 20,4060,1981.

99. DICHLORO-CARBONYL-(DIMETHYLSULFOXIDE)-(O-PHENYLENE-BIS(METHYLPHENYLPHOSPHINE))-RUTHENIUM(II)
BUXMUC S.R.HALL,B.W.SKELTON,A.H.WHITE, AUST.J.CHEM., 36,271,1983.

100. DICHLORO-(TRIS(3-DIMETHYLPHOSPHINOPROPYL)-PHOSPHINE-P,P',P'',P''') RUTHENIUM(II)
DILMIU M.ANTBERG,L.DAHLENBURG, INORG.CHIM.ACTA, 111,73,1986.

101. CHLORO-HYDRIDO-(TRIS(3-DIMETHYLPHOSPHINOPROPYL)-PHOSPHINE-P,P',P'') RUTHENIUM(II)
DUKPII M.ANTBERG,L.DAHLENBURG, ACTA CRYST.,C (CR.STR.COMM.), 42,997,1986.

102. CIS-DICHLORO-(1,4,8,11-TETRATHIACYCLOTETRADECANE)-RUTHENIUM(II) DIHYDRATE
BIGLAE T.-F.LAI,C.-K.POON, J.CHEM.SOC.,DALTON, ,1465,1982.

103. DICHLORO-TETRAKIS(DIMETHYLSULFOXIDE) RUTHENIUM(II)
CDMSOR A.MERCER,J.TROTTER, J.CHEM.SOC.,DALTON, ,2480,1975.

104. CIS-DICHLORO-(DIMETHYLSULFOXIDE-O)-TRIS(DIMETHYLSULFOXIDE-S) RUTHENIUM(II) (ORTHORHOMBIC FORM)
CDMSOR01 W.M.ATTIA,M.CALLIGARIS, ACTA CRYST.,C (CR.STR.COMM.), 43,1426,1987.

105. CIS-DICHLORO-TRIS(DIMETHYL SULFOXIDE-S)-(DIMETHYL SULFOXIDE-O)-RUTHENIUM(II) (RE-DETERMINATION OF A MERCER ET AL, J CHEM SOC DALTON TRANS., 2480,1975, ANTI-TUMOUR AGENT)
CDMSOR02 E.ALESSIO,G.MESTRONI,G.NARDIN,W.M.ATTIA, M.CALLIGARIS,G.SAVA,S.ZORZET, INORG.CHEM., 27,4099,1988.

106. DIMETHYLAMMONIUM TRICHLORO-TRIS(DIMETHYLSULFOXIDE) RUTHENIUM(II)
CDMSRU R.S.MCMILLAN,A.MERCER, B.R.JAMES,J.TROTTER, J.CHEM.SOC.,DALTON, ,1006,1975.

107. TETRAKIS(DIETHYLDITHIOCARBAMATO)-DICHLORO-TRICARBONYL-TRIRUTHENIUM(II)
CLECRU C.L.RASTON,A.H.WHITE, J.CHEM.SOC.,DALTON, ,2422,1975.

108. DICHLORO-(DIMETHYLSULFOXIDE-S)-(1,1,1-TRIS (ETHYLTHIOMETHYL)-ETHANE-S,S',S'')-RUTHENIUM(II)
DOWLOQ D.P.RILEY,J.D.OLIVER, INORG.CHEM., 25,1814,1986.

109. DICHLORO-(DIMETHYLSULFOXIDE-S)-(3-(ETHYLTHIO)-1-((3-(ETHYLTHIO)PROPYL)SULFINYL)PROPANE)-RUTHENIUM(II)
DOWXIW D.P.RILEY,J.D.OLIVER, INORG.CHEM., 25,1821,1986.

110. CHLOROTRIS(N,N-DIETHYLDITHIOCARBAMATO)-RUTHENIUM(IV)
ETCCRU K.W.GIVEN,B.M.MATTSON,L.H.PIGNOLET, INORG.CHEM., 15,3152,1976.

REFERENCES

1. Mutterties, E. L., J. Am. Chem. Soc., (1969), 91, 1636.

2. Britton, D.; Dunitz, J. D., Acta Cryst., Sect. A, (1973), 29, 362.

3. Drew, M. G., Progress in Inorganic Chemistry, (1977), 23, 67.

4. Hoffmann, R.; Beier, B. F.; Muetterties, E. L.; Rossi, A. R., Inorg. Chem., (1977), 16, 511.

5. Kepert, D. L., Progress in Inorganic Chemistry, (1979), 25, 41.

6. Wester, D. W., Ph.D. Dissertation, The University of Florida, 1975.

7. Wester, D. W.; Palenik, G. J., J. Am. Chem. Soc., (1973), 95, 6505.

8. Wester, D. W.; Palenik, G. J., J. Am. Chem. Soc., (1974), 96, 7576.

9. Palenik, G. J.; Wester, D. W.; Rychlewska, U.; Palenik, R. C., Inorg. Chem. (1976), 15, 1814.

10. Palenik, G. J.; Giordano, T., J. Chem. Soc., Dalton Trans., (1987), 1175.

11. McRitchie, D. D.; Palenik, R. C.; Palenik, G. J., Inorg. Chim. Acta, (1976), 20, L27.

12. David, J.; Palenik, G. J., Inorg. Chim. Acta, (1985), 99, L51.

13. J. E. Thomas, and G. J. Palenik, Inorg. Chim. Acta, 44 (1980) L303.

14. J. E. Thomas, M.S. Dissertation, University of Florida, Gainesville, FL, 1980.

15. Giordano, T. J.; Palenik, G. J.; Palenik, R. C.; Sullivan, D. A., Inorg. Chem., (1979), 18, 2245.

16. Palenik, G. J.; Koziol, A. E.; Gawron, M.; Palenik, R. C.; Wester, D. W., Acta Cryst., (1988), C44, 85.

17. Nowatari, H.; Hirabayaski, K.; Yosumari, I., J. Chem. Soc., Faraday Trans., (1976) 2785.

18. Gabe, E. J.; Page, Y. L.; Charland, J. P.; Lee, F. L.; White, P. S., NRCVAX - An Interactive Program System for Structural Analysis, J. Appl. Cryst., (1989), 22, 384.

19. Delledonne, D.; Pelizzi, G.; Pelizzi, C., Acta Cryst., (1987), C43, 1502.

20. Pelizzi, C.; Pelizzi, G., J. Chem. Soc., Dalton Trans., (1980) 1970.

21. Pelizzi, C.; Pelizzi, G.; Predieri, G., J. Organomet. Chem., (1984), 263, 9.

22. Albinati, A.; Pregosin, P. S.; Ruegger, H., Inorg. Chem., (1984), 23, 3223 and references therein.

23. Nelson, J. H.; Alcock, N. W., Inorg. Chem., (1982), 21, 1196.

24. Cotton, F. A.; Wilkinson, G., Advanced Inorganic Chemistry, 4th ed, 1980, John Wiley and Sons, Inc., New York, New York, p. 397,398.

25. Cruickshank, W. J.; Robertson, A. P., Acta Cryst., (1953), 6, 689.

26. Park, J. J.; Collins, D. M.; Hoard, J. L., J. Am. Chem. Soc., (1970), 92, 3636.

27. Nordelli, M.; Pelizzi, C.; Pelizzi, G.; Tarasconi, P., Inorg. Chim. Acta, (1978), 30, 179.

28. Sheldrick, G. M., SHELXTL, a program for crystal structure determination, Revision 4, Nicolet Analytical Instruments, Madison, Wis., August, 1983.

29. Bino, A.; Firm, R.; VanGenderen, M., Inorg. Chim. Acta, (1987), 127, 95.

30. Chung, L-Y.; Constable, E. C.; Khan, M. S.; Lewis, J.; Raithby, P. R.; Vargas, M. D., J. Chem. Soc., Chem. Commun., (1984), 1425.

31. Jahn, H. A.; Teller, E., Proc. R. Soc. London, (1937), 161, 220.

32. Loliger, J.; Scheffold, R., J. Chem. Ed., (1972), 49, 646 and references there in.

33. Sprees,Jr., S.T.; Perumareddi, J. R., Adamson, A. W., J. Am. Chem. Soc., (1968), 90, 6626.

34. Wasson, J. R.; Lorenze, D. R., Inorg. Nucl. Chem. Lett., (1975), 11, 617.

35. Goodman, B. A.; Raynor, J. B.,Advances in Inorganic Chemistry and Radiochemistry, Vol. 13, p.192 (Table XVI), 1970.

36. Wester, D.; Palenik, G. J., Inorg. Chem., (1976), 15, 755.

37. Paolucci, G.; Marangoni, G., Inorg. Chim. Acta, (1977), 24, L5.

38. Masuda, H.; Taga, T.; Osaki, K.; Sugimoto, H.; Mori, M.; Ogoshi, H. Bull. Chem. Soc. Jpn., (1982), 55, 3887. And references there in.

39. Cundari, T. R.; Drago, R. S. Inorg. Chem., (1990), 29, 487.

40. Holm, R. H., Chem. Rev., (1987), 87, 1401.

41. Nagashima, H.; Mukai, K.; Shiota, Y.; Yamaguchi, K.;Ara, K.; Fukahori, T.; Suzuki, H.; Akita, M.; Moro-oka, Y.; Itoh, K. Organometallics, (1990), 9, 799.

42. Bhattacharya, S.; Chakravorty, A.; Cotton, F. A.; Mukherjee, R.; Schwotzer, W. Inorg. Chem., (1984), 23, 1709. And references there in.

43. Perrier, S., Kochi, J. K., Inorg. Chem., (1988), 27, 4165.

44. Griffth, W. P., Ley, S. V., Aldrichimica. Acta, (1990), 23, 13.

45. Porri, L.; Gallazzi, M. C.; Colombo, A.; Allegra, G. Tetrahedron Lett., (1965), 4187.

46. Colombo, A.; Allegra, G. Acta Crystallogr., Sect. B, (1971), 27, 1653.

47. Hitchcock, P. B.; Nixon, J. F.; Sinclair, J. J. Organomet. Chem., (1975), 86, C34.

48. Given, K. W.; Mattson, B. M.; Pignolet, L. H., Inorg. Chem., (1976), 15, 3152.

49. Cox, D. N.; Roulet, R., Inorg. Chem., (1990), 29, 1360.

50. Hiraki, K.; Hidefumi, H. Macromolecules , (1970) 3, 4, 382.

51. Powell, P. Principals of Organometallic Chemistry, 2nd ed.; Chapman and Hill; New York, NY, 1988 (Chapter 6).

52. Albers, M.O.; Liles,D.C.; Robinson, D.J.; Shaver, A.; Singleton, E. Organometallics, (1987), 6, 2347.

53. Boerth, D. W.; Streitwieser, Jr., A. J. Am. Chem. Soc., (1978) 100, 750.

54. Peyerimhoff, S. D.; Buenker, R. J. J. Chem. Phys., (1969), 51, 2528; Theor. Chim. Acta, (1972), 24, 132.

55. Radom, L.; Hariharan, P. C.; Popel, J. A.; Schleyer, P. J. Am. Chem. Soc., (1973), 95, 6531.

56. Lydon, J. E.; Nicholson, J. K.; Show, B. L.; Truter, M. R. Proc. Chem. Soc., (1964), 421.

57. Seddon, E. A.; Seddon, K. R. The Chemistry of Ruthenium; Elsevier; Amsterdam, 1984, (Chapt. 2).

58. Pauling, L. J. Chem. Soc., (1948), 1461.

59. Sanderson,R. T. Science, (1951), 114, 670.

60. Cambridge Structural Database

61. Hancock, R. D., Prog. Inorg. Chem., (1989), 37, 187.

62. Brubaker, G. R.; Johnson, D. W., Coord. Chem. Rev., (1984), 53, 1.

63. Allinger, N. L., Adv. Phys. Org. Chem., (1976), 13, 1.

64. Allinger, N. L., J. Am. Chem. Soc., (1977), 99, 8127.

65. Heimer, N. E.; Swanson, J. T.; Stewart, J. J. P., Frank J. Seiler Research Laboratory, U. S. Air Force Academy, Colorado Springs, CO 80840.

66. Dewar, M. J. S.; Zoebisch, E. G.; Healy, E. F.; Stewart, J. J. P., J. Am. Chem. Soc., (1985), 107, 3902.

67. Pople, J. A.; Beveridge, D. L.; Dobosh, P. A., J. Chem. Phys., (1967), 47, 2026.

68. Ridley, J.; Zerner, M., Theor. Chim. Acta., (1973), 32, 111.

69. Anderson, W. P.; Edwards, W. D.; Zerner, M. C., Inorg. Chem., (1986), 25, 2728.

70. Zerner, M. C.; Loew, G. H.; Kirchner, R. F.; Mueller-Westerhoff, U. T., J. Am. Chem. Soc., (1980), 102, 589.

71. Head, J. D.; Zerner, M. C., Chem. Phys. Lett., (1985), 122, 264.

72. Edwards, W. D.; Zerner, M. C., Theor. Chim. Acta., (1987), 72, 347.

73. Hancock, R. D.; Dobson, S. M.; Evers, A.; Ngwenya, M. P.; Wade, P. W.; Boeyens, J. C. A.; Wainwright, K. P., J. Am. Chem. Soc., (1988), 110, 2788.

74. Boeyens, J. C. A.; Cotton, F. A.; Han, S., Inorg. Chem., (1985), 24, 1750.

75. Allinger, N. L.; Yuh, Y. H., Department of Chemistry, The University of Georgia, Athens, Georgia 30602. MM2-PC Version available form Quantum Chemistry Program Exchange (QCPE), 5th ed., (1990), #QCMP004 (1977 version) or #QCMP010 (An interactive version for PC's).

76. ALCHEMY II, Tripos Associates, Inc., a subsidairy of Evans and Sutherland, 1699 South Hanley Road, Suit 303, St. Louis, Missouri 63144 (1988).

BIOGRAPHICAL SKETCH

The author was born in Los Angeles, California, on May 18, 1962. Shortly thereafter he moved to Canby, Minnesota, where he attended primary and secondary school. After graduating from Canby Public High School in 1980, he attended St. John's University in Collegeville, Minnesota, obtaining a B.S. in chemistry in 1984. After taking a year and one-half off to work, he began graduate studies at South Dakota State University, Brookings, South Dakota, where he obtained a M.S. in chemistry in 1987. He then moved to Gainesville, Florida, and began a Ph.D. program in chemistry at the University of Florida.

I certify that I have read this study and that in my opinion it conforms to acceptable standards of scholarly presentation and is fully adequate, in scope and quality, as a dissertation for the degree of Doctor of Philosophy.

Gus J. Palenik, Chair
Professor of Chemistry

I certify that I have read this study and that in my opinion it conforms to acceptable standards of scholarly presentation and is fully adequate, in scope and quality, as a dissertation for the degree of Doctor of Philosophy.

James M. Boncella
Assistant Professor of Chemistry

I certify that I have read this study and that in my opinion it conforms to acceptable standards of scholarly presentation and is fully adequate, in scope and quality, as a dissertation for the degree of Doctor of Philosophy.

R. Carl Stoufer
Associate Professor of Chemistry

I certify that I have read this study and that in my opinion it conforms to acceptable standards of scholarly presentation and is fully adequate, in scope and quality, as a dissertation for the degree of Doctor of Philosophy.

James D. Winefordner
Graduate Research Professor of Chemistry

I certify that I have read this study and that in my opinion it conforms to acceptable standards of scholarly presentation and is fully adequate, in scope and quality, as a dissertation for the degree of Doctor of Philosophy.

Frank Blanchard
Professor of Geology

This dissertation was submitted to the Graduate Faculty of the Department of Chemistry in the College of Liberal Arts and Sciences and to the Graduate School and was accepted as partial fulfillment of the requirements for the degree of Doctor of Philosophy.

May 1991

Dean, Graduate School

UNIVERSITY OF FLORIDA
3 1262 08285 411 7